# Mechanistic insights into secondary metabolite production through interspecies communication

By

Deepa Deepta Acharya

A dissertation submitted in partial fulfillment of the requirements for the degree of

Doctor of Philosophy (Pharmaceutical Science)

at the University of Wisconsin–Madison 2019

Date of the final examination: 3<sup>rd</sup> May 2019

The dissertation is approved by the following members of the Final Oral Committee:

Tim S. Bugni, Professor, Pharmaceutical Science Lingjun Li, Professor, Pharmaceutical Science Charles T. Lauhon, Associate Professor, Pharmaceutical Science Jennifer Golden, Assistant Professor, Pharmaceutical Science Jennifer Reed, Associate Professor, Chemical and Biological Engineering This dissertation is dedicated to my parents, Mr. Piyush K. Acharya and Mrs. Gouri Acharya for their love and steadfast belief in me.

### Acknowledgment

First and foremost, I would like to express my gratitude to my advisor, Dr. Tim Bugni for his mentorship and support, and for giving me the opportunity to work with him at the end of what was an uncertain second year of graduate school. Aside from the invaluable scientific knowledge I gained from him, I sincerely appreciate his kindness and the time he spent in coaching me to be a better scientist. I would also like to thank my thesis committee: Prof. Lingjun Li, Prof. Charles Lauhon, Prof. Jennifer Reed and Prof. Jennifer Golden for their guidance and advice on my projects.

I would like to especially thank Dr. Navid Adnani for initiating me in the Bugni lab and for being an excellent guide and friend to me. His critical work in the lab went on to become the foundation of my thesis and as a result, I am grateful to him for teaching me everything he knew about co-cultures. I am also thankful to the many past and current members of the Bugni group who have made working in the lab not only intellectually stimulating but extremely supportive and fun. In particular, Srikar Adibhatla, Dr. Ken Barns, Doug Braun, Shaurya Chanana, Jon Fitzgerald, Dr. Dinith Jayanetti, Dr. Rene Ramos, Chris Thomas, I-Wei Tsai, Jiaxuan Yan and Dr. Fan Zhang, have each inspired me through the exemplary work they do and their friendship.

Special thanks go to several colleagues and collaborators without whom the projects would not have been possible. Dr. Ian Miller (Jason Kwan lab), Yusi Cui (Lingjun Li lab) and Mark Berres (Bioinformatics Resource Center) have all made significant contributions to my interdisciplinary project. The National Magnetic Resonance Facility at Madison (NMRFAM), the School of Pharmacy Analytical Instrumentation Center (AIC), the UW-Madison Biotech Center and the scientists who work there, Dr. Paulo Cobra, Dr. Cameron Scarlett, Dr. Thomas

Stringfellow, Dr. Sandra Bondurant, Molly Pellitteri-Hahn and Gary Girdaukas have all been a great resource for NMR, mass spectrometry and gene expression experiments.

I am indebted to the friends I made here in Madison who have become like family. Their companionship through the years has made the ups and downs of graduate school more enjoyable and have kept me motivated.

Finally, I would like to express my profound gratitude for my parents and sisters. Their unconditional love and support inspire me in everything I do.

### **Abstract**

The 'omics' era of the past decade resulted in a paradigm shift in the field of natural products. Recent genomics studies of different Actinobacteria, a class of prolific producers of therapeutic natural products, showed that they contain numerous 'cryptic' or 'silent' biosynthetic gene clusters (BGCs) that remain inactive under standard laboratory growth conditions. Therefore, triggering these silent BGCs could be the key to further exploit this untapped bacterial natural resource. Co-culture has proven to be a remarkable tactic to elicit the production of novel secondary metabolites in various Actinobacteria. Research in our laboratory found that a *Rhodococcus* sp. induces a *Micromonospora* sp. to produce an antibiotic, keyicin when co-cultured together. In this dissertation, the mechanism of interspecies interaction in bacteria was studied to understand how bacteria regulate their BGC activation (Chapter 1).

Differences in the transcription and translation of keyicin producing *Micromonospora* sp. in monoculture and co-culture were evaluated to determine the regulatory bottleneck for the corresponding BGC, *kyc* (Chapter 2). Increase in transcription was found not only for *kyc* but also several other BGCs within the organism. Moreover, small molecule signaling was found to be key for keyicin production. Quorum sensing regulators like exogenously added acyl homoserine lactones and diketopiperizines isolated from the inducing *Rhodococcus* sp., led to keyicin production (Chapter 3).

Additional co-culture combinations were found to produce secondary metabolites that neither participating species produced in monoculture, using LCMS based metabolomics. The isolation and structure elucidation of these co-culture specific compounds were reported. Biosynthetic analyses also helped determine the producing organism in these cases (Chapter 4 and 5).

The amalgamation of several omics techniques was powerful in tracking the process of biosynthesis of keyicin from the genome to the metabolite. These interdisciplinary approaches can be utilized to systematically study interspecies interaction, which will equip us with the knowledge to activate other similarly regulated BGCs.

## **Table of Contents**

ACKNOWLEDGMENT	I
ABSTRACT	IV
LIST OF TABLES	IX
LIST OF FIGURES	X
CHAPTER 1: INTRODUCTION	1
1.1 RECENT ADVANCES IN ANTIBIOTIC DRUG DISCOVERY FROM BACTERIA	1
$1.2\mathrm{Extracellular}$ chemical communication for secondary metabolite production .	4
1.3 Inter-species communication for activating silent biosynthetic gene clusters	7
1.4 Thesis Summary	9
1.5 References	11
CHAPTER 2: OMICS TECHNOLOGIES TO UNDERSTAND SILENT BIOSYNTHETIC G	ENE
CLUSTER ACTIVATION IN MICROMONOSPORA SP. WMMB235	17
2.1 Introduction:	17
2.2 RESULTS AND DISCUSSION:	18
2.3 CONCLUSION	32
2.4 Methods:	33
2.5 References	39
CHAPTER 3: EFFECTS OF QUORUM SENSING AND SMALL MOLECULE CHEMICAI	٠
SIGNALING ON ACTIVATION OF KYC	45
3.1 Introduction	45
3.2 RESULTS AND DISCUSSION	48
3.3 CONCLUSION	57

3.4 MATERIALS AND METHODS	57
3.5 References	61
CHAPTER 4: COMPOUNDS FROM CO-CULTURE AND M	MONO-CULTURE OF
ACTINOMYCETES	65
4. 1 Introduction	65
4. 2 RESULTS AND DISCUSSION:	66
4.3 CONCLUSIONS	75
4.4 MATERIALS AND METHODS	75
4.5 References	81
CHAPTER 5: MECHANISTIC INSIGHT INTO INTERSPE	CIES INTERACTION OF GUT
SYMBIONTS	84
5.1 Introduction	84
5.2 RESULTS AND DISCUSSION:	86
5.3 CONCLUSION	91
5.4 MATERIALS AND METHODS	92
5.5 References	94
CHAPTER 6: CONCLUSIONS AND FUTURE WORK	97
6.1 CONCLUDING REMARKS	97
6.2 Future Work	99
6.3 References	100
APPENDIX 1	101
SUPPLEMENTARY DATA FOR CHAPTER 2	101
ADDENDIY 2	100

SUPPLEMENTARY DATA FOR CHAPTER 2	109
APPENDIX 3	125
SUPPLEMENTARY DATA FOR CHAPTER 4	125
APPENDIX 4	156
SUPPLEMENTARY DATA FOR CHAPTER 5	156

## **List of Tables**

Table 2-1.	BGCs identified within the Micromonospora sp. WMMB235	. 25
Table 2-2.	WMMB235-embedded BGC2 genes	27
Table 2-3.	WMMB235-embedded BGC9	.29
Table 4-1.	NMR for 1 (600 MHz, CD3OD)	69
Table 4-2.	BGCs identified within WMMA2032.	71
Table 4-3.	BGCs homologous to cluster 2 from WMMA2032	72
Table 4-4.	NMR for 5 (CD3OD, 600MHz)	. 74

# **List of Figures**

Figure 1-1. The diverse classes of antibiotics discovered from Actinobacteria	2
<b>Figure 1-2.</b> Structure of A-factor, the γ-butyrolactones from Streptomyces griseus	5
Figure 1-3. Structure of different acyl homoserine lactones	6
Figure 1-4. Structure of Thailandamide A	7
Figure 1-5. Structure of keyicin	9
Figure 2-1. Structure of co-culture-dependent polyketide Keyicin.	19
Figure 2-2. Summary of kyc cluster orf expression profiles	20
Figure 2-3. Summary of quantitative proteomics studies	21
Figure 2-4. GNPS and Cytoscape visualization of Keyicin analog masses	24
<b>Figure 2-5.</b> Global changes in BGC expression profiles in co-cultured WMMB235	26
<b>Figure 2-6.</b> Summary of KEGG mapping for WMMB235 monoculture versus co-culture	30
<b>Figure 2-7.</b> Dotplot of the clusters kyc from Micromonospora sp	32
Figure 3-1. Schematic of co-culture interactions and subsequent activation of silent BGC ky	c 48
Figure 3-2. AHL inducers of keyicin	50
<b>Figure 3-3.</b> Metabolomic analysis of WMMB235-WMMC960 coculture	52
<b>Figure 3-4.</b> Keyicin induction using inducers from WMMA185	55
<b>Figure 4-1.</b> Principal component analysis of WMMA2032, WMMA184 and their co-culture.	67
<b>Figure 4-2.</b> Sephadex LH-20 fractionation of cocultures and monocultures.	68
Figure 4-3. (A) Structure of Chrysophanol (B) Structure of GTRI-02	69
Figure 4-5. Putative BGC (Cluster 2) of Type II PKS	70
Figure 4-4. Structures of actinorhodin (left) and granaticin (right)	70
<b>Figure 4-6.</b> Structures of compounds isolated from <i>Microbulbifer</i> sp	73

Figure 4-7. Structures of compounds isolated from WMMB235 monoculture	. 74
Figure 5-1. A polyketide synthase cluster in L. reuteri R2lc provides competitive advantage	. 85
<b>Figure 5-2.</b> L. reuteri-pks inhibits 100-23 in a time dependent manner	. 88
<b>Figure 5-3.</b> Mass spectra of R2lc and R2lc Δpks2-PKS	. 89
<b>Figure 5-4.</b> R2lc-PKS inhibits 100-23 in a cell-to-cell contact dependent manner	. 90

### **Chapter 1: Introduction**

### 1.1 Recent advances in antibiotic drug discovery from bacteria

Natural products are undeniably one of the fundamental pillars of modern medicine. The vast chemical diversity and breadth of pharmacological activity in naturally derived compounds is remarkable.<sup>1,2</sup> Interestingly, natural products of many clinically relevant classes (Figure 1) have been discovered from Actinobacteria.<sup>3</sup> However, drug discovery efforts from these sources over the last few decades have led to disappointing returns owing to rediscovery of known molecules.<sup>4</sup> The failure to identify new compounds, particularly those with antimicrobial activity, has compounded the national health crisis of antimicrobial resistance.<sup>5</sup> However, two key realizations have led to a resurgence in the field of natural products: first, 99% of bacterial species have not yet been cultured for natural product isolation studies;<sup>6</sup> and second, the genomic potential of cultured bacteria far exceeds the molecules discovered so far.<sup>7-9</sup>

Historically, terrestrial Actinomycetes have overshadowed any other source for natural product drug discovery, primarily because they devote up to 10% of their genome to the biosynthesis of secondary metabolites and as a result, are prolific producers of bioactive molecules. <sup>10,11</sup> However, they are only a small fraction of the bacterial species that exist. Consequently, exploring newer bacterial sources has provided a valuable way to discover new natural products. Recently, underexplored sources such as marine bacteria have been recognized as valuable in the pursuit of new chemical scaffolds. <sup>12–14</sup> Specifically, marine invertebrate associated bacteria provide a niche for unique secondary metabolites. Sponges are among the most productive sources of natural products, in part because 35% of their biomass is composed of a rich and diverse community of bacteria. <sup>15</sup> Our lab and many other labs have investigated these marine invertebrates for new

species of bacteria and have found great success in discovering new bioactive molecules from them.  $^{16-18}$ 

β-lactam (Pennicillin G)

Rifamycin SV

Macrolide (Eryhthromycin)

Tetracycline

Aminoglycoside (Streptomycin)

$$\begin{array}{c} & & & \\ & &$$

Glycopeptide (Vancomycin)

Figure 1-1. The diverse classes of antibiotics discovered from Actinobacteria

Furthermore, the genomics era and the ease of whole genome sequencing have brought within our grasp the knowledge of the entire biosynthetic potential of different microbes. <sup>19</sup> The reduction in sequencing cost in the past decade has resulted in an explosion of genomic data for several bacteria, both cultured and uncultured from wide variety of ecological niches. Our increased understanding of the biosynthetic enzymology of gene clusters has made it possible to evaluate the genomic potential of microbes in silico. The breakthrough in this field was the discovery that genes involved in the production of a secondary metabolites are clustered in a contiguous fashion and include the associated regulatory genes. Together, these collections of genes are called biosynthetic gene clusters (BGCs). The enzymatic assembly line format of a polyketide synthase (PKS) and a non-ribosomal peptide synthetase (NRPS) BGC make elegant use of simple building blocks such as malonyl CoA and amino acids units, respectively to make complex compounds with different functionalities and activities. <sup>20,21</sup> These large enzymatic domains maintain their core structures, but small variations in the biosynthetic architecture can account for drastic differences in the final metabolites.<sup>22</sup> Programming the biosynthetic logic into *in silico* methods for identifying BGCs and secondary metabolites has revolutionized drug discovery from microbes. Utilizing profile Hidden Markov Models based on several experimentally characterized cluster domains enables the prediction of BGCs in uncharacterized bacteria, directly from their genome. Several bioinformatics programs, such as AntiSmash<sup>23,24</sup> and PRISM,<sup>25</sup> can perform these analyses in an automated fashion. These have been used extensively throughout this thesis for analysis of the genomes studied herein.

What was particularly striking from the genomics explosion was the exceedingly large number of BGCs for which no corresponding metabolites have yet been identified. These BGCs have been referred to as cryptic, silent, or orphan.<sup>13,26</sup> More recently, the term orphan gene cluster has been

adopted in an attempt to not overstate our knowledge about the cluster. Many orphan BGCs remained inactive in standard laboratory growth conditions. For example, in Streptomyces coelicolor A3(2), six groups of structurally distinct metabolites have been discovered by traditional methods, but analysis of its genome have identified 16 additional orphan BGCs including NRPSs, PKSs, terpene synthases and NRPS-independent siderophore synthases.<sup>27</sup> Similarly, the complete genome sequencing of Saccharopolyspora erythraea has revealed that only 3 out of 25 biosynthetic gene clusters have been characterized and associated with a secondary metabolite.<sup>7</sup> Nevertheless, with the right conditions in the form of environmental stimuli, expression of orphan BGCs may be switched "on". To achieve the full potential of bacterial natural product chemistry, it is essential to develop methods that harness these silent BGCs.<sup>26</sup> Different strategies have been utilized to coax the bacteria into producing these orphan metabolites including: i) altering growth conditions, <sup>28</sup> ii) addition of chemical elicitors, <sup>29,30</sup> iii) targeted genetic modifications, <sup>31</sup> iv) alterations to transcriptional machineries<sup>32</sup> and v) heterologous expression methods.<sup>33,34</sup> While several new metabolites have been discovered as a result of these efforts, systematic understanding of how silent BGCs can be activated is still lacking. In this regard, it is crucial to realize that bacteria in nature exist in complex ecosystems where they communicate and regulate their gene expression accordingly.

# 1.2 Extracellular chemical communication for secondary metabolite production

It has long been speculated that production of secondary metabolites results from specific environmental stimuli.<sup>35,36</sup> Although factors such as nutrient medium or temperature have profound impacts on the type and quantity of natural products produced, research has demonstrated that bacterial communication is key to regulation for some BGCs.<sup>37</sup> Extracellular communication may

occur through physical interaction<sup>38</sup> or through chemical signals,<sup>39</sup> via intra- and inter- species interactions.<sup>40</sup> Numerous studies have shown that interactions between bacterial cells, either within the same or different species, played a significant role in secondary metabolite production, as outlined below.

In *Streptomyces* sp., production of antibiotics is dependent on the growth phase and accumulation of auto-regulators. In particular, A-factor, a type of γ -butyrolactone (Figure 1-2) controls the biosynthesis of streptomycin in *Streptomyces griseus*.<sup>39</sup> First discovered in 1967 by Khokhlov,<sup>41</sup> this class of signals share a 2, 3-disubstituted γ-butyrolactone scaffold with different side-chains governing their strain specificity. These compounds can diffuse through the cytoplasmic membrane and their accumulation results in the transcriptional activation of streptomycin by binding to the repressor protein ArpA in *S. griseus*.<sup>42–46</sup> Although proteins analogous to ArpA are often cluster specific, they are also known to cause global or pleiotropic changes that affect both morphology and antibiotic production.

Figure 1-2. Structure of A-factor, the y-butyrolactones from *Streptomyces griseus*.

An alternate signaling pathway in Gram-positive bacteria is through modified oligopeptides that are part of a "two-component system" and depend on phosphorylation to activate a DNA-response regulator. This pathway is used by *Staphylococcus aureus* to exercise its virulence. At high cell density, secretion of the autoinducing peptide initiates a cascade of activity that results in the production of toxins and proteases.<sup>47,48</sup>

Similarly, autoregulation through the use of small molecules is prevalent in many Gramnegative bacteria and is the basis of what is known as quorum sensing. First discovered in

Figure 1-3. Structure of different acyl homoserine lactones

bioluminescent marine bacteria *Vibrio fischeri*, quorum sensing is a chemical-based signaling pathway to modulate transcription and/or other responses to environmental stimuli<sup>48</sup>. The canonical system has two major components: LuxI, which synthesizes the signaling molecule acylhomoserine lactone and a corresponding response regulator protein, LuxR, which is a transcription factor. Closely associated with the cell density of the producing species, the AHLs accumulate in the cells over time and above a certain threshold, initiate several downstream processes including virulence and secondary metabolite production. In *Burkholderia thailandensis*, quorum sensing is responsible for regulating production of a polyketide thailandamide A.<sup>49</sup> Analysis of the *B. thailandensis* genome showed that biosynthesis is regulated by a protein, ThaA which has binding motifs similar to LuxR. Knocking this gene out leads to increased production of the compound, demonstrating that intra-species communication through chemical signaling is crucial to secondary metabolite production.

Figure 1-4. Structure of Thailandamide A

It is clear that bacterial communication through small molecules plays a significant role in the regulation of BGCs housed within a bacterium. However, only a few studies have demonstrated the impact of exogenous small molecules either from another species or from the environment. For example, it has been shown that γ-butyrolactones, which are considered species specific, may be involved in interspecies crosstalk. Recio *et al.* have found that a small molecule called PI factor from pimaricin producing *Streptomyces natalensis* serves as the autoregulator for this species. Interestingly, they have demonstrated that production of pimaricin can be restored in a *S. natalensis* mutant lacking in PI factor when A-factor from *Streptomyces griseus* is added to the culture. Another study has shown that a mutant *Streptomyces venezuelae*, also lacking its own γ-butyrolactone can produce the antibiotic jadomycin by intercepting the γ-butyrolactone produced by *S. coelicolor*. These findings show that not only do bacterial species communicate among themselves, they also alter the expression of their biosynthetic genes in response to chemical signaling.

# 1.3 Inter-species communication for activating silent biosynthetic gene clusters

Intracellular communication is crucial to autoregulate group behavior, as described above. However, bacteria constantly interact with other species in naturally occurring ecosystems, either through mutually beneficial or competitive exchanges.<sup>52</sup> As a result, co-culturing of bacteria in the lab setting is a simple and useful representation of the complex interactions that exist in nature.

One of the earliest examples of co-culture that has led to the isolation of a novel secondary metabolite is that of a marine fungus with a marine bacterial strain, CNJ-328, leading to the production of pestalone<sup>53</sup>. Numerous subsequent examples of fungal-bacterial co-cultures have shown that inter-Kingdom interactions can lead to the discovery of newer compounds.<sup>53-57</sup> In contrast, relatively fewer inquiries have been made into bacterial-bacterial cocultures. However, new research shows that bacterial crosstalk can often prompt the synthesis of bioactive compounds for defensive or symbiotic purposes.<sup>58</sup> For instance, a number of diketopiperizines with antibiotic activity against *Vibrio anguillarum* have been discovered through co-culture with a set of marine bacteria.<sup>59</sup> Onaka *et al.* have found that several *Streptomyces* sp. can be driven to produce unique secondary metabolites when co-cultured with mycolic acid containing bacteria, such as *Tsukamurella pulmonis* and *Rhodococcus erythropolis*. They have reported the structure of novel compounds like alchivemycin, niizalactams and chojalactones with antibiotic or cytotoxic effects.<sup>38,60,61</sup>

Our lab has adapted the co-culture technique to show that marine bacteria can be coaxed to produce the products of silent BGCs in the presence of interspecies interaction. Systematic large-scale study of hundreds of co-cultures has shown differential metabolic production between monoculture and co-cultures.<sup>62</sup> In particular, a co-culture pair of *Micromonospora* sp. WMMB235 and *Rhodococcus* sp. WMMA185 has been found to produce a novel antibiotic, keyicin, which is encoded in the BGC, *kyc* housed within the genome of WMMB235 (Figure 1-5).<sup>63</sup>

While it is evident that bacterial co-cultures hold great promise in discovering new secondary metabolites, it is unclear how and why they interact. Similarly, the downstream effects of interspecies interactions have not been characterized. Understanding the mechanism by which co-cultures activate silent BGCs will be crucial to fully exploiting this technique in antibiotic drug discovery from bacteria.

**Figure 1-5.** Structure of keyicin, produced by *Micromonospora* sp. WMMB235 in the presence of *Rhodococcus* sp. WMMA185

### 1.4 Thesis Summary

This thesis aims to expand on the knowledge of how interspecies interaction regulates the biosynthesis of secondary metabolites in bacteria. Co-cultures of marine actinobacteria as well as gut bacteria were studied using multidisciplinary approaches in an effort to elucidate the mechanism of interaction between two bacterial species and the changes that occur in their biosynthetic processes as a result. Overall, this work shows the advantages of using co-culture as a fermentation technique to activate otherwise silent BGCs a using multi-omics approach.

The interspecies interaction between *Micromonospora* sp. WMMB235 and *Rhodococcus* sp. WMMA185 and its implication for keyicin production have been studied in detail. Genome wide transcriptomics using RNA-Seq and proteomics using isobaric tagging have been applied to pinpoint where regulation of keyicin biosynthesis differs between monoculture and co-culture. By comparing the transcription level of *kyc* in WMMB235 between monoculture and co-culture conditions, it was found that the regulatory bottleneck existed at the transcription level. Transcriptomics analysis also demonstrated that expression of several other BGCs in WMMB235 were greatly improved upon co-culturing. The mechanism of interaction was shown to be mediated by small molecules produced by WMMA185. In parallel, quorum sensing modulators, like certain acyl homoserine lactones were shown to activate keyicin production.

Isolation of compounds unique to co-cultures was also reported for other marine bacteria. In particular, co-cultures of *Micromonospora* sp. WMMA2032 with *Dietzia* sp. WMMA184, and WMMB235 with *Microbulbifer* sp. C694 were analyzed due to preliminary evidence that new molecules were produced through interspecies interaction. Additionally, metabolomics studies of two strains of gut bacterium, *Lactobacillus reuteri* were conducted to understand the mechanism of competition between them, whereby one outcompeted the other.

### 1.5 References

- (1) Newman, D. J.; Cragg, G. M. Natural Products as Sources of New Drugs over the Last 25 Years. *J.Nat Prod.* **2007**, *70* (0163–3864 (Print)), 461–477.
- (2) Koehn, F. E.; Carter, G. T. The Evolving Role of Natural Products in Drug Discovery. *Nat. Rev. Drug Discov.* **2005**, *4* (MARCH), 0.
- (3) Barka, E. A.; Vatsa, P.; Sanchez, L.; Gaveau-Vaillant, N.; Jacquard, C.; Klenk, H.-P.; Clément, C.; Ouhdouch, Y.; van Wezel, G. P. Taxonomy, Physiology, and Natural Products of Actinobacteria. *Microbiol. Mol. Biol. Rev.* **2016**, *80* (1), 1–43.
- (4) Rutledge, P. J.; Challis, G. L. Discovery of Microbial Natural Products by Activation of Silent Biosynthetic Gene Clusters. *Nat. Rev. Microbiol.* **2015**, *13* (8), 509–523.
- (5) Piddock, L. J. The Crisis of No New Antibiotics—What Is the Way Forward? *Lancet Infect. Dis.* **2012**, *12* (3), 249–253.
- (6) Amann, R. I.; Ludwig, W.; Schleifer, K.-H. *Phylogenetic Identification and In Situ*Detection of Individual Microbial Cells without Cultivation; 1995; Vol. 59.
- (7) Oliynyk, M.; Samborskyy, M.; Lester, J. B.; Mironenko, T.; Scott, N.; Dickens, S.; Haydock, S. F.; Leadlay, P. F. Complete Genome Sequence of the Erythromycin-Producing Bacterium Saccharopolyspora Erythraea NRRL23338. *Nat. Biotechnol.* 2007, 25 (4), 447–453.
- (8) Bentley, S.; Chater, K.; Cerdeño-Tárraga, a-M.; Challis, G. L.; Thomson, N. R.; James, K. D.; Harris, D. E.; Quail, M. a; Kieser, H.; Harper, D.; et al. Complete Genome Sequence of the Model Actinomycete Streptomyces Coelicolor A3(2). *Nature* 2002, 417 (6885), 141–147.
- (9) Omura, S.; Ikeda, H.; Ishikawa, J.; Hanamoto, A.; Takahashi, C.; Shinose, M.; Takahashi, Y.; Horikawa, H.; Nakazawa, H.; Osonoe, T.; et al. Genome Sequence of an Industrial Microorganism Streptomyces Avermitilis: Deducing the Ability of Producing Secondary Metabolites. *Proc. Natl. Acad. Sci. U. S. A.* 2001, 98 (21), 12215–12220.
- (10) Genilloud, O. Actinomycetes: Still a Source of Novel Antibiotics. *Nat. Prod. Rep.* **2017**, *34* (10), 1203–1232.
- (11) Nett, M.; Ikeda, H.; Moore, B. S. Genomic Basis for Natural Product Biosynthetic Diversity in the Actinomycetes. *Nat. Prod. Rep.* **2009**, *26* (11), 1362.
- (12) Abdelmohsen, U. R.; Bayer, K.; Hentschel, U. Diversity, Abundance and Natural Products

- of Marine Sponge-Associated Actinomycetes. Nat. Prod. Rep. 2014, 31 (3), 381–399.
- (13) Udwary, D. W.; Zeigler, L.; Asolkar, R. N.; Singan, V.; Lapidus, A.; Fenical, W.; Jensen, P. R.; Moore, B. S. Genome Sequencing Reveals Complex Secondary Metabolome in the Marine Actinomycete Salinispora Tropica. Proc. Natl. Acad. Sci. U. S. A. 2007, 104 (25), 10376–10381.
- (14) Fenical, W.; Jensen, P. R. Developing a New Resource for Drug Discovery: Marine Actinomycete Bacteria. *Nat. Chem. Biol.* **2006**, *2* (12), 666–673.
- (15) Hentschel, U.; Piel, J.; Degnan, S. M.; Taylor, M. W. Genomic Insights into the Marine Sponge Microbiome. *Nat. Publ. Gr.* **2012**, *10*.
- (16) Wyche, T. P.; Piotrowski, J. S.; Hou, Y.; Braun, D.; Deshpande, R.; McIlwain, S.; Ong, I. M.; Myers, C. L.; Guzei, I. a.; Westler, W. M.; et al. Forazoline A: Marine-Derived Polyketide with Antifungal in Vivo Efficacy. *Angew. Chemie Int. Ed.* 2014, 53 (43), 11583–11586.
- (17) Zhang, F.; Barns, K.; Hoffmann, F. M.; Braun, D. R.; Andes, D. R.; Bugni, T. S. Thalassosamide, a Siderophore Discovered from the Marine-Derived Bacterium *Thalassospira Profundimaris. J. Nat. Prod.* 2017, 80 (9), 2551–2555.
- (18) Zhang, F.; Braun, D. R.; Ananiev, G. E.; Hoffmann, F. M.; Tsai, I.-W.; Rajski, S. R.; Bugni, T. S. Biemamides A–E, Inhibitors of the TGF-β Pathway That Block the Epithelial to Mesenchymal Transition. *Org. Lett.* **2018**, *20* (18), 5529–5532.
- (19) Kjærbølling, I.; Vesth, T. C.; Frisvad, J. C.; Nybo, J. L.; Theobald, S.; Kuo, A.; Bowyer, P.; Matsuda, Y.; Mondo, S.; Lyhne, E. K.; et al. Linking Secondary Metabolites to Gene Clusters through Genome Sequencing of Six Diverse Aspergillus Species. *Proc. Natl. Acad. Sci. U. S. A.* 2018, 115 (4), E753–E761.
- (20) Michael A. Fischbach, A.; Walsh, C. T. Assembly-Line Enzymology for Polyketide and Nonribosomal Peptide Antibiotics: Logic, Machinery, and Mechanisms. **2006**.
- (21) Nguyen, T.; Ishida, K.; Jenke-Kodama, H.; Dittmann, E.; Gurgui, C.; Hochmuth, T.; Taudien, S.; Platzer, M.; Hertweck, C.; Piel, J. Exploiting the Mosaic Structure of Trans-Acyltransferase Polyketide Synthases for Natural Product Discovery and Pathway Dissection. *Nat. Biotechnol.* **2008**, *26* (2), 225–233.
- (22) Van Lanen, S. G.; Shen, B. Microbial Genomics for the Improvement of Natural Product Discovery. **2006**.

- (23) Weber, T.; Blin, K.; Duddela, S.; Krug, D.; Kim, H. U.; Bruccoleri, R.; Lee, S. Y.; Fischbach, M. A.; Müller, R.; Wohlleben, W.; et al. AntiSMASH 3.0—a Comprehensive Resource for the Genome Mining of Biosynthetic Gene Clusters. *Nucleic Acids Res.* **2015**, 43 (W1), W237–W243.
- (24) Blin, K.; Wolf, T.; Chevrette, M. G.; Lu, X.; Schwalen, C. J.; Kautsar, S. A.; Suarez Duran, H. G.; de los Santos, E. L. C.; Kim, H. U.; Nave, M.; et al. AntiSMASH 4.0—Improvements in Chemistry Prediction and Gene Cluster Boundary Identification. Nucleic Acids Res. 2017, 45 (W1), W36–W41.
- (25) Skinnider, M. A.; Dejong, C. A.; Rees, P. N.; Johnston, C. W.; Li, H.; Webster, A. L. H.; Wyatt, M. A.; Magarvey, N. A. Genomes to Natural Products PRediction Informatics for Secondary Metabolomes (PRISM). *Nucleic Acids Res.* **2015**, *43* (20), gkv1012.
- (26) Hertweck, C. Hidden Biosynthetic Treasures Brought to Light. *Nat. Chem. Biol.* **2009**, *5* (7), 450–452.
- (27) Challis, G. L. Exploitation of the Streptomyces Coelicolor A3(2) Genome Sequence for Discovery of New Natural Products and Biosynthetic Pathways. *J. Ind. Microbiol. Biotechnol.* **2014**, *41* (2), 219–232.
- (28) Lincke, T.; Behnken, S.; Ishida, K.; Roth, M.; Hertweck, C. Closthioamide: An Unprecedented Polythioamide Antibiotic from the Strictly Anaerobic Bacterium Clostridium Cellulolyticum. *Angew. Chemie* **2010**, *122* (11), 2055–2057.
- (29) Moore, J. M.; Bradshaw, E.; Seipke, R. F.; Hutchings, M. I.; McArthur, M. *Use and Discovery of Chemical Elicitors That Stimulate Biosynthetic Gene Clusters in Streptomyces Bacteria*, 1st ed.; Elsevier Inc., 2012; Vol. 517.
- (30) Seyedsayamdost, M. R. High-Throughput Platform for the Discovery of Elicitors of Silent Bacterial Gene Clusters. *Proc. Natl. Acad. Sci. U. S. A.* **2014**, *111* (20), 7266–7271.
- (31) Laureti, L.; Song, L.; Huang, S.; Corre, C.; Leblond, P.; Challis, G. L.; Aigle, B. Identification of a Bioactive 51-Membered Macrolide Complex by Activation of a Silent Polyketide Synthase in Streptomyces Ambofaciens. *Proc. Natl. Acad. Sci. U. S. A.* **2011**, *108* (15), 6258–6263.
- (32) Hosaka, T.; Ohnishi-Kameyama, M.; Muramatsu, H.; Murakami, K.; Tsurumi, Y.; Kodani, S.; Yoshida, M.; Fujie, A.; Ochi, K. Antibacterial Discovery in Actinomycetes Strains with Mutations in RNA Polymerase or Ribosomal Protein S12. *Nat. Biotechnol.*

- **2009**, 27 (5), 462–464.
- (33) Xin Lin; Russell Hopson, and; Cane\*, D. E. Genome Mining in Streptomyces Coelicolor: Molecular Cloning and Characterization of a New Sesquiterpene Synthase. **2006**.
- (34) Chou, W. K. W.; Fanizza, I.; Uchiyama, T.; Komatsu, M.; Ikeda, H.; Cane, D. E. Genome Mining in *Streptomyces Avermitilis*: Cloning and Characterization of SAV\_76, the Synthase for a New Sesquiterpene, Avermitilol. *J. Am. Chem. Soc.* **2010**, *132* (26), 8850–8851.
- (35) Hallada, T. C.; Fountoulakis, J. M.; Sosa, M. S.; Masurekar, P. S.; Kaplan, L. Pneumocandins from Zalerion Arboricola. II. Modification of Product Spectrum by Mutation and Medium Manipulation. *J. Antibiot. (Tokyo).* 2012, 45 (12), 1867–1874.
- (36) Connors, N.; Petersen, L.; Hughes, R.; Saini, K.; Olewinski, R.; Salmon, P. Residual Fructose and Osmolality Affect the Levels of Pneumocandins B 0 and C 0 Produced by Glarea Lozoyensis. *Appl Microbiol Biotechnol* **2000**, *54*, 814–818.
- (37) Scherlach, K.; Hertweck, C. Triggering Cryptic Natural Product Biosynthesis in Microorganisms. **2009**.
- (38) Onaka, H.; Mori, Y.; Igarashi, Y.; Furumai, T. Mycolic Acid-Containing Bacteria Induce Natural-Product Biosynthesis in Streptomyces Species. *Appl. Environ. Microbiol.* **2011**, 77 (2), 400–406.
- (39) Bibb, M. J. Regulation of Secondary Metabolism in Streptomycetes. *Curr. Opin. Microbiol.* **2005**, *8* (2), 208–215.
- (40) Schroeckh, V.; Scherlach, K.; Nützmann, H.-W.; Shelest, E.; Schmidt-Heck, W.; Schuemann, J.; Martin, K.; Hertweck, C.; Brakhage, A. A. Intimate Bacterial-Fungal Interaction Triggers Biosynthesis of Archetypal Polyketides in Aspergillus Nidulans. *Proc. Natl. Acad. Sci. U. S. A.* **2009**, *106* (34), 14558–14563.
- (41) Khokhlov, A. S.; Anisova, L. N.; Tovarova, I. I.; Kleiner, E. M.; Kovalenko, I. V.; Krasilnikova, O. I.; Kornitskaya, E. Y.; Pliner, S. A. Effect of A-Factor on the Growth of Asporogenous Mutants of Streptomyces Griseus, Not Producing This Factor. *Zeitschrift* für allgemeine Mikrobiologie. 1973, pp 647–655.
- (42) Horinouchi, S.; Suzuki, H.; Nishiyama, M.; Beppu, T. Nucleotide Sequence and Transcriptional Analysis of the Streptomyces Griseus Gene (AfsA) Responsible for A-

- Factor Biosynthesis. J. Bacteriol. 1989, 171 (2), 1206–1210.
- (43) Chater, K. F.; Bibb, J. 2 Regulation of Bacterial Antibiotic Production. 1997.
- (44) Gomez-Escribano, J.; Alt, S.; Bibb, M. Next Generation Sequencing of Actinobacteria for the Discovery of Novel Natural Products. *Mar. Drugs* **2016**, *14* (4), 78.
- (45) Takano, E. Gamma-Butyrolactones: Streptomyces Signalling Molecules Regulating Antibiotic Production and Differentiation. *Current Opinion in Microbiology*. **2006**, pp 287–294.
- (46) Ohnishi, Y.; Kameyama, S.; Onaka, H.; Horinouchi, S. The A-Factor Regulatory Cascade Leading to Streptomycin Biosynthesis in Streptomyces Griseus: Identification of a Target Gene of the A-Factor Receptor. *Mol. Microbiol.* **1999**, *34* (1), 102–111.
- (47) Lyon, G. J.; Novick, R. P. Peptide Signaling in Staphylococcus Aureus and Other Gram-Positive Bacteria. *Peptides* **2004**, *25*, 1389–1403.
- (48) Waters, C. M.; Bassler, B. L. Quorum Sensing: Communication in Bacteria. *Annu. Rev. Cell Dev. Biol.* **2005**, *21* (1), 319–346.
- (49) Ishida, K.; Lincke, T.; Behnken, S.; Hertweck, C. Induced Biosynthesis of Cryptic Polyketide Metabolites in a Burkholderia Thailandensis Quorum Sensing Mutant. **2010**.
- (50) Recio, E.; Colinas, Á.; Rumbero, Á.; Aparicio, J. F.; Martín, J. F. PI Factor, a Novel Type Quorum-Sensing Inducer Elicits Pimaricin Production in Streptomyces Natalensis. *J. Biol. Chem.* **2004**, 279 (40), 41586–41593.
- (51) Nodwell, J. R. Are You Talking to Me? A Possible Role for ??-Butyrolactones in Interspecies Signalling. *Mol. Microbiol.* **2014**, *94* (3), 483–485.
- (52) Adnani, N.; Rajski, S. R.; Bugni, T. S. Symbiosis-Inspired Approaches to Antibiotic Discovery. *Nat. Prod. Rep.* **2017**, *34* (7), 784–814.
- (53) Cueto, M.; Jensen, P. R.; Kauffman, C.; Fenical, W.; Lobkovsky, E.; Clardy, J. Pestalone, a New Antibiotic Produced by a Marine Fungus in Response to Bacterial Challenge. *J. Nat. Prod.* **2001**, *64* (11), 1444–1446.
- (54) Brakhage, A. A.; Schroeckh, V. Fungal Secondary Metabolites Strategies to Activate Silent Gene Clusters. *Fungal Genet. Biol.* **2011**, *48* (1), 15–22.
- (55) Sonnenbichler, J.; Dietrich, J.; Peipp, H. Secondary Fungal Metabolites and Their Biological Activities, V. Investigations Concerning the Induction of the Biosynthesis of Toxic Secondary Metabolites in Basidiomycetes. *Biol. Chem. Hoppe. Seyler.* **1994**, *375*

- (1), 71-80.
- (56) Meyer, V.; Stahl, U. The Influence of Co-Cultivation on Expression of the Antifungal Protein in Aspergillus Giganteus. *J. Basic Microbiol.* **2003**, *43* (1), 68–74.
- (57) Nützmann, H.; Reyes-dominguez, Y.; Scherlach, K.; Schroeckh, V.; Horn, F. Bacteria-Induced Natural Product Formation in the Fungus Aspergillus Nidulans Requires Saga / Ada-Mediated Histone Acetylation. *Pnas* **2011**, *108* (34), 14282–14287.
- (58) Zarins-Tutt, J. S.; Barberi, T. T.; Gao, H.; Mearns-Spragg, A.; Zhang, L.; Newman, D. J.; Goss, R. J. M. Prospecting for New Bacterial Metabolites: A Glossary of Approaches for Inducing, Activating and Upregulating the Biosynthesis of Bacterial Cryptic or Silent Natural Products. *Nat. Prod. Rep.* 2016, 33, 54–72.
- (59) Fdhila, F.; Vazquez, V.; Sánchez, J. L.; Riguera, R. DD-Diketopiperazines: Antibiotics Active against Vibrio Anguillarum Isolated from Marine Bacteria Associated with Cultures of Pecten Maximus. *J. Nat. Prod.* **2003**, *66* (10), 1299–1301.
- (60) Hoshino, S.; Okada, M.; Wakimoto, T.; Zhang, H.; Hayashi, F.; Onaka, H.; Abe, I. Niizalactams A-C, Multicyclic Macrolactams Isolated from Combined Culture of Streptomyces with Mycolic Acid-Containing Bacterium. J. Nat. Prod. 2015, 78 (12), 3011–3017.
- (61) Hoshino, S.; Wakimoto, T.; Onaka, H.; Abe, I. Chojalactones A-C, Cytotoxic Butanolides Isolated from Streptomyces Sp. Cultivated with Mycolic Acid Containing Bacterium. *Org. Lett.* **2015**, *17* (6), 1501–1504.
- (62) Adnani, N.; Vazquez-Rivera, E.; Adibhatla, S.; Ellis, G.; Braun, D.; Bugni, T. Investigation of Interspecies Interactions within Marine Micromonosporaceae Using an Improved Co-Culture Approach. *Mar. Drugs* 2015, 13 (10), 6082–6098.
- (63) Adnani, N.; Chevrette, M. G.; Adibhatla, S. N.; Zhang, F.; Yu, Q.; Braun, D. R.; Nelson, J.; Simpkins, S. W.; McDonald, B. R.; Myers, C. L.; et al. Coculture of Marine Invertebrate-Associated Bacteria and Interdisciplinary Technologies Enable Biosynthesis and Discovery of a New Antibiotic, Keyicin. ACS Chem. Biol. 2017, 12 (12), 3093–3102.

### Chapter 2: Omics Technologies to Understand Silent Biosynthetic Gene Cluster Activation in *Micromonospora* sp. WMMB235

Portions of this chapter have been submitted to ACS Chemical Biology as:

Acharya, D. D.; Miller I. J.; Cui Y., Braun, D.; Berres M.; Styles, M. J.; Li, L.; Kwan, J.C.; Rajski, S. R.; Blackwell, H. E.; Bugni, T. S. Omics Technologies to Understand Silent Biosynthetic Gene Cluster Activation in *Micromonospora* sp. WMMB235

### 2.1 Introduction:

Widespread genome mining efforts in Actinobacteria aimed at unveiling new compounds for drug discovery, discovered that these genomes contained biosynthetic gene clusters (BGCs) in far greater number than previously anticipated. The genomics revolution was fueled in part by the increased understanding of secondary metabolite biosynthesis and the availability of numerous bioinformatics pipelines that could assess the biosynthetic potential of an organism. The result of the extensive genomic analyses demonstrated that many BGCs remained silent and inaccessible. In other words, under standard laboratory conditions, their products were either produced in diminishingly small quantities or were altogether absent. These findings made clear that genomic information alone was insufficient to access new secondary metabolites since regulatory mechanisms prevented the expression of many BGCs. Therefore, an approach correlating genomic information with feasibility of metabolite production and isolation requires the integration of transcriptomic, proteomic, and metabolomic methods.

In an effort to activate silent BGCs, co-culturing of multiple organisms has been found to facilitate interspecies communication, triggering biosynthesis of co-culture dependent natural products. Consistent with this observation, previous work in our laboratory showed that *Micromonospora* sp. WMMB235 when co-cultured with a *Rhodococcus* sp. WMMA185 produced

a new antibiotic named keyicin (1). Keyicin (1) was identified as a glycosylated anthracycline with a characteristic red color constructed by a type II PKS gene cluster, kyc housed within the WMMB235 genome. 16 Importantly, the WMMA185 genome did not contain any putative BGC capable of producing keyicin.<sup>17</sup> In isolation, neither bacterium was capable of producing keyicin (1). Despite the excitement and significance of this finding, little was known about how the presence of each microbe during fermentation enabled interspecies interactions that changed the metabolic profile either, both, The of or participants. Micromonospora WMMB235/Rhodococcus sp. WMMA185 co-culture provided an excellent system to study changes in gene expression and regulatory mechanisms resulting from inter-species communication. We report herein the application of transcriptomics and proteomics to understand how WMMA185 triggered kyc activation and subsequent keyicin (1) production by WMMB235. Such multi-omics methods enable elucidation of inter-species communications and interactions in bacterial co-culture.

#### 2.2 Results and Discussion:

#### Transcriptomic activation of the kyc cluster and Keyicin production in co-culture

Early sequencing efforts made clear that keyicin assembly in co-culture could be ascribed only to WMMB235.  $^{16,18}$  To evaluate how *kyc* biosynthetic genes were impacted by the presence of WMMA185, we collected cells from days 2 and 5 of the cultures for WMMB235, WMMA185 and their co-culture in triplicate. LC/MS and colorimetric analyses ( $\lambda$ max = 470 nm) revealed that 1 was not produced in substantial quantities until day 4 of fermentation. In parallel, total RNA from each of these samples was extracted and processed to yield mRNA. Illumina sequencing of each mRNA collection enabled alignments of the resulting RNASeq data for the two genomes in

order to parse transcript reads for WMMB235 (producer). The aggregate value of reads per kb/million reads aligning to annotated ORFs (RPKMO) of the gene clusters was calculated from the number of reads for each gene in the cluster that could be mapped to the genome. <sup>19</sup> This value was normalized to cluster length to ensure accurate representation of the smaller gene clusters in the genome relative the large kyc cluster. Overall, the kyc cluster started out with similar RPKMO values of 1303.0 and 1849.1 on day 2 in monoculture and co-culture, respectively, which suggested a similar level of expression in both conditions. These values changed drastically at day 5 to 267 in monoculture and 2267.7 in co-culture. The relative RPKMO values were representative of the extent of gene expression that eventually led to the production of keyicin. Therefore, a higher RPKMO value in co-culture compared to monoculture was consistent with significantly increased transcription of the *kyc* cluster in the presence of WMMA185 and the commensurate reduction of the same transcripts over time in monocultured WMMB235.

Further differential gene expression analyses (DGE) were conducted on day 5 data using EdgeR software<sup>20</sup> to quantitate expression of each WMMB235 gene in co-culture relative to

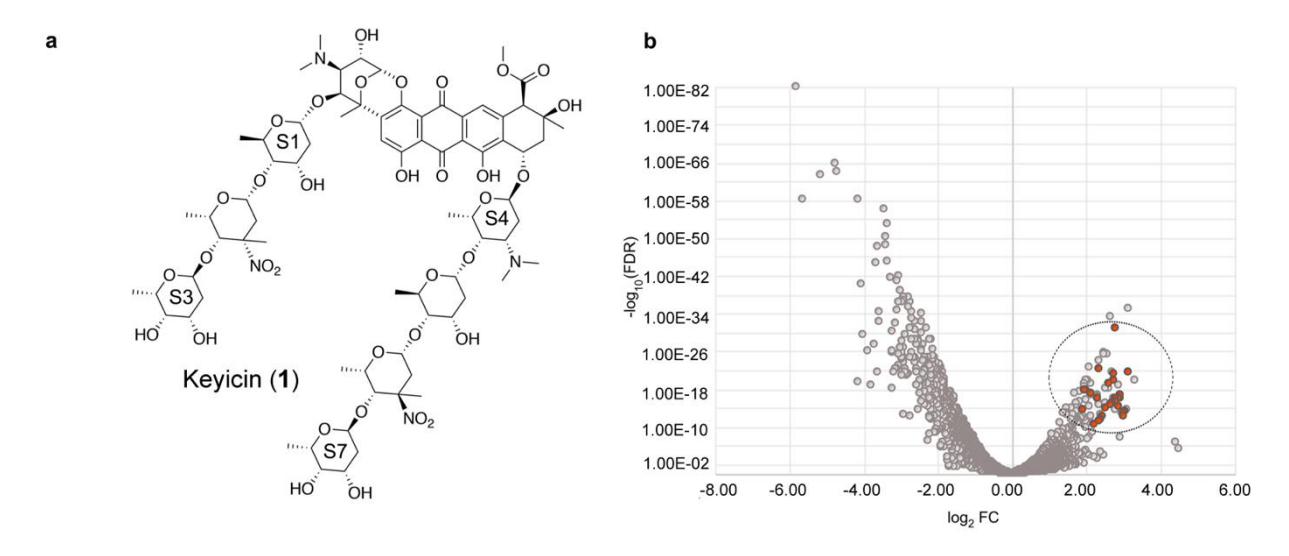


**Figure 2-1**. Structure of co-culture-dependent polyketide Keyicin **1** (**A**) and differential gene expression from WMMB235 genome in co-culture with Rhodococcus sp. WMMA185 (**B**). Genes from the kyc gene cluster are indicated as red spheres within the circled (dashed lines) region.

monoculture as a fold-change of read counts, along with the significance of this difference as adjusted p-value or false discovery rate (FDR). The volcano plot in Figure 2-1B revealed that putative *kyc* cluster genes were among the most upregulated and had the lowest rates of false discovery. In fact, the vast majority of *orfs* within the *kyc* cluster showed at least a 2-fold (to the log<sub>2</sub>) increase in gene expression. These transcriptomic analyses suggested that the presence of WMMA185 induced the transcriptional activation of the *kyc* cluster. We posited that, in the absence of this challenging competitor, WMMB235 channeled resources to other metabolic machineries unrelated to the assembly of 1. Of course, the co-culture situation was different; here,

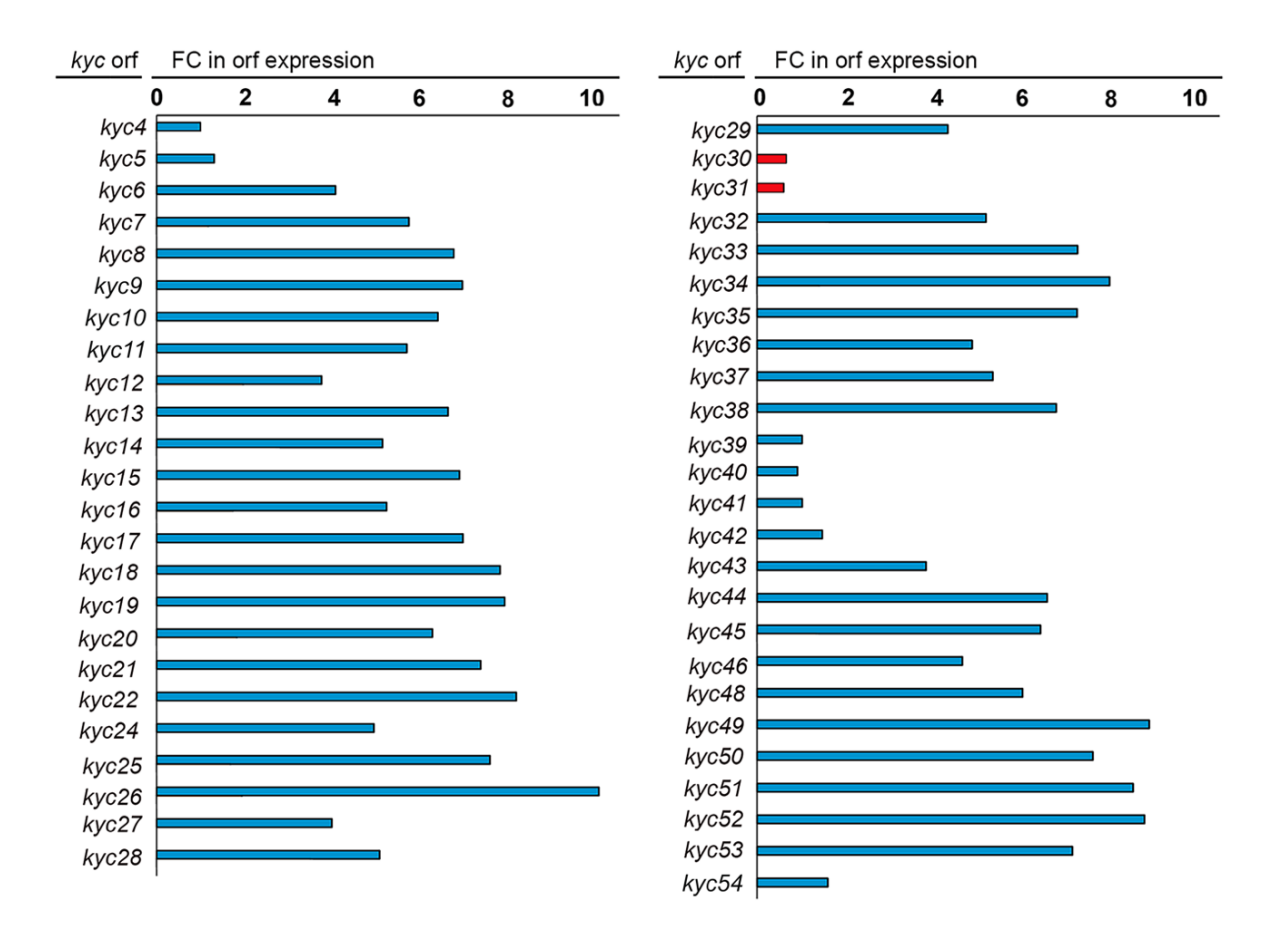


**Figure 2-2.** Summary of *kyc* cluster *orf* expression profiles in WMMB235/WMMA185 co-culture compared to those generated in WMMB235 monoculture. Out of 49 *orfs* within the *kyc* cluster, only 6 undergo less than a 4-fold increase in expression and two (*kyc30*, 31 *in red*) appear to be suppressed in co-culture. That these *orfs* appear to be dispersed at 3-4 different groupings within the *kyc* cluster suggests that *kyc* cluster regulation calls for more than just one global regulator. FC, fold change. False Discovery Rate (q-value) for each gene expression change <<0.01.

the antibiotic properties of keyicin seemed highly beneficial to its producer and, commensurately, *kyc* transcripts were much more pronounced in the day 2 co-culture case relative to either monoculture scenario (days 2 and 5).

Further in-depth transcriptomics analysis of the *kyc* cluster revealed that effectively all *orfs* within the cluster showed some level of over expression. Only *kyc4*,5,30,31,39-42,53 showed less than a 4-fold increase in expression relative to WMMB235 monoculture (Figure 2-2); *kyc30* and *kyc31* were slightly suppressed under co-culturing (FC < 1.0). With respect to *kyc* cluster-specific changes, it was clear that the overwhelming majority of *kyc* cluster elements in WMMB235 monoculture suffered from limited transcription relative to co-culture. Not surprisingly, several regulatory genes that control transcription existed within the *kyc* cluster. Particularly interesting was the *luxR* gene (kyc5), known to play a crucial role in regulation via quorum sensing. Transcriptional activation via this route will be discussed in detail in Chapter 3.

## Isobaric tagging reveals important proteomic profiles unique to WMMB235/WMMA185 coculture.

We used quantitative proteomics approach to evaluate WMMB235/WMMA185 co-cultures to identify unique elements of co-culture that could be clearly correlated to *kyc* cluster activation and biosynthesis of **1**. Proteomics initiatives were carried out on 5-day long and 8-day long fermentations

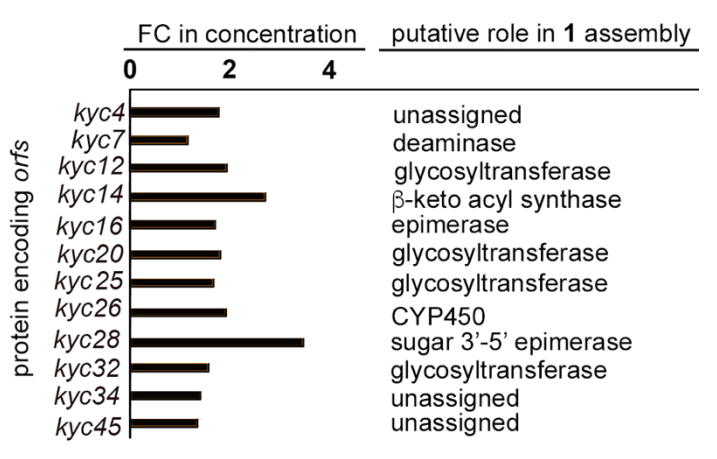


**Figure 2-3.** Summary of quantitative proteomics studies of WMMB235 fermented in WMMA185 supernatant (*Rhodococcus* cell free) for 8 d. Fold change, FC. N=3, P<0.05

in order to most accurately capture protein levels. To reduce the complexity of samples subjected to proteomics we employed a simulated co-culture system wherein the supernatant of WMMA185 (5 d fermentation) was used as the WMMB235 growth medium. This enabled us to more confidently assign proteomic signatures to the keyicin producer and not *Rhodococcus* products. Protein samples from each of these conditions (in triplicate) were labelled in parallel using established isobaric DiLeu tagging methods,<sup>21</sup> and combined for analysis via LC-MS/MS. Labelling each sample with a different reporter ion in this manner, allowed us to multiplex all samples and generate quantitative data on proteins of WMMB235 origin.

Importantly, a marginal number (12) of putative biosynthetic proteins coded for by the kyc cluster were identified from the 8-day fermentation of WMMB235 (Figure 2-2); these included four glycosyltransferases (GTs) (Kyc12, Kyc20, Kyc25, Kyc32) all of which were significantly upregulated in co-culture, as well as the putative deaminase (Kyc4),  $\Box$ -keto acyl synthase (Kyc14), epimerase (Kyc16), cytochrome P<sub>450</sub> (Kyc26) and the dTDP-4-dehydrorhamnose 3,5-epimerase (Kyc28). The GTs Kyc12, Kyc20, and Kyc32 were all homologous to AknK, which was shown to be the GT responsible for adding the second and third 2-deoxy-L-fucose moieties during aclacinomycin biosynthesis (MIBiG: BGC0000191).<sup>22</sup> Kyc25, on the other hand shared 61% identity with CosG, a glycosyltransferase known to transfer aminodeoxysugars like L-rhodosamine during biosynthesis of cosmomycin D (MIBiG: BGC0001074).<sup>23</sup> In depth sequence analyses for Kyc28 revealed 69% similarity to the sugar 3'-5' epimerase SnogF (Accession no.: A0QSK5.1) involved in the deoxyhexose pathway required for nogalamycin assembly.<sup>24</sup> Interestingly, this protein was one of the few proteins found in our preliminary proteomics study to be predominant in the co-culture compared to the WMMB235 monoculture. 16 Additionally, Kyc26 was reported to have 42% protein identity with SnogN, 16 which is also considered to be involved in the

deoxyhexose pathway in the biosynthesis of nogalamine.<sup>25</sup> The closest homologue to Kyc16 was a putative NDP-sugar 4-ketoreductase encoded within the versipelostatin gene cluster (MIBiG: BGC0001204). Importantly, Kyc14 with 65% identity with AknC, also from the aclacinomycin biosynthetic pathway, was the only *kyc orf* product found thus far that played a role in the biosynthesis of the keyicin aglycone. Overarchingly, the predominance of GTs at later fermentation times (day 8 or later) relative to other enzymes involved in keyicin assembly suggested initial aglycone construction followed by glycosylation. The GTs involved in keyicin production appeared to function as true tailoring enzymes. This was consistent with other anthracycline biosynthetic studies where hydroxylated aglycone intermediates added exogenously to fermentation systems serve as efficient substrates for glycosylation.<sup>26-28</sup>

The prominent changes in GT production found in co-culture versus monoculture inspired us to investigate the prospect that keyicin analogs or precursors might be generated during co-culture and other related keyicin-generating conditions but may have evaded detection. This notion was further supported by the clear presence of many other compounds with distinct retention times in co-culture extracts, all of which contained a chromophore with unique absorption at  $\lambda = 470$  nm, and MS/MS signals at m/z = 550.1692 and 586.1899 representative of the keyicin aglycone (Appendix). The relationship of these molecules with keyicin could be easily identified by subjecting the liquid chromatography tandem mass spectrometry (LC-MS/MS) analyses of co-culture extracts collected over a fermentation period of 14 days to Global Natural Product Social (GNPS) Molecular Networking<sup>29</sup> and subsequent visualization by Cytoscape<sup>30</sup> (Figure 2-3). By tracking the node representative of keyicin (m/z 805.347), we identified the subcluster that contained the keyicin analogs/intermediates. On mapping the AUC (Area Under Curve) of extracted ion chromatogram for each of the parent masses identified in the cluster at each time

point, we discovered that many of these signals initially increased in intensity and then gradually subsided with time consistent with the biosynthetic progression leading ultimately to keyicin and away from incompletely glycosylated intermediates or precursors. For example, a doubly-charged peak on the chromatogram corresponding to m/z values of 661.3050 and 645.7829 seemed to show a distinct temporal pattern. Here we propose that these signals represented differentially glycosylated analogs of keyicin. The m/z value of 645.7829 was consistent with decilonitrose, <sup>16</sup> the adduct resulting from the absence of keyicin's terminal 2-deoxy-fucose (S7, Figure 2-1). Additionally, the absence of both S3 and S7 (Figure 2-1) manifests would be reflected by the m/z signal at 661.395 (Appendix).

That co-culture driven transcriptomic enhancements were much more dramatic than those seen at the proteomics level suggested that the production of 1 in WMMB235 monoculture was most likely limited at a transcriptional level. Having identified changes to the transcriptomic and proteomic profile, as well as, the players in keyicin production, and realizing that these changes likely invoke co-culture-dependent changes that go beyond changes in *kyc* expression, transcriptional changes considerate of the whole WMMB235 genome.

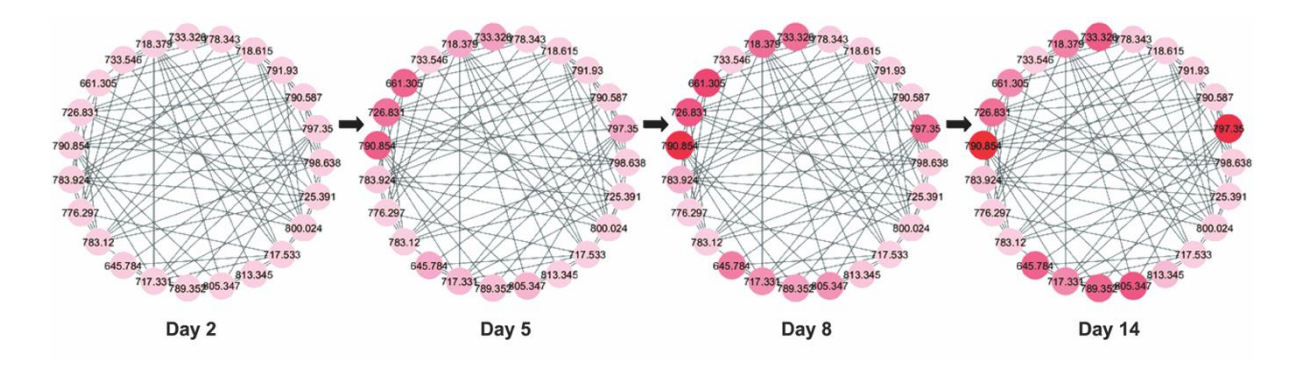


**Figure 2-4.** GNPS and Cytoscape visualization of Keyicin analog masses (from LC-MS/MS of cocultured WMMB235) reflect varying extents of glycosylation over time (Days 2, 5, 8, and 14). Continuous color mapping for each node in the network represent the relative concentrations of the species for which MS data is shown. Color intensities correlate to concentrations of each species for which MS data is acquired.

# Impacts of co-culture on the WMMB235 genome revealed by transcriptomics

WMMB235 Transcriptomic evaluation of the Micromonospora sp. genome WMMB235/WMMA185 co-cultures dramatically expanded what we knew about kyc activation as well as the modulation of other WMMB235 embedded BGCs. We extended the transcriptomics analyses to other BGCs present within WMMB235. Since biosynthetic genes group together on bacterial chromosomes, these could be computationally identified using different algorithms. AntiSmash data processing for the WMMB235 genome<sup>18</sup> revealed the presence of 50 putative BGCs, whereas PRISM processing of the same data set revealed the presence of 10 putative BGCs. The abundance of BGCs found by AntiSmash could be attributed to the low confidence/high novelty algorithm of ClusterFinder to identify BGCs. This probabilistic algorithm was optimized for detecting unknown types of gene clusters and consequently gave relatively high rates of false positives in the results. <sup>31–33</sup> Consequently, we restricted our transcriptomics analyses to only BGCs that resulted from PRISM; as expected, these same BGCs were also identified by AntiSmash processing of the WMMB235 genome.

**Table 2-1.** BGCs identified within the Micromonospora sp. WMMB235 genome as annotated by PRISM. Assigned cluster numbers correlate to all subsequent Tables and Figures.

BGC#	Cluster annotation	Closest Known Homologous BGC (% genes showing similarity) (MIBiG number)
1	Keyicin	Aclacinomycin <sup>34</sup> (72%) (BGC0000191)
2	AT-less PKS	Leinamycin <sup>35–37</sup> (15%) (BGC0001101)
3	Type II PKS	Xantholipin <sup>38</sup> (16%) (BGC0000279)
4	NRPS-T1PKS	Bleomycin <sup>39,40</sup> (12%) (BGC0000963)
5	NRPS-T1PKS	Azicemicin <sup>41</sup> (13%) (BGC0000202)
6	NRPS-T1PKS	
7	Enediyne	Tiancimycin <sup>42</sup> (19%) (BGC0001378)
8	AHBA BGC	Rifamycin <sup>43</sup> (35%) (BGC0000137)
9	T1PKS	Chlorizidine A <sup>44,45</sup> (7%) (BGC0001172)
10	Lanthipeptide	-

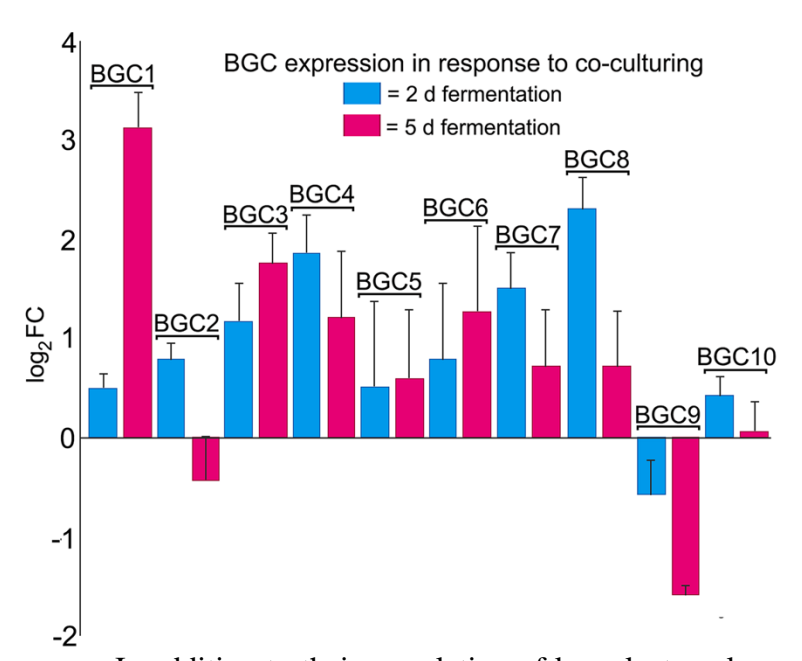


Figure 2-5: Global changes in BGC expression profiles in cocultured WMMB235 shown as logarithm of the fold change (FC) with base 2. The RPKMO over all the ORFs annotated by PRISM for each cluster were used to calculate the overall FCs. BGC numbers correlating to Table 2-1 are above each relevant bar and expression profiles were obtained following 2d (blue) or 5d (purple) fermentations. N=3.

In addition to their correlation of kyc cluster elements (transcripts and protein levels) to the production and structure of **1**, transcriptomics on the WMMB235 revealed that many other putative BGCs (annotated using PRISM) undergo transcriptomic changes in response to co-culture with *Rhodococcus* sp. WMMA185. These included, as summarized in Table 2-1, several hybrid NRPS-Type I PKS gene clusters (BGCs4, 5, 6, 8), a type II PKS (BGC3), an AT-less Type I PKS (BGC2), and clusters encoding a putative enediyne (BGC7) and lanthipeptide (BGC10). Impressively, of the 10 putative BGCs identified, nine were positively impacted by the presence of WMMA185 during fermentation and of these, *kyc* was the dominantly impacted cluster (Figure 2-5). This transcriptomics finding was especially interesting since all 10 BGCs, except for *kyc* which had 79% similarity to aclacinomycin, had little similarity to known clusters in the MIBiG repository, making them orphan clusters (Table 2-1); tentative mapping of BGCs 2–10 showed the presence of *luxR orfs* embedded within BGCs 3 and 8. These findings bolstered our hypothesis that new chemical scaffolds are yet to be found in WMMB235 and that co-culturing, may enable a host of new natural product discoveries.

Co-culturing WMMB235 with WMMA185 appeared to impair transcription for only two BGCs within the WMMB235 genome, BGC 2, a Type I PKS–NRPS hybrid with a trans acyltransferase (AT) domain, and BGC9, which is a Type I PKS. The closest homologous cluster for BGC2 was that of leinamycin<sup>35–37</sup> (MIBiG: BGC0001101) with only 15% similarity. This cluster, in particular was interesting as its expression was enhanced early on during co-culturing but was then slightly repressed by day 5. Perhaps most interesting about this finding was that, of the BGC2 orfs suppressed in co-culture at day 5, those involving transport were the most strongly represented. Though further studies await, we envisioned that diminished transporter production with respect to BGC2 may represent some form of defense by way of restricted extracellular access.

**Table 2-2:** WMMB235-embedded BGC2 genes downregulated upon co-culturing with Rhodococcus sp. WMMA185.

ID	NCBI accession number	Log₂FC Day 5 (Co/Mono)	NCBI Annotation (putative function of the gene product)	Homologue	MiBIG cluster
BFV98 _00820	OHX01627.1	-1.48600927	hypothetical protein	AAN85518.1	BGC0001101
BFV98 _00815	OHX01626.1	-1.41694817	enoyl-CoA hydratase	AAN85519.1	BGC0001101
BFV98 _00940	OHX01649.1	-1.24897815	ABC transporter	AAN85531.1	BGC0001101
BFV98 _00860	OHX01634.1	-1.20094237	ABC transporter	AAP85349.1	BGC0000233
BFV98 _00865	OHX01635.1	-1.18908439	ABC transporter	AAG32068.1	BGC0000026
BFV98 _00925	OHX01646.1	-1.1046561	ABC transporter substrate- binding protein	AAN85534.1	BGC0001101
BFV98 _00915	OHX01644.1	-1.07446882	polyketide β-ketoacyl:ACP synthase	ADI59526.1	BGC0001091
BFV98 _00910	OHX01643.1	-1.07396388	phosphopantetheine-binding protein	AAW33973.1	BGC0000255

BGC9 was the smallest BGC identified of the 10 found in the WMMB235 genome and was a Type I PKS with only 7% similarity to any known BGC - Chlorizidine A (MIBiG:

BGC0001172) (Table 2-1). For BGC2, eight genes had >1 log negative fold change (Table 2-2) on day 5, which notably included all the transporter genes. For BGC9, *orf* downregulation was prominent and consistent over the full course of co-culture fermentation. BGC9 suppression, as reflected by Figure 2-5 was dramatic relative to all other BGCs noted. A point-by-point assessment of specific *orfs* within BGC9 that were negatively impacted by co-culturing is shown by Table 2-3. Unlike the BGC2 case, there was no one group or type of gene that bore the brunt of downregulation although it was clear that elements of the PKS machinery for BGC9 were clearly impacted by co-culturing. We posited that this may simply be a random event or, more enticingly, this may represent one means by which WMMB235 turned down production of a BGC9 encoded product. This may benefit the organism by allowing raw materials to be more wisely used given the competitive conditions of co-culturing, or it may be a direct means of self-defense.

Analysis of the WMMB235 genome alluded to the fact that this organism may employ LuxR-based quorum sensing systems in embedded BGCs (Chapter 3). BGC8 (Figures 2-5, 2-6) was found to contain 184.203 kbp of information and to encode for a hybrid NRPS - Type I PKS cluster with 22 modules and with 3-amino-5-hydroxy benzoic acid (AHBA) as a predicted substrate in one of the synthetase/ligase domains (Appendix). A large group of natural products in the family of ansamycins, mitomycins and saliniketals utilized AHBA as a precursor <sup>46</sup> although BGC8 was only 35% similar to the closest ansamycin BGC of rifamycin (MIBiG: BGC0000137). Interestingly, it contained two *luxR* genes both of which code for products with 36% similarity to GdmRII (ABI93788.1). GdmRI and GdmRII are known homologs of LuxR proteins that positively regulate the production of geldanamycin in *Streptomyces hygroscopicus* 17997. <sup>47</sup> This suggested that BGC8, in addition to *kyc*, may also be regulated using small molecule inducers. Notably, although BGC8 was an orphan cluster, similar clusters were present in other *Micromonospora* spp.

such as *Micromonospora* sp. strain B006.<sup>48</sup> Finally, it warranted noting that, besides *kyc* and BGC 8, these transcriptomics studies revealed the presence of two *luxR* genes within the Type II PKS-encoding BGC 3. It was clear that WMMB235 embedded BGCs harbored the potential to widely exploit LuxR-based QS pathways, presumably to regulate secondary metabolism in response to assorted cellular challenges.

**Table 2-3:** WMMB235-embedded BGC9 genes downregulated upon co-culturing with Rhodococcus sp. WMMA185.

ID	NCBI accession number	Log₂FC Day 5 (Co/Mono)	NCBI Annotation (putative function of the gene product)	Homologue	MiBIG Cluster
BFV98 _26800	OHX06338.1	-2.14562736	acyl carrier protein (ACP)	AHA12082.1	BGC0001172
BFV98 _26795	OHX06337.1	-1.92477769	β-ketoacyl-ACP synthase II	CUI25675.1	BGC0001353
BFV98 _26855	OHX06349.1	-1.89956036	pyruvate dehydrogenase (acetyl-transferring)- homodimeric type	A0R0B0.1	-
BFV98 _26790	OHX06336.1	-1.70957738	hypothetical protein	A3Q339.1	-
BFV98 _26830	OHX06344.1	-1.44829961	copper resistance protein CopC	Q56797.1	-
BFV98 _26805	OHX06339.1	-1.27058731	3-oxoacyl-ACP synthase	CBW54661.1	BGC0000971
BFV98 _26835	OHX06345.1	-1.24636114	tRNA-synthetase class I	CAG14955.2	BGC0000253
BFV98 _26810	OHX06340.1	-1.10536628	biotin attachment protein	AJO72737.1	BGC0001381
BFV98 _26775	OHX06333.1	-1.07607101	hypothetical protein	-	-

# **Changes in global KEGG categorization**

Analysis of transcriptomics and genomics data for WMMB235 monocultures versus WMMB235/WMMA185 co-cultures using Kyoto Encyclopedia of Genes & Genomes (KEGG)

software revealed further insight into changes that occurred within WMMB235 during co-culture and that likely have a bearing on the expression of the *kyc* and other BGCs and their products.

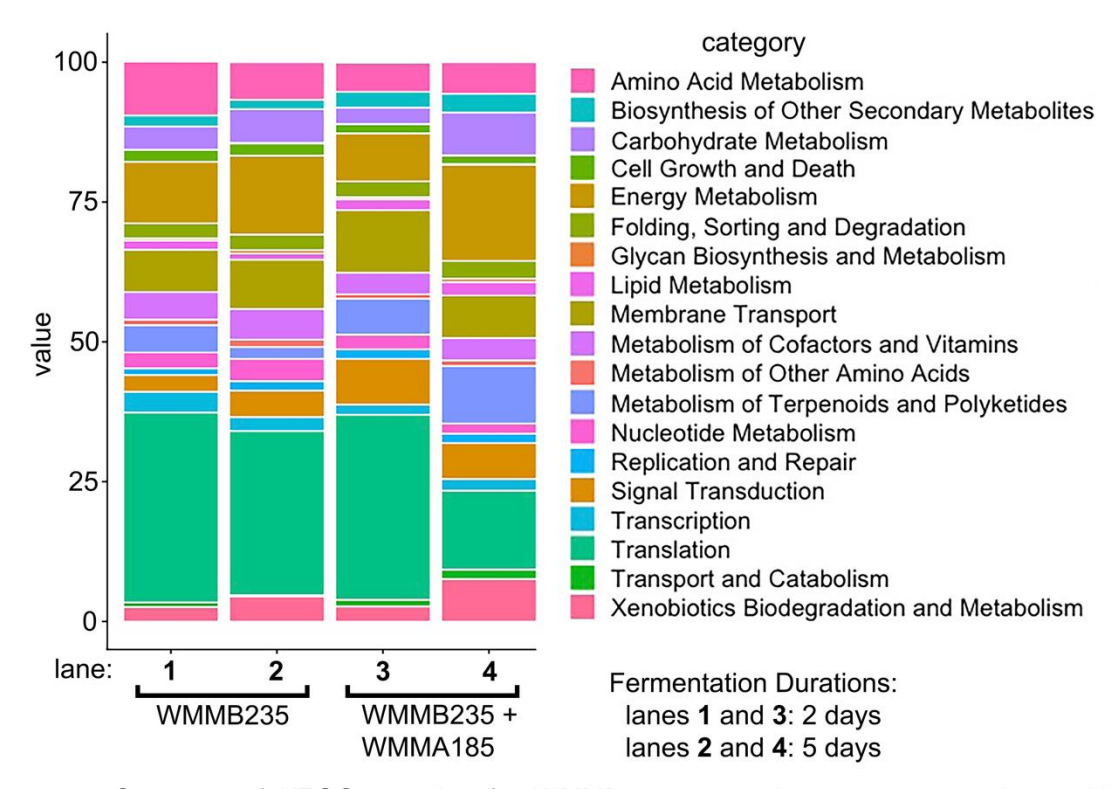


**Figure 2-6.** Summary of KEGG mapping for WMMB235 monoculture versus co-culture with WMMA185. Lane contents are shown by combination of bracketing and lane coding below the categories listing. Co-culturing and duration of fermentations both impact gene expression within WMMB235. Categories of function not abundant enough to depict graphically involved cell communication, cell motility, and signal molecules and interaction. All other categories are depicted in one or more of lanes 1–4.

As reflected in Figure 2-6, significant shifts were seen based on the duration of fermentation (2d vs. 5d) as well as the presence or absence of WMMA185. Particularly interesting were the significant increases in carbohydrate metabolism, energy metabolism and metabolism of terpenoids and polyketides observed in co-culture at day 5 (Figure 2-6, lane 4). Perhaps also noteworthy was the apparent reduction in translational capacity at day 5 in co-culture relative to WMMB235 monoculture. Notably, these changes were reflective of altered gene expression with respect to the whole WMMB235 genome and most certainly encompass changes that have a bearing on keyicin production. Indeed, it was likely that the results of these KEGG studies could

be understood, in part, by the transcriptomics changes depicted in Figure 2-5. In essence, the results showed in Figures 2-5 and 2-6 were clearly related; whereas Figure 2-5 conveyed *kyc* cluster specific changes, Figure 2-6 provided a more global view of how WMMB235 genome readout and processing change in response to co-culturing with WMMA185.

The detailed investigations into WMMB235 shed considerable light on the biosynthetic potential and regulation of BGCs within the organism. However, unlike *Streptomyces* spp.,<sup>49</sup> genetic manipulation of *Micromonospora* sp. was neither well documented nor well understood. But the exciting ramifications of manipulating the biosynthetic and regulatory machinery in a *Micromonospora* sp. made it necessary to explore this possibility further.

#### Investigation into Micromonospora aurantiaca

AntiSmash analysis of the *kyc* cluster provided information on other putative BGCs that existed in closely related organisms and were homologous to *kyc*. From this, we identified a gene cluster housed in the ATCC strain of *Micromonospora aurantiaca* where 98% of the genes showed similarity with *kyc*. In depth study of the *M. aurantiaca* genome indeed showed that the two gene clusters had full synteny and high nucleotide identity, although the order of genes was reversed (Figure 2-7). The genome of *M. aurantiaca* was sequenced nearly a decade ago, and as a result it has superior annotation through the automatic NCBI annotation pipelines. It has close similarity to an organism that were genetically engineered to produce secondary metabolites.<sup>50</sup> This was exciting since *M. aurantiaca* could prove to be more amenable to genetic manipulation and further study using molecular biology tools.

To analyze whether the regulatory mechanism of the *kyc*-like BGC within *M. aurantiaca* was similar to that in WMMB235, we first tested if this bacterium could produce keyicin. We

found that just like in WMMB235, *kyc* was silent in this strain – attested by the fact that no keyicin was detected in 500 μL microscale or 100 mL cultures over a period of 14 days using LC/MS. Consequently, we studied the impact of co-culturing with WMMA185 on *M. aurantiaca*'s ability to produce keyicin. In microscale culture, two out of three replicates showed positive results commensurate with the hypothesis that both species regulated the keyicin BGC similarly.

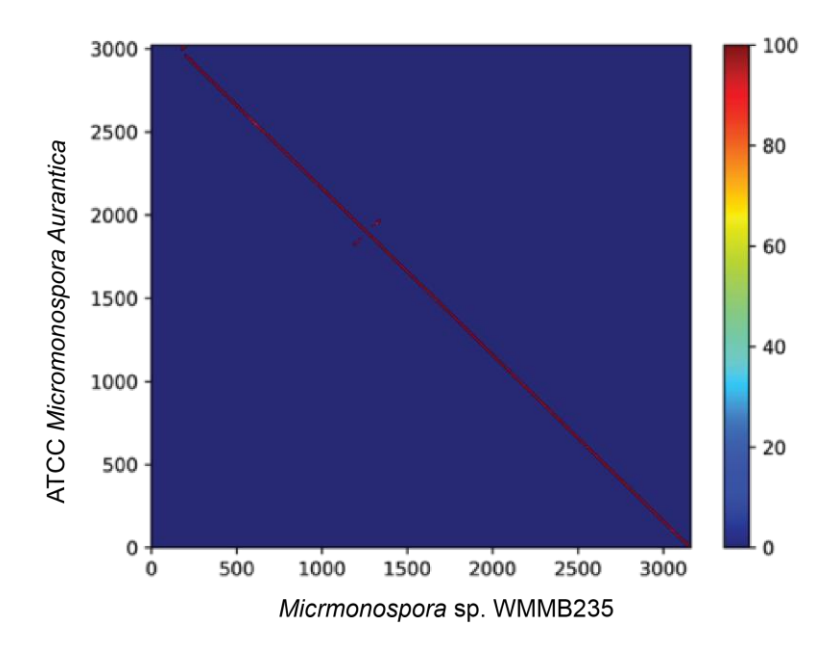


**Figure 2-7:** Dot plot of the clusters *kyc* from *Micromonospora* sp. versus the putative cluster from ATCC strain of *Micromonospora Aurantiaca*, showing perfect alignment between each other.

## 2.3 Conclusion

In sum, the ability to track transcriptomic and proteomic information in relation to WMMB235/WMMA185 co-culture and subsequent keyicin production shed significant insight into the activation of *kyc*, an otherwise silent BGC. The correlation of these omics data and keyicin biosynthesis supported the notion that, by comparing BGC host transcriptomes, proteomes and metabolomes between monoculture and co-culture scenarios, the identification of biosynthetic bottlenecks in monoculture as well as strategies by which to circumvent or overcome such

bottlenecks is readily feasible. Our findings suggested that monocultured WMMB235 suffers from one or more transcriptionally-based bottlenecks with respect to keyicin assembly. This logic was apparent when comparing transcriptomic and proteomic profiles of WMMB235 monoculture versus WMMB235/WMMA185 (or related) systems. At the same time, delineating possible regulatory differences in mono and co-cultures is envisioned to expand our understanding of microbial combinations able to activate cryptic BGCs.

# 2.4 Methods:

# **Transcriptomics**

WMMA185 and WMMB235 were grown in monoculture and co-culture as described before in triplicate. Aliquots of 1.5 mL were taken from day 2 and day 5 for each sample and frozen at -80°C. At the end of the experiment, the samples were thawed and centrifuged to collect the cell mass. Cells were lysed by freezing the samples in liquid nitrogen and mechanically breaking it down in a mortar and pestle. The RNA was extracted using RNAeasy Plus Mini Kit according to manufacturer's instructions (Appendix) and sent to UW-Madison Biotech Center for sequencing, quality control and read mapping. Briefly, the ribosomal RNA was depleted using Ribo-Zero rRNA removal kit (Epicentre) and TruSeq Total RNA v2 Illumina library was prepared. The samples were subjected to Illumina HiSeq 2500 at 1x100bp read length. Extensive QC was conducted on the resultant sequencing data (SI) showed high quality reads. The filtered RNA sequences were aligned with Bowtie 2<sup>51</sup> to contigs in the WMMB235 assembly using the end-to-end alignment options "-very-sensitive -no-discordant -no-unal". The WMMB235 assembly was annotated with Prokka<sup>52</sup> and normalized reads per kbp of gene per million (RPKM) reads was calculated for each ORF annotated. Differential gene expression for RNA-Seq results from day 5

was analyzed using EdgeR with GLM after alignment of each of the two species WMMB235 and WMMA185 to a 'hybrid' genome created from both. Functional Kyoto Encyclopedia of Genes and Genomes (KEGG) categories were assigned to the predicted protein sequences for WMMB235 using MEGAN<sup>53</sup> using previously described methods.<sup>54</sup> KEGG trees were uncollapsed two levels in MEGAN and all assignments except for "organismal systems" and "human diseases" were exported to .csv file (with the columns "read name" and "KEGG name"). Calculated RPKM values and the MEGAN .csv table were used to calculate proportions of the WMMb235 transcriptome that corresponded to each KEGG category.

#### **Proteomics**

WMMA185 was grown in 100 mL culture in triplicate in ASW-D media for a period of 5 days. The content of each of these culture flasks was then vacuum filtered through 0.2 μm PES filters (Thermo Scientific<sup>TM</sup> Nalgene<sup>TM</sup> Rapid-Flow<sup>TM</sup> Sterile Disposable Filter Units) and transferred to three new flasks. These were inoculated with WMMB235 and incubated in a shaker. Aliquots after 5 and 8 days of culture were taken and frozen in -80C freezer. The cells were lysed using a lysis buffer (10 mL) containing 8 M urea (4.8048 g), 50 mM Tris Base (60.57 mg), 5 mM CaCl2 (5.5 mg), 20 mM NaCl (17.5 mg), 1 EDTA-free Roche protease inhibitor tablet (11836170001), 1 Roche PhosSTOP phosphatase inhibitor tablet (04906845001) and 25 μL of 12.1 N HCl (to make pH ~8). To 100 μl of cell lysate 500 μl of lysis buffer was added. This was vortexed and subsequently sonicated with a probe sonicator by applying twelve 15 second pulses at 50% amplitude, each followed by a 30 second rest period. Care was taken to ensure the sample was kept cold. The sample then underwent trypsin digestion using 2 μg of trypsin and incubating

for 18 hours at 37° C. Subsequently, the samples were labelled using Dileu (SI), following published protocol.<sup>55</sup>

Labeled day 5 or day 8 bacterial peptides were combined respectively as 6-plex mixtures. The mixtures were purified by strong cation exchange liquid chromatography (SCX LC) with a PolySULFOETHYL A column (200mm  $\times$  2.1 mm, 5  $\mu$ m, 300 Å, PolyLC, Columbia, MD). Elutes containing labeled peptides were collected by a FC-4 fraction collector (Rainin Dynamax) and dried under vacuum. Samples were then fractioned with a Kinetex C18 column (5  $\mu$ m, 100 Å, Phenomenex, Torrance, CA) at pH=10 into 8 fractions. Each fraction was dried under vacuum for several times.

Peptides in each fraction was reconstituted in 0.1% Formic Acid (FA) and subjected to reversed phase LC-MS/MS analysis with an Orbitrap Fusion Lumos Tribrid mass spectrometer (Thermo Fisher Scientific, San Jose, CA) interfaced with a Dionex Ultimate 3000 UPLC system (Thermo Fisher Scientific, San Jose, CA). Peptides were loaded onto a 75  $\mu$ m inner diameter micro capillary column custom-packed with 15 cm of Bridged Ethylene Hybrid C18 particles (1.7  $\mu$ m, 130 Å, Waters). Labeled peptide were separated with a 120min gradient from 3% to 30% ACN with 0.1% FA, followed by 10 min to 75% ACN and then 10 min to 95% ACN. After that, the column was equilibrated at 3% ACN for 15 min to prepare for the next injection. Survey scans of peptide precursors from 350 to 1500 m/z were performed at a resolving power of 60K and an AGC target of 2×105 with a maximum injection time of 100 ms. The top 20 intense precursor ions were selected and subjected to the HCD fragmentation at a normalized collision energy of 27% followed by tandem MS acquisition at a resolving power of 30K and an AGC target of 5×104, with a maximum injection time of 54 ms and a lower mass limit of 110 m/z. Precursors were subjected to a dynamic exclusion of 45s with a 10 ppm mass tolerance.

Raw files were processed with PEAKS Studio (Bioinformatics Solutions Inc., Waterloo, ON, Canada). Trypsin was selected as the enzyme with the maximum two missed cleavages. Spectra were first annotated by de novo sequencing then searched by PEAKS 7.0 against a transcriptome predicted protein database for WMB235, where the parent mass error tolerance was set to be 25.0 ppm and fragment mass tolerance was 0.3 Da. Fixed modifications included DiLeu labels on peptide *N*-termini and lysine residues (+145.12801 Da) and carbamidomethylation on cysteine residues (+57.02146 Da). Dynamic modifications included oxidation of methionine residues (+15.99492 Da), deamidation of asparagine and glutamine residues (+0.98402 Da). Quantitation was performed with a reporter ion integration tolerance of 20 ppm with the peptide score threshold of 20.0. Protein quantitative ratios were calculated using unique peptides. Reporter ion ratios for protein groups were exported to Excel workbook and Student t-test was performed with biological triplicates. Proteins that had >50%-fold change and p<0.05 were filtered as significantly changed.

#### **Metabolomics**

WMMB235 and WMMA185 cultures grown in triplicate for transcriptomics analysis were allowed to grow for 14 days and were also used to collect aliquots of 1.5 mL for metabolomic analyses. The collected samples were processed using solid phase extraction and analyzed using UHPLC/UV/qTOF-HRESI-MS/MS.<sup>16,56</sup> Briefly, solubilized extracts in 10:1 H<sub>2</sub>O: MeOH were subjected to automated SPE using a Gilson GX-271 liquid handling system. Briefly, extracts were loaded onto EVOLUTE ABN SPE cartridges (25 mg absorbent mass, 1 mL reservoir volume; Biotage, S4 Charlotte, NC), washed with water and eluted with MeOH (500 μL) directly into an LC/MS-certified vial. LC/MS data were acquired using a Bruker MaXis ESI-qTOF mass spectrometer (Bruker, Billerica, MA) coupled with a Waters Acquity UPLC system (Waters,

Milford, MA) operated by Bruker Hystar software. Chromatographic separations were achieved with a gradient of MeOH and H2O (containing 0.1% formic acid) on an RP C-18 column (Phenomenex Kinetex 2.6µm, 2.1 x 100 mm; Phenomenex, Torrance, CA) at a flow rate of 0.3 mL/min. The method was as follows: 1-12 min (10%-97% MeOH in H<sub>2</sub>O) and 12-14 min (97% MeOH). Full scan mass spectra (m/z 150–1550) were measured in positive ESI mode. The mass spectrometer was operated using the following parameters: capillary, 4.5 kV; nebulizer pressure, 1.2 bar; dry gas flow, 8.0 L/min; dry gas temperature, 205 °C; scan rate, 2 Hz. Tune mix (ESI-L low concentration; Agilent, Santa Clara, CA) was introduced through a divert valve at the end of each chromatographic run for automated internal calibration. The full scan spectra were followed by MS/MS spectra acquisition at variable scan speed ranging from 0.5 Hz to 2 Hz. CID energy varied linearly from 30, 25, 20 eV for 500 m/z 50, 40, 35 eV for 1000 m/z and 70, 50, 45 eV for 2000 m/z for charge states of 1, 2 and 3 respectively and had a mass range of 500 m/z to 1500 m/z. The precursor list was set to exclude precursor ions for 1.00 min after 3 spectra with the same precursor ion have been acquired. Bruker DataAnalysis 4.2 software was used for analysis of chromatograms and to convert MS/MS data from .d files to mzXML. These files were then uploaded to the Mass Spectrometry Interactive Virtual Environment (MASSive) server (https://massive.ucsd.edu/ProteoSAFe/static/massive.jsp) and networked using the GNPS pipeline.<sup>29</sup> Parent ions with at least three fragments were considered in the network. A cosine similarity score of 0.7 for the fragmentation spectra was used. The resulting networks were visualized using Cytoscape 3.5.1 (www. cytoscape.org/cy3.html).<sup>30</sup> The network containing parent ions representative of keyicin (m/z 805.34 and 797.35) was extracted and further analyzed. For each of the ion in the network, the AUC was calculated from the corresponding LC-MS data using the integrate method in the DataAnalysis software. These values were analyzed in Cytoscape to color the nodes using continuous mapping color for each day.

# 2.5 References

- (1) Ziemert, N.; Alanjary, M.; Weber, T. The Evolution of Genome Mining in Microbes a Review. *Nat. Prod. Rep.* **2016**, *33* (8), 988–1005.
- (2) Machado, H.; Tuttle, R. N.; Jensen, P. R. Omics-Based Natural Product Discovery and the Lexicon of Genome Mining. *Curr. Opin. Microbiol.* **2017**, *39*, 136–142.
- (3) Weber, T. In Silico Tools for the Analysis of Antibiotic Biosynthetic Pathways. *Int. J. Med. Microbiol.* **2014**, *304*, 230–235.
- (4) Hertweck, C. Hidden Biosynthetic Treasures Brought to Light. *Nat. Chem. Biol.* **2009**, *5* (7), 450–452.
- (5) Udwary, D. W.; Zeigler, L.; Asolkar, R. N.; Singan, V.; Lapidus, A.; Fenical, W.; Jensen, P. R.; Moore, B. S. Genome Sequencing Reveals Complex Secondary Metabolome in the Marine Actinomycete Salinispora Tropica. Proc. Natl. Acad. Sci. U. S. A. 2007, 104 (25), 10376–10381.
- (6) Fenical, W.; Jensen, P. R. Developing a New Resource for Drug Discovery: Marine Actinomycete Bacteria. *Nat. Chem. Biol.* **2006**, *2* (12), 666–673.
- (7) Abdelmohsen, U. R.; Grkovic, T.; Balasubramanian, S.; Kamel, M. S.; Quinn, R. J.; Hentschel, U. Elicitation of Secondary Metabolism in Actinomycetes. *Biotechnol. Adv.* 2015, 33 (6), 798–811.
- (8) Gross, H. Strategies to Unravel the Function of Orphan Biosynthesis Pathways: Recent Examples and Future Prospects. *Appl. Microbiol. Biotechnol.* **2007**, *75* (2), 267–277.
- (9) Scherlach, K.; Hertweck, C. Triggering Cryptic Natural Product Biosynthesis in Microorganisms. **2009**.
- (10) Bentley, S.; Chater, K.; Cerdeño-Tárraga, a-M.; Challis, G. L.; Thomson, N. R.; James, K. D.; Harris, D. E.; Quail, M. a; Kieser, H.; Harper, D.; et al. Complete Genome Sequence of the Model Actinomycete Streptomyces Coelicolor A3(2). *Nature* 2002, 417 (6885), 141–147.
- (11) Rateb, M. E.; Hallyburton, I.; Houssen, W. E.; Bull, A. T.; Goodfellow, M.; Santhanam, R.; Jaspars, M.; Ebel, R. Induction of Diverse Secondary Metabolites in Aspergillus Fumigatus by Microbial Co-Culture. *RSC Adv.* **2013**, *3* (34), 14444.
- (12) Bertrand, S.; Bohni, N.; Schnee, S.; Schumpp, O.; Gindro, K.; Wolfender, J.-L. Metabolite

- Induction via Microorganism Co-Culture: A Potential Way to Enhance Chemical Diversity for Drug Discovery. *Biotechnol. Adv.* **2014**, *32* (6), 1180–1204.
- (13) Kurosawa, K.; Ghiviriga, I.; Sambandan, T. G.; Lessard, P. A.; Barbara, J. E.; Rha, C.; Sinskey, A. J. Rhodostreptomycins, Antibiotics Biosynthesized Following Horizontal Gene Transfer from Streptomyces Padanus to Rhodococcus Fascians. *J. Am. Chem. Soc.* 2008, 130 (4), 1126–1127.
- (14) Cueto, M.; Jensen, P. R.; Kauffman, C.; Fenical, W.; Lobkovsky, E.; Clardy, J. Pestalone, a New Antibiotic Produced by a Marine Fungus in Response to Bacterial Challenge. *J. Nat. Prod.* **2001**, *64* (11), 1444–1446.
- (15) Pishchany, G.; Mevers, E.; Ndousse-Fetter, S.; Horvath, D. J.; Paludo, C. R.; Silva-Junior, E. A.; Koren, S.; Skaar, E. P.; Clardy, J.; Kolter, R.; et al. Amycomicin Is a Potent and Specific Antibiotic Discovered with a Targeted Interaction Screen. *Proc. Natl. Acad. Sci. U. S. A.* 2018, 115 (40), 10124–10129.
- (16) Adnani, N.; Chevrette, M. G.; Adibhatla, S. N.; Zhang, F.; Yu, Q.; Braun, D. R.; Nelson, J.; Simpkins, S. W.; McDonald, B. R.; Myers, C. L.; et al. Coculture of Marine Invertebrate-Associated Bacteria and Interdisciplinary Technologies Enable Biosynthesis and Discovery of a New Antibiotic, Keyicin. ACS Chem. Biol. 2017, 12 (12), 3093–3102.
- (17) Adnani, N.; Braun, D. R.; McDonald, B. R.; Chevrette, M. G.; Currie, C. R.; Bugni, T. S. Complete Genome Sequence of Rhodococcus Sp. Strain WMMA185, a Marine Sponge-Associated Bacterium. *Genome Announc.* **2016**, *4* (6), e01406-16.
- (18) Adnani, N.; Braun, D. R.; Mcdonald, B. R.; Chevrette, M. G.; Currie, C. R.; Bugni, T. S. Draft Genome Sequence of Micromonospora Sp. Strain WMMB235, a Marine Ascidian-Associated Bacterium Downloaded From. 2019, 5, 1369–1385.
- (19) Mandlik, A.; Livny, J.; Robins, W. P.; Ritchie, J. M.; Mekalanos, J. J.; Waldor, M. K. RNA-Seq-Based Monitoring of Infection-Linked Changes in Vibrio Cholerae Gene Expression. *Cell Host Microbe* **2011**, *10* (2), 165–174.
- (20) Robinson, M. D.; McCarthy, D. J.; Smyth, G. K. EdgeR: A Bioconductor Package for Differential Expression Analysis of Digital Gene Expression Data. *Bioinformatics* 2010, 26 (1), 139–140.
- (21) Frost, D. C.; Rust, C. J.; Robinson, R. A. S.; Li, L. Increased *N,N* -Dimethyl Leucine Isobaric Tag Multiplexing by a Combined Precursor Isotopic Labeling and Isobaric Tagging

- Approach. Anal. Chem. 2018, 90 (18), 10664–10669.
- (22) Lu, W.; Leimkuhler, C.; Oberthür, M.; Kahne, D.; Walsh, C. T. AknK Is an L-2-Deoxyfucosyltransferase in the Biosynthesis of the Anthracycline Aclacinomycin A †. **2004**.
- (23) Garrido, L. M.; Lombó, F.; Baig, I.; Nur-e-Alam, M.; Furlan, R. L. A.; Borda, C. C.; Braña, A.; Méndez, C.; Salas, J. A.; Rohr, J.; et al. Insights in the Glycosylation Steps during Biosynthesis of the Antitumor Anthracycline Cosmomycin: Characterization of Two Glycosyltransferase Genes. *Appl. Microbiol. Biotechnol.* **2006**, *73* (1), 122–131.
- (24) Torkkell, S.; Kunnari, T.; Palmu, K.; Hakala, J.; Ma¨ntsa¨la¨, P.; Ma¨ntsa, M.; Ma¨ntsa¨la, M.; Ma¨ntsa¨la¨, M.; Ylihonko, K. Identification of a Cyclase Gene Dictating the C-9 Stereochemistry of Anthracyclines from Streptomyces Nogalater. *Antimicrob. Agents Chemother.* 2000, 44 (2), 396–399.
- (25) Torkkell, S.; Kunnari, T.; Palmu, K.; Maè, P.; Hakala, J.; Ylihonko, K. The Entire Nogalamycin Biosynthetic Gene Cluster of Streptomyces Nogalater: Characterization of a 20-Kb DNA Region and Generation of Hybrid Structures. *Mol Genet Genomics* 2001, 266, 276–288.
- (26) Yoshimoto, A.; Johdo, O.; Takatsuki, Y.; Ishikura, T.; Sawa, T.; Takeuchi, T.; Umezawa, H. New Anthracycline Antibiotics Obtained by Microbial Glycosidation of .BETA.-Isorhodomycinone and .ALPHA.2-Rhodomycinone. *J. Antibiot. (Tokyo).* 1984, 37 (8), 935–938.
- (27) Matsuzawa, Y.; Yoshimoto, A.; Oki, T.; Naganawa, H.; Takeuch, T.; Umezawa, H. Biosynthesis of Anthracycline Antibiotics by Streptomyces Galilaeus. II. Structure of New Anthracycline Antibiotics Obtained by Microbial Glycosidation and Biological Activity. *J. Antibiot. (Tokyo).* **1980**, *33* (11), 1341–1347.
- (28) Oki, T.; Yoshimoto, A.; Matsuzawa, Y.; Takeuchi, T.; Umezawa, H. Biosynthesis of Anthracycline Antibiotics by Streptomyces Galilaeus. I. Glycosidation of Various Anthracyclinones by an Aclacinomycin-Negative Mutant and Biosynthesis of Aclacinomycins from Aklavinone. *J. Antibiot. (Tokyo).* **1980**, *33* (11), 1331–1340.
- Wang, M.; Carver, J. J.; Phelan, V. V; Sanchez, L. M.; Garg, N.; Peng, Y.; Nguyen, D.-T.
   D. D.; Watrous, J.; Kapono, C. A.; Luzzatto-Knaan, T.; et al. Sharing and Community
   Curation of Mass Spectrometry Data with Global Natural Products Social Molecular

- Networking. Nat. Biotechnol. 2016, 34 (8), 828–837.
- (30) Shannon, P.; Markiel, A.; Ozier, O.; Baliga, N. S.; Wang, J. T.; Ramage, D.; Amin, N.; Schwikowski, B.; Ideker, T. Cytoscape: A Software Environment for Integrated Models of Biomolecular Interaction Networks. *Genome Res* **2003**, *13* (Karp 2001), 2498–2504.
- (31) Weber, T.; Blin, K.; Duddela, S.; Krug, D.; Kim, H. U.; Bruccoleri, R.; Lee, S. Y.; Fischbach, M. A.; Müller, R.; Wohlleben, W.; et al. AntiSMASH 3.0—a Comprehensive Resource for the Genome Mining of Biosynthetic Gene Clusters. *Nucleic Acids Res.* **2015**, 43 (W1), W237–W243.
- (32) Medema, M. H.; Fischbach, M. A. Computational Approaches to Natural Product Discovery. *Nat. Chem. Biol.* **2015**, *11* (9), 639–648.
- (33) Cimermancic, P.; Medema, M. H.; Claesen, J.; Kurita, K.; Wieland Brown, L. C.; Mavrommatis, K.; Pati, A.; Godfrey, P. A.; Koehrsen, M.; Clardy, J.; et al. Insights into Secondary Metabolism from a Global Analysis of Prokaryotic Biosynthetic Gene Clusters. *Cell* **2014**, *158* (2), 412–421.
- (34) Chung, J.-Y.; Fujii, I.; Harada, S.; Sankawa, U.; Ebizuka, Y. Expression, Purification, and Characterization of AknX Anthrone Oxygenase, Which Is Involved in Aklavinone Biosynthesis in Streptomyces Galilaeus. *J. Bacteriol.* **2002**, *184* (22), 6115–6122.
- (35) Cheng, Y.-Q.; Tang, G.-L.; Shen, B. Identification and Localization of the Gene Cluster Encoding Biosynthesis of the Antitumor Macrolactam Leinamycin in Streptomyces Atroolivaceus S-140. *J. Bacteriol.* **2002**, *184* (24), 7013–7024.
- (36) Cheng, Y.-Q.; Tang, G.-L.; Shen, B. Type I Polyketide Synthase Requiring a Discrete Acyltransferase for Polyketide Biosynthesis. *Proc. Natl. Acad. Sci.* **2003**, *100* (6), 3149–3154.
- (37) Tang, G.-L.; Cheng, Y.-Q.; Shen, B. Leinamycin Biosynthesis Revealing Unprecedented Architectural Complexity for a Hybrid Polyketide Synthase and Nonribosomal Peptide Synthesise. *Chem. Biol.* **2004**, *11* (1), 33–45.
- (38) Zhang, W.; Wang, L.; Kong, L.; Wang, T.; Chu, Y.; Deng, Z.; You, D. Unveiling the Post-PKS Redox Tailoring Steps in Biosynthesis of the Type II Polyketide Antitumor Antibiotic Xantholipin. *Chem. Biol.* **2012**, *19* (3), 422–432.
- (39) Du, L.; Sánchez, C.; Chen, M.; Edwards, D. J.; Shen, B. The Biosynthetic Gene Cluster for the Antitumor Drug Bleomycin from Streptomyces Verticillus ATCC15003 Supporting

- Functional Interactions between Nonribosomal Peptide Synthetases and a Polyketide Synthase. *Chem. Biol.* **2000**, *7* (8), 623–642.
- (40) Galm, U.; Wang, L.; Wendt-Pienkowski, E.; Yang, R.; Liu, W.; Tao, M.; Coughlin, J. M.; Shen, B. In Vivo Manipulation of the Bleomycin Biosynthetic Gene Cluster in Streptomyces Verticillus ATCC15003 Revealing New Insights into Its Biosynthetic Pathway. *J. Biol. Chem.* **2008**, 283 (42), 28236–28245.
- (41) Ogasawara, Y.; Liu, H. Biosynthetic Studies of Aziridine Formation in Azicemicins. *J. Am. Chem. Soc.* **2009**, *131* (50), 18066–18068.
- (42) Ge, H.-M.; Huang, T.; Rudolf, J. D.; Lohman, J. R.; Huang, S.-X.; Guo, X.; Shen, B. Enediyne Polyketide Synthases Stereoselectively Reduce the β-Ketoacyl Intermediates to β- d -Hydroxyacyl Intermediates in Enediyne Core Biosynthesis. *Org. Lett.* 2014, *16* (15), 3958–3961.
- (43) August, P. R.; Tang, L.; Yoon, Y. J.; Ning, S.; Müller, R.; Yu, T.-W.; Taylor, M.; Hoffmann, D.; Kim, C.-G.; Zhang, X.; et al. Biosynthesis of the Ansamycin Antibiotic Rifamycin: Deductions from the Molecular Analysis of the Rif Biosynthetic Gene Cluster of Amycolatopsis Mediterranei S699. *Chem. Biol.* **1998**, *5* (2), 69–79.
- (44) Alvarez-Mico, X.; Jensen, P. R.; Fenical, W.; Hughes, C. C. Chlorizidine, a Cytotoxic 5 *H* -Pyrrolo[2,1- *a*] Isoindol-5-One-Containing Alkaloid from a Marine *Streptomyces* Sp. *Org. Lett.* **2013**, *15* (5), 988–991.
- (45) Mantovani, S. M.; Moore, B. S. Flavin-Linked Oxidase Catalyzes Pyrrolizine Formation of Dichloropyrrole-Containing Polyketide Extender Unit in Chlorizidine A. *J. Am. Chem. Soc.* 2013, 135 (48), 18032–18035.
- (46) Kang, Q.; Shen, Y.; Bai, L.; Gorls, H.; Lin, W. H.; Peschel, G.; Hertweck, C.; Aoki, H.; Imanaka, H.; Speedie, M. K.; et al. Biosynthesis of 3,5-AHBA-Derived Natural Products. *Nat. Prod. Rep.* **2012**, *29* (2), 243–263.
- (47) He, W.; Lei, J.; Liu, Y.; Wang, Y. The LuxR Family Members GdmRI and GdmRII Are Positive Regulators of Geldanamycin Biosynthesis in Streptomyces Hygroscopicus 17997. *Arch Microbiol* **2008**, *189*, 501–510.
- (48) Braesel, J.; Crnkovic, C. M.; Kunstman, K. J.; Green, S. J.; Maienschein-Cline, M.; Orjala, J.; Murphy, B. T.; Eustáquio, A. S. Complete Genome of Micromonospora Sp. Strain B006 Reveals Biosynthetic Potential of a Lake Michigan Actinomycete. *J. Nat. Prod.* 2018, 81

- (9), 2057–2068.
- (49) Gomez-Escribano, J. P.; Bibb, M. J. Heterologous Expression of Natural Product Biosynthetic Gene Clusters in Streptomyces Coelicolor: From Genome Mining to Manipulation of Biosynthetic Pathways. J. Ind. Microbiol. Biotechnol. 2014, 41 (2), 425– 431.
- (50) Sakai, A.; Mitsumori, A.; Furukawa, M.; Kinoshita, K.; Anzai, Y.; Kato, F. Production of a Hybrid 16-Membered Macrolide Antibiotic by Genetic Engineering of Micromonospora Sp. TPMA0041. J. Ind. Microbiol. Biotechnol. 2012, 39 (11), 1693–1701.
- (51) Langmead, B.; Salzberg, S. L. Fast Gapped-Read Alignment with Bowtie 2. *Nat. Methods* **2012**, *9* (4), 357–359.
- (52) Seemann, T. Prokka: Rapid Prokaryotic Genome Annotation. *Bioinformatics* **2014**, *30* (14), 2068–2069.
- (53) Huson, D. H.; Weber, N. Microbial Community Analysis Using MEGAN. *Methods Enzymol.* **2013**, *531*, 465–485.
- (54) Miller, I. J.; Vanee, N.; Fong, S. S.; Lim-Fong, G. E.; Kwan, J. C. Lack of Overt Genome Reduction in the Bryostatin-Producing Bryozoan Symbiont " Candidatus Endobugula Sertula" *Appl. Environ. Microbiol.* **2016**, 82 (22), 6573–6583.
- (55) Frost, D. C.; Greer, T.; Li, L. High-Resolution Enabled 12-Plex DiLeu Isobaric Tags for Quantitative Proteomics. *Anal. Chem.* **2015**, 87 (3), 1646–1654.
- (56) Adnani, N.; Vazquez-Rivera, E.; Adibhatla, S.; Ellis, G.; Braun, D.; Bugni, T. Investigation of Interspecies Interactions within Marine Micromonosporaceae Using an Improved Co-Culture Approach. *Mar. Drugs* **2015**, *13* (10), 6082–6098.

# Chapter 3: Effects of quorum sensing and small molecule chemical signaling on activation of *kyc*

Portions of this chapter have been submitted to ACS Chemical Biology as:

Acharya, D. D.; Miller I. J.; Cui Y., Braun, D.; Berres M.; Styles, M. J.; Li, L.; Kwan, J.C.; Rajski, S. R.; Blackwell, H. E.; Bugni, T. S. Omics Technologies to Understand Silent Biosynthetic Gene Cluster Activation in *Micromonospora* sp. WMMB235

## 3.1 Introduction

One of the seminal findings in the field of natural products drug discovery is that many of the bacterial biosynthetic gene clusters (BGCs) that code for specialized molecules are in reality, not expressed in the setting in which they are usually studied. But substantial evidence now supports the fact that extracellular communication plays a key role in the expression of genes, including BGCs. In gram negative bacteria, communication commonly occurs via quorum sensing (QS). In fact, the realization that QS among microbial organisms plays a critical role in dictating how microbes govern themselves is one of the most important discoveries in microbiology over the last 20 years. Microbial QS entails the generation of extracellular chemical signals that accumulate in the local environment. Once they reach a threshold concentration (and thus a "quorum" of cells has accrued), the transcription of group-specific genes is activated. Ultimately, these QS-driven changes in transcription constitute the expression of group-beneficial behaviors including virulence and biofilm formation. Accordingly, it comes as no surprise that numerous campaigns to devise new anti-virulence agents have targeted bacterial QS systems.

Thus, it is in this *intraspecies* realm that QS has mostly captured the imagination of drug discovery scientists by influencing microbial secondary metabolic pathways. In short, it is now clear that QS mechanisms offer one means of activating (or "de-repressing") otherwise silent biosynthetic gene clusters (BGCs), leading to the production of new natural products. For instance, elegant work by Hertweck and co-workers revealed the critical role that LuxR-based QS plays in silencing the biosynthesis of thailandamide A lactone in wild-type Burkholderia thailandensis.<sup>3</sup> Subsequent work by Seyedsayamdost and co-workers recently showed that the QS-controlled transcriptional regulator ScmR serves as a global gatekeeper of secondary metabolism in Burkholderia thailandensis E264<sup>11</sup> and a repressor of numerous BGCs. Greenberg and co-workers have shown that QS in B. thailandensis impacts biosynthetic gene clusters that code for the synthesis of malleobactin, malleilactone, quinolones, rhamnolipids and others. <sup>12</sup> Importantly, all of these QS systems are of the LuxI/LuxR class that is typical of Gram-negative bacteria. These systems consist of a LuxI-type synthase that produces a diffusible N-acyl L-homoserine lactone (AHL) signal, and a LuxR-type receptor that binds the AHL and activates transcription of QScontrolled genes. AHLs constitute the extracellular chemical signals by which bacteria communicate en route to self-governance and are well known as LuxR activators and crucial quorum sensing agents. 13–15

Similarly, Gram-positive bacteria are known to have an analogous extracellular signaling mechanisms, as discussed in detail in Chapter 1. Notably, small molecule signals such as A-factor (of the γ-butyrolactone family) and auto-inducing peptides most commonly found in *Streptomyces* sp. are the basis for activation of many important secondary metabolite gene clusters.<sup>2</sup> Recently, other signaling molecules like the butanolides and the furans have been discovered to control biosynthesis of antibiotics in *Streptomyces avermitilis* and *Streptomyces coelicolor*, respectively.<sup>16</sup>

Although our understanding of small molecule induction for activating BGCs have increased over the last few decades, majority of these pathways are based in intraspecies communication. In fact only a few reports exist, that explore the phenomenon by which a bacterial species intercepts a signaling molecule that it does not intrinsically make and subsequently utilizes it to regulate its biosynthetic output.<sup>17</sup>

By extension, the relevance of interspecies associations to BGC activation processes holds tremendous promise and now constitutes an area of active investigation within our laboratory. The activation of otherwise silent or "orphan" biosynthetic gene clusters (BGCs) is a particularly exciting application of chemical signaling pathways since it is now well established that microbial genetic diversity and possibilities far exceed previous expectations with respect to secondary metabolism and the natural product-based drug leads to which they give rise.

From chapter 2 and the work cited therein, it is clear that co-culturing different microbes can activate silent BGCs: co-culturing of *Micromonospora* sp. WMMB235 and a *Rhodococcus* sp. WMMA185, enabled the production of a new glycosylated anthracycline constructed by a large type II PKS, keyicin<sup>18</sup> through transcriptional activation. Despite the excitement and significance of this finding, little is known about how these organisms communicate to generate keyicin. In this chapter, we aim to elucidate the different mechanisms by which keyicin production is initiated. Here, we hypothesize that the metabolites resulting from co-cultures are likely attributable to interspecies QS mechanisms, by a two-part analysis. First, we test the hypothesis that a LuxR homolog, embedded within the keyicin BGC (*kyc*) in WMMB235 dictates keyicin production in a fashion consistent with QS; and second, that small molecule signals produced by WMMA185 direct the activation of *kyc* and therefore production of keyicin.

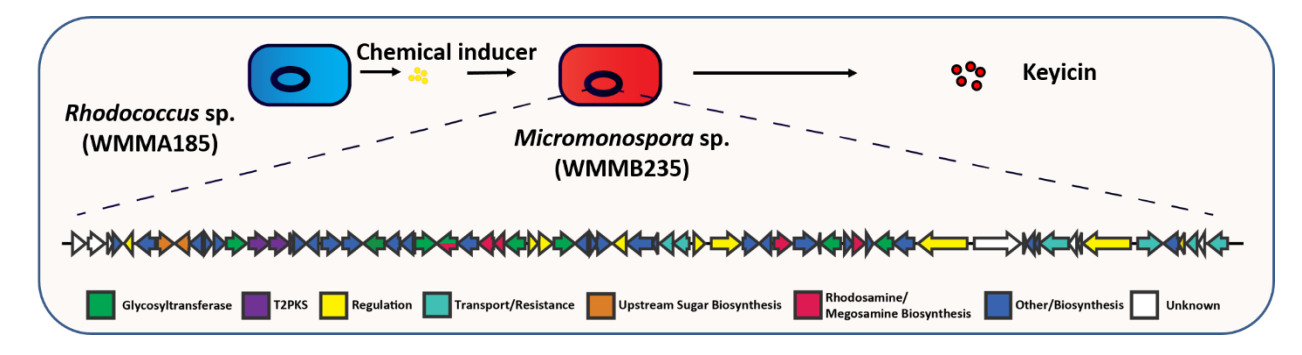


**Figure 3-1.** Schematic of co-culture interactions and subsequent activation of silent BGC *kyc*, by a *Rhodococcus*-derived small molecule.

# 3.2 Results and Discussion

# Keyicin production is small moleculetriggered

Early studies on keyicin production, conducted by Adnani *et al.* in our lab, revealed WMMB235 as the producer of keyicin (1), in co-culture.<sup>18</sup> This conclusion was supported primarily by two key findings. First, was that only WMMB235 harbored a BGC (*kyc*) able to code for all the machinery anticipated to be

necessary for keyicin assembly (Figure 3-1); this was first illuminated using PRISM<sup>19</sup> and AntiSmash<sup>20–22</sup> to process the WMMB235 genome. Both analyses identified *kyc* as an anthracycline type biosynthetic gene cluster housing several glycosyltransferases (GTs) essential to keyicin assembly. Secondly, fermentations in which the two microbial species were separated

with a 0.2 µm cell impermeable membrane led, over time, to inhibit *Rhodococcus* sp. WMMA185 growth and increased keyicin production; this assay highlighted the antibacterial properties of keyicin as well the absence of any required interspecies cell-cell contacts.<sup>18</sup>

Although the above-mentioned assay showed that physical interaction was unnecessary, it did not rule out the possibility that live cells of WMMA185 were needed to facilitate the production of keyicin. Consequently, we carried out experiments to gain further insights into the mechanism of interaction between the two species. We found that keyicin production, as detected by colorimetric analyses (λ<sub>max</sub> = 470 nm) from WMMB235, could be triggered by subjecting WMMB235 to supernatant from monocultured *Rhodococcus* sp. WMMA185. When inoculated into cell free media of a WMMA185 culture grown for 4 days, WMMB235 clearly generated 1 as reflected by production of keyicin's unique chromophore. This result clearly put to rest any possibility that WMMB235 and WMMA185 were involved in a dynamic communication system that required both participants to be alive or active. Moreover, this campaign suggested that WMMA185 produces a small molecule inducer of keyicin biosynthesis even in the absence of WMMB235, bringing to light the prospect that QS may play an important, though not exclusive, role in triggering *kyc* BGC activation.

#### A role for quorum sensing through LuxR in kyc cluster activation?

Our ability to definitively demonstrate that transcriptomic activation of *kyc* within WMMB235 leads to the production of **1**, coupled with the realization that pathway-specific regulators often cluster within or proximal to BGCs,<sup>2</sup> inspired us to search the *kyc* cluster for regulatory gene candidates. From this inquiry was identified, among others, a *luxR* family transcriptional regulator termed herein *kyc5*. Predicated on LuxR's well established and vital role

in QS in assorted microbial systems<sup>4,23,24</sup> we posited that Kyc5 activation (via AHL exposure) may trigger keyicin production. Accordingly, we investigated the impact of established LuxR-selective ligands upon keyicin production. A library of 96 AHLs and related analogs (both natural products and synthetics) were screened for the ability to trigger keyicin production by monocultures of WMMB235.

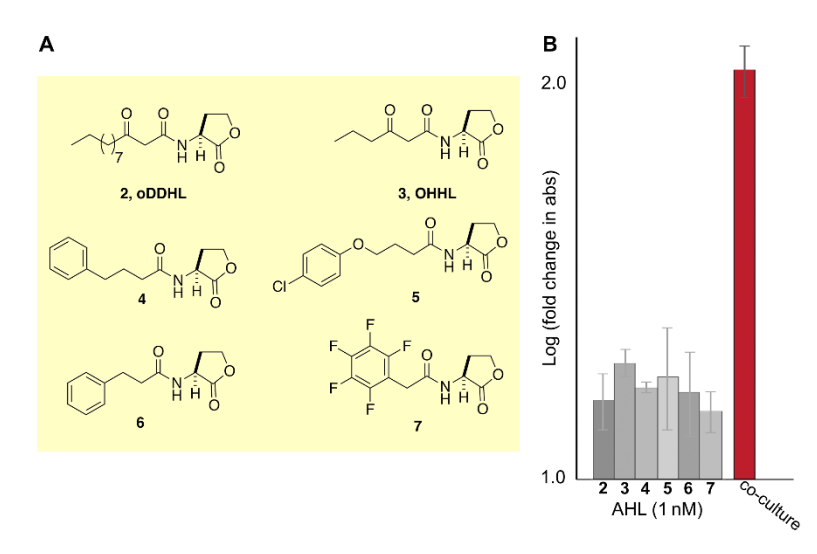


Figure 3-2. AHL inducers of keyicin. (A) Six out of 96 AHLs screened for kyc cluster activation and subsequent keyicin production: 2 and 3 are natural AHLs whereas 4–7 are synthetic. (B) Increase in keyicin production shown as positive log fold change in the absorbance at 470 nm on treatment with AHLs compared to untreated monoculture. Co-culture with WMMA185 shown as positive control (red bar).

A range of putative LuxR ligand concentrations were investigated and, even at the lowest concentration (1 nM), six compounds (Figure 3-2A) were found to activate keyicin production. The fold change in production of 1 was calculated by measuring the absorbance of cell supernatants of WMMB235 spiked with inducers (in DMSO) compared to its monoculture treated with DMSO alone. AHL-triggered keyicin production by WMMB235 was not as pronounced as in the WMMB235/WMMA185 co-culture system (Figure 3-2B), indicating that production of 1 is subject to more than just one regulatory element. This, combined with the absence of any decipherable LuxI homolog in the WMMA185 genome, <sup>25</sup> suggested that the LuxR pathway in the WMMA185/WMMB235 co-culture system may respond to alternative (non-AHL) signals. Alternatively, *kyc* activation may be triggered by an altogether different mechanism. Although *luxI/luxR* are well studied in Gram-negative bacteria, it is only recently that these have been found

not only in Gram-positive bacteria but also other kingdom representatives.<sup>26,27</sup> In fact, several genomic studies across different species have found many QS-related *luxR* type genes that are unpaired to a cognate *luxI* to synthesize the signaling molecule, and thus encode "orphan" LuxR receptors or "solos".<sup>28,29</sup> This supports our hypothesis that an "orphan" luxR in *Micromonospora* sp. may be involved in inter-species communication by interacting with the small molecule signal from *Rhodococcus* sp. It is altogether possible that keyicin production may require pathways in addition to or even instead of LuxR. For instance, efficient production of pyocyanin, a phenazine virulence factor produced by *Pseudomonas aeruginosa* calls upon a total of three separate, but interwoven regulatory systems.<sup>30</sup> The results of Figure 3-2 may reflect a similar scenario, in which LuxR-type signaling plays an important but not exclusive role in *kyc* cluster activation.

# Impact on keyicin production induced by gram-negative bacteria

The results supporting the hypothesis the QS plays a role in inter-species communication between WMMB235 and WMMA185 warranted subsequent orthogonal investigations. Although the co-culture of these bacterial species was inspired by the mycolic acid containing bacterial co-cultures spearheaded by Onaka et al.,<sup>31</sup> we demonstrated that their mechanism of interaction is distinctly different. To analyze the broader landscape of possible inducers and bolstered by our knowledge that Gram-negative bacteria extensively rely on LuxIR based QS,<sup>32</sup> we tested a panel of 22 proteobacteria to potentially recapitulate the coculture interaction between WMMB235 and WMMA185. Proteobacteria are a major phylum of Gram-negative bacteria and do not contain mycolic acid, thereby using them as inducers directed our search for mechanistic insights away from what is known for Actinobacterial cocultures. Interestingly, two of the 22 bacteria indeed showed positive results – both *Rhodovulum* sp. WMMC316 and *Pseudomonas* sp. WMMC960 led

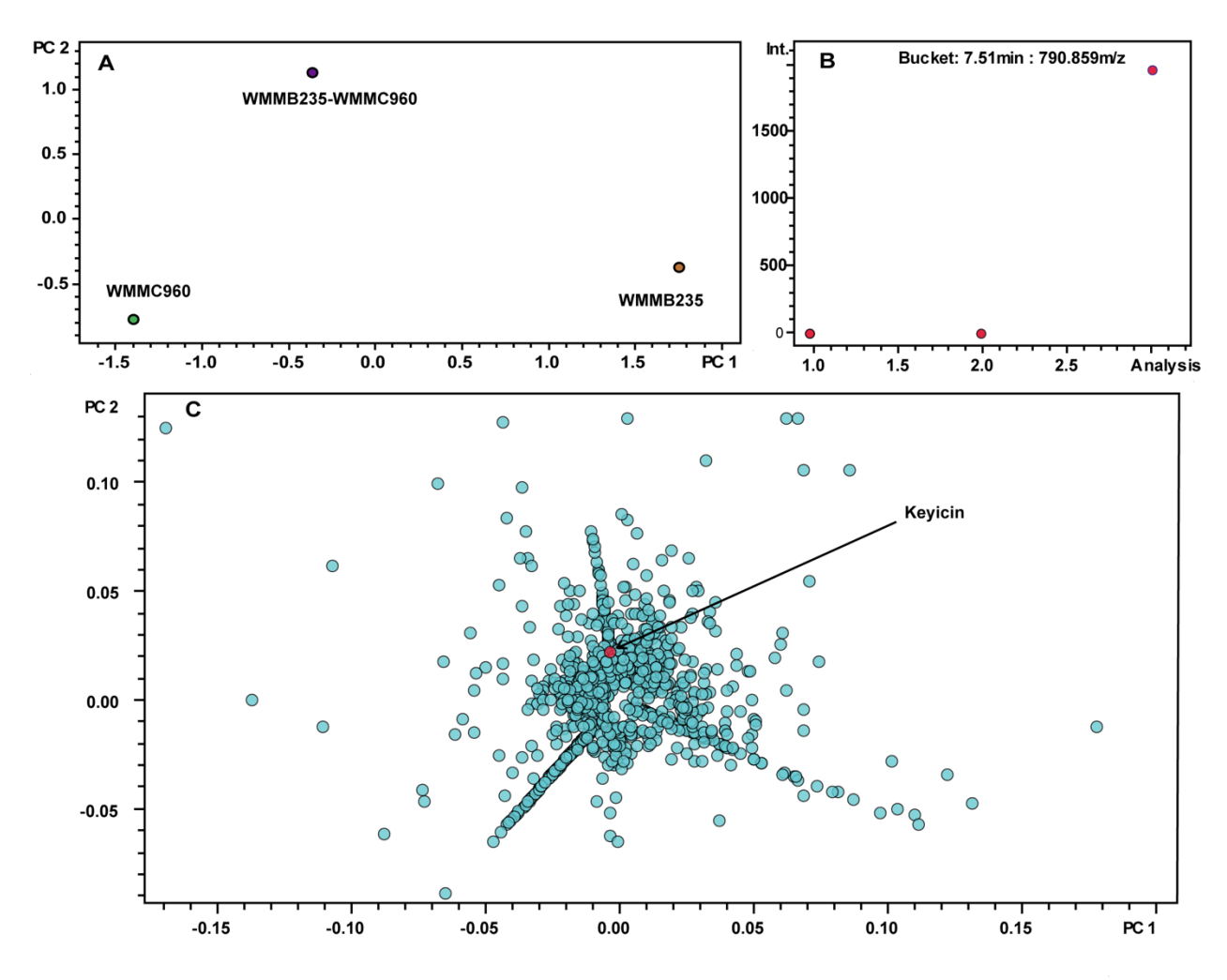


**Figure 3-3.** Metabolomic analysis of WMMB235-WMMC960 coculture using Principal Component Analysis. (A) Score plot for WMMB235, WMMC960 and their coculture (B) Bucket statistic showing the presence of keyicin ion (*m/z*: 790.859) exclusively in the coculture (C) Loadings plot for PCA showing all the metabolites; Keyicin is spatially placed where the coculture is in the scores plot.

to the production of keyicin. Each of these two species were grown in monoculture and in coculture with WMMB235 in 500 µL cultures for a metabolomics study using the platform developed in our lab previously.<sup>33</sup> A spectral intensity table of mass-to-charge ratio and retentiontime pairs was generated from the LCMS profiles of WMMB235-WMMC960 cultures, which was further analyzed using principal component analysis (PCA) (Figure 3-3). The bucket statistic plot (Figure 3-3B) showed the presence of keyicin ions only in the co-culture but not in either of the monocultures. Despite this, the ion was not as spatially separated from the center of the loadings plot because the intensity of the keyicin ion was not as high as the other compounds uniquely produced in the co-culture. Nevertheless, the finding that Gram-negative bacteria, in particular a *Pseudomonas* sp. can trigger *kyc* transcription corroborates the fact that QS is involved in the activation of silent BGCs through inter-species communication.

#### Small molecule signal (s) from *Rhodococcus* sp. WMMA185

The foray into understanding activation of keyicin through quorum sensing signals complemented the basic model of interspecies interaction between WMMB235 and WMMA185. While the modest production of keyicin gave us important insight into how WMMB235 may perceive exogenous molecules for activating transcription, the challenge to discover the native molecules of WMMA185 remained. As mentioned previously, cell-free supernatant from a Day 5 WMMA185 culture induced keyicin production. This implied that the small molecule inducers generated by WMMA185, are still the primary driver of keyicin activation in the co-culture system. Thus, efforts to isolate and identify these inducers were undertaken. Predicated on the fact that WMMA185 produced the signal intrinsically and released it into the medium, we grew 20L of the bacteria with Diaion HP20 beads, which were subsequently extracted using acetone. As expected, these crude extracts resulted in the production of keyicin when incubated with WMMB235 for 2 weeks, at a concentration of 100 µg/mL in DMSO. Keyicin was detected similarly as before, using UV/Vis absorption spectroscopy. Multiple fractionation approaches from here on gave us clues as to the chemical nature of the signals. Two factors were critical in the discovery of the chemical signals: one, the active compound(s) proved to be very potent, and two, they were produced at very low quantities.

The WMMA185 acetone extracts were consecutively fractionated using C-18 and LH-20, and assayed for their ability to elicit keyicin production at concentrations of 10  $\mu$ g/mL, 50  $\mu$ g/mL and 100  $\mu$ g/ml. Two fractions active at the lowest concentration were further separated into 20 fractions

directly into 96 deep-well (1 mL) plates with each run being 20 mins long. At this stage, the wells were dried, and 3 µg/ml of the resulting semi-pure extracts were dissolved in DMSO and incubated with WMMB235. The wells that were active contained the putative inducers of keyicin production and were characterized using LCMS and NMR.

Mass spectrometric analysis yielded the following 3 compounds from the active wells: m/z: [M+H] 180.1088 (**8**), 205.0971 (**9**) and 261.1232 (**10**). The HRMS-ESI data gave us the molecular formula for each of the compounds as  $C_{10}H_{13}NO_2$ ,  $C_{11}H_{12}N_2O_2$  and  $C_{14}H_{16}N_2O_3$ , respectively (Appendix). Interestingly, compounds **8** and **10** eluted in the same well and were structurally related. Prominent features in both these compounds based on 1-D  $^1H$  NMR were the two doublet peaks at  $\delta$  6.71 and  $\delta$  7.02 ppm. These were representative of the tyrosine like p-OH phenyl groups. Additionally, the chemical shift at  $\delta$  4.2 present in both 9 and 10 was typical of an alphaproton in amino acids. The fact that these compounds were eluted at low MeOH:  $H_2O$  composition during the fractionation alluded to the fact that they were hydrophilic in nature. Further inspection of the NMR data using HSQC, COSY and HMBC (Appendix) resulted in the identification of the compounds as N-(4-hydroxyphenethyl) acetamide (**8**), and diketopiperazines (DKPs) cyclo-(Gly-L-Phe) (**9**) and cyclo-(L-Pro-L-Tyr) (**10**). Subsequent advanced Marfey's analysis helped establish the absolute configuration of the diketopiperazines.

The observation that DKPs were among the compounds that induced the production of keyicin is interesting in the light of two studies that showed that DKPs can regulate QS systems

much like the AHLs. Holden *et al.* found that three compounds from multiple *Pseudomonas* spp., cyclo (Ala-*L*-Val) and cyclo (*L*-Pro-*L*-Tyr) and cyclo (*L*-Phe-*L*-Pro) all activated an AHL based biosensor.<sup>34</sup> This study was followed up by Venturi and co-workers, who isolated four cyclic dipeptides from fractions also derived from *Pseudomonas aeruginosa*, that activated quorum sensing systems in *Chromobacterium violaceum* and *Agrobacterium tumefaciens*.<sup>35</sup> These compounds were cyclo (*L*-Pro-*L*-Tyr), cyclo (*L*-Pro-*L*-Leu), cyclo (*L*-Phe-*L*-Pro) and cyclo (*L*-Val-*L*-Leu). Interestingly, both the studies (Holden and Venturi) found cyclo (*L*-Pro-*L*-Tyr) (10) as a possible activator of quorum sensing.

# Keyicin production assay using synthetically made inducers

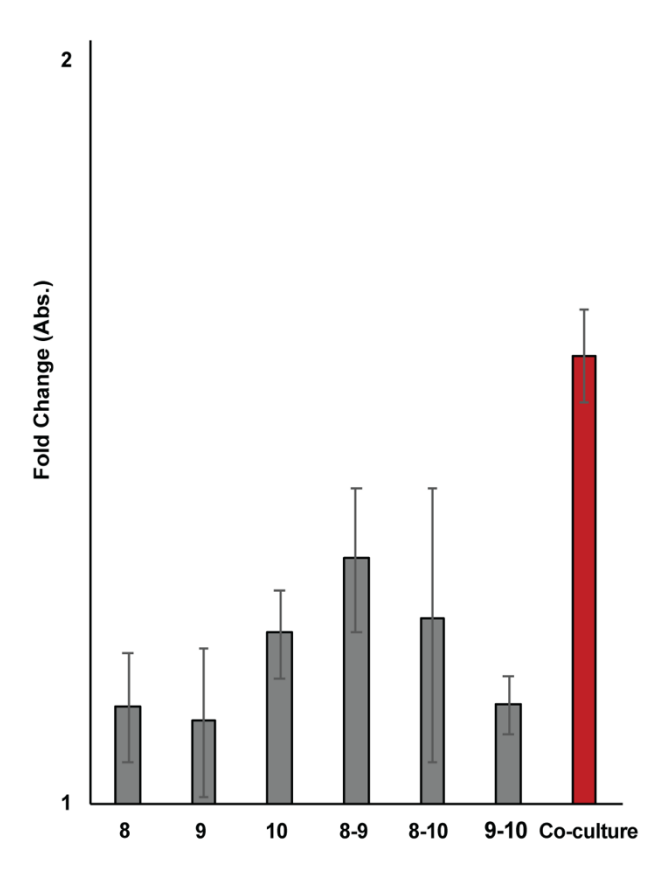


**Figure 3-4.** Keyicin induction using inducers from WMMA185. Absorbance value shown for 8, 9 and 10 at 100nM, and for combination of 8-9, 8-10 and 9-10 at 1nM each.

In order to confirm the activity of the inducers isolated from WMMA185, we purchased the synthetic versions of 8, 9 and 10 and used them in the keyicin activation assay. Surprisingly, the three compounds showed moderate activity at all the concentrations tested (Figure 3-4). Just like the AHLs, these compounds were dissolved in DMSO and controls of both mono- and coculture were spiked with 1% DMSO before incubation. In addition, we conducted combination studies using equal concentration of each of two compounds

tested at a time (Figure 3-4). The concentrations shown (100nM for 8, 9, and 10 and 1nM each for 8-9, 8-10, and 9-10) were chosen since they provided the highest induction across a range of concentrations tested. This assay showed increased production of keyicin compared to monoculture. Neither the compounds alone nor in combination, were able to induce WMMB235 to produce keyicin to the same extent as co-culture with either live cells or with supernatant of WMMA185. This suggested that there may be other compounds involved in the pathway that activated keyicin and may require a more dynamic interplay between different molecules in tandem.

# Impact of exogenous molecules on kyc activation

It was clear from the studies detailed above that activation of the *kyc* cluster may be achieved via multiple routes encompassing different types of inducer molecules. Although studies of silent BGC induction via non-native small molecules are limited (as discussed in Chapter 1), a recent discovery by Pishchany *et al.* found that interspecies communication facilitated by sugar molecules, such as galactose, N-acetyl-glucosamine (GlcNAc), glucosamine, xylose, and arabinose, led to the production of an orphan compound called amycomicin. This was based on previous studies that showed that xylose and GlcNAc can alter gene regulation in *Streptomyces* spp. <sup>37,38</sup>

Based on these results, we investigated the effect of these sugars on the production of keyicin. Galactosamine, N-acetyl glucosamine, galactose, lactose, sucrose, maltose, and arabinose at 10mM concentration were added to the ASW-D media before inoculation with WMMB235. However, none of these compounds were able to yield the red coloration indicative of keyicin. This signals that activation of *kyc* may be unrelated to the nutrient based trigger that is common in

*Streptomyces* sp. and does indeed require bona fide chemical communication and interaction with the transcriptional activator in WMMB235.

# 3.3 Conclusion

The co-culture of WMMB235 and WMMA185 proved to be an excellent representation of how bacterial communication may provide us access to compounds hitherto not isolated. Gaining mechanistic insights into this interaction could establish a working model for activating silent BGCs in other bacteria. In this chapter, we showed that WMMB235 responded to chemical signals by activating the transcription of *kyc*, resulting in the production of a novel antibiotic keyicin. Quorum sensing through the interplay of the *luxR* gene clustered within *kyc* may be one of several pathways by which the cluster was activated. This study also added to the investigation of the role of cyclic dipeptides into not just extracellular signaling but in activation of AHL responsive regulators.

#### 3.4 Materials and methods

#### Acyl homoserine lactone assay

Seed cultures of WMMB235 were grown in five 10 mL ASW-D media (SI). After three days of culture, polypropylene square 96-deepwell microplates (Enzyscreen, The Netherlands) containing 500 μL ASW-D were inoculated with 15 μL of WMMB235 and 5 μL AHL dissolved in DMSO at five concentrations were added to it in triplicate. Monocultures and co-culture controls were also inoculated as described before (17). The culture plates were incubated at 30 °C for fourteen days and shaken at 300 rpm. Subsequently, the plates were centrifuged at 3,000 RPM for 20 min (Eppendorf<sup>TM</sup> Centrifuge 5810R) and the supernatants were transferred to a Corning<sup>TM</sup>

Clear Polystyrene 96-Well Microplate and the absorption at 470 nm was recorded using a BioTek Synergy microplate reader.

#### **Isolation of inducers from WMMA185**

A total of 20L of WMMA185 was grown in AWS-D media with HP20 beads (70g/L) for 5 days. The HP20 beads were filtered, washed and extracted with acetone. The resulting 25g of crude extract was solubilized in 1mL DMSO, 6mL MeOH and water and subjected to large scale bench top ENV+ fractionation. The column was first washed with 100% water, to remove salt and media components, and subsequently extracted with 25%, 50%, 75% and 100% MeOH in water. 470 mg of the active fraction 3 (75% MeOH) was collected and partially subjected to LH20 fractionation in water into 7 fractions. Active fractions 5 and 7 were each further fractionated into 20 wells by RP-HPLC using Phenomenex Luna C18 analytical column (250 × 4.6 mm, 5μm), MeOH/0.1% acetic acid water as the solvent in the following gradient: 0-2 min, 10% MeOH; 2 min-14.50 min, 10-50% MeOH; 14.50 min-19 min, 50-100% MeOH; 19 min-22 min 100% MeOH; 22 min-22.50 min 100-10% MeOH and held at 10% till 27 min. Wells 14 in each case were active.

# Absolute configuration of cyclic dipeptides

The absolute configurations of 1 and 2 were elucidated via application of Marfey's advanced method. <sup>39</sup> L- and DL-FDLA were synthesized as previously reported. <sup>40</sup> Cyc(Gly-Phe) (9) (0.2 mg) and cyc(Pro-Tyr) (10) (0.2 mg) were each hydrolyzed with 6 N HCl (500  $\mu$ L) for 4 h at 110 °C and dried under vacuum. The acid hydrolysates were each dissolved in 100  $\mu$ L of H<sub>2</sub>O and split into two equal portions. Each portion was mixed with 1 N NaHCO<sub>3</sub> (80  $\mu$ L) and 100  $\mu$ L of L- or DL-FDLA (10 mg/mL in acetone). Each solution was stirred for 1 h at 40 °C. The reaction was quenched with 1 N HCl (80  $\mu$ L) and dried under vacuum. A portion of each product was dissolved in CH<sub>3</sub>OH (1:1) for UHPLC/HRMS analysis. Separation of the derivatives was achieved

with a Phenomenex Kinetex C18 reversed-phase column (2.6  $\mu$ m, 2.1 × 100 mm) at a flow rate of 0.3 mL/min and with a linear gradient of H2O (containing 0.1% formic acid) and CH3OH (90:10 to 3:97 over 12 min, and held for 2 min at CH<sub>3</sub>OH/H<sub>2</sub>O (97:3). The absolute configuration of the amino acid was determined by comparing the retention times of the L- and DL-FDLA derivatives, which were identified by HRMS.

# **Sugar induction:**

Seven sugars were tested for activation of kyc cluster: galactosamine, N-acetyl glucosamine, galactose, lactose, sucrose, maltose and arabinose. They were added to 10 mL ASW-D media to make a final concentration of 10mM for each sugar. The spiked ASW-D was used as the test growth media for WMMB235 in microscale culture and analyzed after 14 days of growth.

# **HRESI-TOF-MS** and PCA analysis

WMMB235 and the proteobacteria inducers were grown in microscale using the protocol published before.<sup>33</sup> Half of the 500μL culture was used for metabolomic study. For this, the samples were processed through a SPE column (EVOLUTE ABN SPE cartridges, 25 mg absorbent mass, 1 mL reservoir volume; Biotage, S4 Charlotte, NC). Subsequently, LC/MS data were acquired using a Bruker MaXis ESI-Q-TOF mass spectrometer (Bruker, Billerica, MA, USA) coupled with a Waters Acquity UPLC system (Waters, Milford, MA, USA) operated by Bruker Hystar software. A gradient comprised of MeOH and H2O (containing 0.1% formic acid) was used on an RP C-18 column (Phenomenex Kinetex 2.6 μm, 2.1 mm × 100 mm; Phenomenex, Torrance, CA, USA) at a flow rate of 0.3 mL/min. The method consisted of a linear gradient from MeOH/H2O (10%/90%) to MeOH/H2O (97%/3%) in 12 min, then held for two minutes at MeOH/H2O (97%/3%). Full scan mass spectra (*m/z* 150–1550) were measured in positive ESI

mode. The mass spectrometer was operated using the following parameters: capillary, 4.5 kV; nebulizer pressure, 1.2 bar; dry gas flow, 8.0 L/min; dry gas temperature, 205 °C; scan rate, 2 Hz. Tune mix (ESI-L low concentration; Agilent, Santa Clara, CA) was introduced through a divert valve at the end of each chromatographic run for automated internal calibration. Bruker Data Analysis 4.2 was used for analysis of chromatograms.

# **Bucketing and PCA of LC/MS Data**

Bucketing LC/MS data and PCA was performed using Bruker Profile Analysis 4.1. LC/MS bucketing was performed using the following parameters: data selection and processing, Find Molecular Features; spectrum type, line; spectrum polarity, positive; spectral range, 2–11 min and m/z = 150–1500; advanced bucketing, 20 seconds and 20 mDa window; normalization, Sum of bucket values in analysis. PCA was performed on bucket tables using a Pareto scaling algorithm.

# 3.5 References

- (1) Hertweck, C. Hidden Biosynthetic Treasures Brought to Light. *Nat. Chem. Biol.* **2009**, *5* (7), 450–452.
- (2) Bibb, M. J. Regulation of Secondary Metabolism in Streptomycetes. *Curr. Opin. Microbiol.* **2005**, *8* (2), 208–215.
- (3) Ishida, K.; Lincke, T.; Behnken, S.; Hertweck, C. Induced Biosynthesis of Cryptic Polyketide Metabolites in a Burkholderia Thailandensis Quorum Sensing Mutant. **2010**.
- (4) Bassler, B. L. How Bacteria Talk to Each Other: Regulation of Gene Expression by Quorum Sensing. *Curr. Opin. Microbiol.* **1999**, *2* (6), 582–587.
- (5) Whiteley, M.; Diggle, S. P.; Greenberg, E. P. Progress in and Promise of Bacterial Quorum Sensing Research. *Nature* **2017**, *551* (7680), 313–320.
- (6) Welsh, M. A.; Blackwell, H. E. Chemical Probes of Quorum Sensing: From Compound Development to Biological Discovery. *FEMS Microbiol. Rev.* **2016**, *40* (5), 774–794.
- (7) Papenfort, K.; Bassler, B. L. A Vibrio Cholerae Autoinducer–Receptor Pair That Controls Biofilm Formation. *Nat. Chem. Biol.*
- (8) Rutherford, S. T.; Bassler, B. L. Bacterial Quorum Sensing: Its Role in Virulence and Possibilities for Its Control. *Cold Spring Harb. Perspect. Med.* **2012**, *2* (11), a012427.
- (9) Rasko, D. A.; Sperandio, V. Anti-Virulence Strategies to Combat Bacteria-Mediated Disease. *Nat. Rev. Drug Discov.* **2010**, *9* (2), 117–128.
- (10) Njoroge, J.; Sperandio, V. Jamming Bacterial Communication: New Approaches for the Treatment of Infectious Diseases. *EMBO Mol. Med.* **2009**, *1* (4), 201–210.
- (11) Mao, D.; Bushin, L. B.; Moon, K.; Wu, Y.; Seyedsayamdost, M. R. Discovery of ScmR as a Global Regulator of Secondary Metabolism and Virulence in Burkholderia Thailandensis E264. *Proc. Natl. Acad. Sci.* 2017, 114 (14), E2920–E2928.
- (12) Majerczyk, C.; Brittnacher, M.; Jacobs, M.; Armour, C. D.; Radey, M.; Schneider, E.; Phattarasokul, S.; Bunt, R.; Greenberg, E. P. Global Analysis of the Burkholderia Thailandensis Quorum Sensing-Controlled Regulon. 2014.
- (13) Campbell, J.; Lin, Q.; Geske, G. D.; Blackwell, H. E. New and Unexpected Insights into the Modulation of LuxR-Type Quorum Sensing by Cyclic Dipeptides. *ACS Chem. Biol.* 2009, 4 (12), 1051–1059.
- (14) Stacy, D. M.; Welsh, M. A.; Rather, P. N.; Blackwell, H. E. Attenuation of Quorum

- Sensing in the Pathogen *Acinetobacter Baumannii* Using Non-Native *N* -Acyl Homoserine Lactones. *ACS Chem. Biol.* **2012**, *7* (10), 1719–1728.
- (15) Moore, J. D.; Rossi, F. M.; Welsh, M. A.; Nyffeler, K. E.; Blackwell, H. E. A Comparative Analysis of Synthetic Quorum Sensing Modulators in *Pseudomonas Aeruginosa*: New Insights into Mechanism, Active Efflux Susceptibility, Phenotypic Response, and Next-Generation Ligand Design. *J. Am. Chem. Soc.* 2015, *137* (46), 14626–14639.
- (16) Arakawa, K. Manipulation of Metabolic Pathways Controlled by Signaling Molecules, Inducers of Antibiotic Production, for Genome Mining in Streptomyces Spp. Antonie Van Leeuwenhoek 111.
- (17) Recio, E.; Colinas, Á.; Rumbero, Á.; Aparicio, J. F.; Martín, J. F. PI Factor, a Novel Type Quorum-Sensing Inducer Elicits Pimaricin Production in Streptomyces Natalensis. *J. Biol. Chem.* **2004**, 279 (40), 41586–41593.
- (18) Adnani, N.; Chevrette, M. G.; Adibhatla, S. N.; Zhang, F.; Yu, Q.; Braun, D. R.; Nelson, J.; Simpkins, S. W.; McDonald, B. R.; Myers, C. L.; et al. Coculture of Marine Invertebrate-Associated Bacteria and Interdisciplinary Technologies Enable Biosynthesis and Discovery of a New Antibiotic, Keyicin. ACS Chem. Biol. 2017, 12 (12), 3093–3102.
- (19) Skinnider, M. A.; Dejong, C. A.; Rees, P. N.; Johnston, C. W.; Li, H.; Webster, A. L. H.; Wyatt, M. A.; Magarvey, N. A. Genomes to Natural Products PRediction Informatics for Secondary Metabolomes (PRISM). *Nucleic Acids Res.* 2015, 43 (20), gkv1012.
- (20) Medema, M. H.; Blin, K.; Cimermancic, P.; De Jager, V.; Zakrzewski, P.; Fischbach, M. A.; Weber, T.; Takano, E.; Breitling, R. AntiSMASH: Rapid Identification, Annotation and Analysis of Secondary Metabolite Biosynthesis Gene Clusters in Bacterial and Fungal Genome Sequences. *Nucleic Acids Res.* 2011, 39 (SUPPL. 2), 339–346.
- (21) Blin, K.; Medema, M. H.; Kazempour, D.; Fischbach, M. A.; Breitling, R.; Takano, E.; Weber, T. AntiSMASH 2.0--a Versatile Platform for Genome Mining of Secondary Metabolite Producers. *Nucleic Acids Res.* **2013**, *41* (Web Server issue), 204–212.
- (22) Weber, T.; Blin, K.; Duddela, S.; Krug, D.; Kim, H. U.; Bruccoleri, R.; Lee, S. Y.; Fischbach, M. A.; Müller, R.; Wohlleben, W.; et al. AntiSMASH 3.0—a Comprehensive Resource for the Genome Mining of Biosynthetic Gene Clusters. *Nucleic Acids Res.* **2015**, 43 (W1), W237–W243.

- (23) Waters, C. M.; Bassler, B. L. Quorum Sensing: Communication in Bacteria. *Annu. Rev. Cell Dev. Biol.* **2005**, *21* (1), 319–346.
- (24) Gerdt, J. P.; Wittenwyler, D. M.; Combs, J. B.; Boursier, M. E.; Brummond, J. W.; Xu, H.; Blackwell, H. E. Chemical Interrogation of LuxR-Type Quorum Sensing Receptors Reveals New Insights into Receptor Selectivity and the Potential for Interspecies Bacterial Signaling. ACS Chem. Biol. 2017, acschembio.7b00458.
- (25) Adnani, N.; Braun, D. R.; McDonald, B. R.; Chevrette, M. G.; Currie, C. R.; Bugni, T. S. Complete Genome Sequence of Rhodococcus Sp. Strain WMMA185, a Marine Sponge-Associated Bacterium. *Genome Announc.* **2016**, *4* (6), e01406-16.
- (26) Polkade, A. V.; Mantri, S. S.; Patwekar, U. J.; Jangid, K. Quorum Sensing: An Under-Explored Phenomenon in the Phylum Actinobacteria. *Front. Microbiol.* **2016**, *7* (February), 1–13.
- (27) Santos, C. L.; Correia-Neves, M.; Moradas-Ferreira, P.; Mendes, M. V. A Walk into the LuxR Regulators of Actinobacteria: Phylogenomic Distribution and Functional Diversity. *PLoS One* **2012**, *7* (10), e46758.
- (28) Venturi, V.; Ahmer, B. M. M. Editorial: LuxR Solos Are Becoming Major Players in Cell–Cell Communication in Bacteria. *Front. Cell. Infect. Microbiol.* **2015**, *5*, 89.
- (29) Covaceuszach, S.; Degrassi, G.; Venturi, V.; Lamba, D. Structural Insights into a Novel Interkingdom Signaling Circuit by Cartography of the Ligand-Binding Sites of the Homologous Quorum Sensing LuxR-Family. *Int. J. Mol. Sci.* 2013, 14 (10), 20578– 20596.
- (30) Higgins, S.; Heeb, S.; Rampioni, G.; Fletcher, M. P.; Williams, P.; Cámara, M. Differential Regulation of the Phenazine Biosynthetic Operons by Quorum Sensing in Pseudomonas Aeruginosa PAO1-N. *Front. Cell. Infect. Microbiol.* **2018**, *8*, 252.
- (31) Onaka, H.; Mori, Y.; Igarashi, Y.; Furumai, T. Mycolic Acid-Containing Bacteria Induce Natural-Product Biosynthesis in Streptomyces Species. *Appl. Environ. Microbiol.* **2011**, 77 (2), 400–406.
- (32) Parsek, Matthew R.; Greenberg, E. P. Acyl-Homoserine Lactone Quorum Sensing in Gram-Negative Bacteria: A Signaling Mechanism Involved in Associations with Higher Organisms. **2000**, *97* (16), 8789–8793.
- (33) Adnani, N.; Vazquez-Rivera, E.; Adibhatla, S.; Ellis, G.; Braun, D.; Bugni, T.

- Investigation of Interspecies Interactions within Marine Micromonosporaceae Using an Improved Co-Culture Approach. *Mar. Drugs* **2015**, *13* (10), 6082–6098.
- (34) Holden, M. T. G.; Ram Chhabra, S.; De Nys, R.; Stead, P.; Bainton, N. J.; Hill, P. J.; Manefield, M.; Kumar, N.; Labatte, M.; England, D.; et al. Quorum-Sensing Cross Talk: Isolation and Chemical Characterization of Cyclic Dipeptides from Pseudomonas Aeruginosa and Other Gram-Negative Bacteria. *Mol. Microbiol.* 2002, 33 (6), 1254–1266.
- (35) Degrassi, G.; Aguilar, C.; Bosco, M.; Zahariev, S.; Pongor, S.; Venturi, V. Plant Growth-Promoting Pseudomonas Putida WCS358 Produces and Secretes Four Cyclic Dipeptides: Cross-Talk with Quorum Sensing Bacterial Sensors.
- (36) Pishchany, G.; Mevers, E.; Ndousse-Fetter, S.; Horvath, D. J.; Paludo, C. R.; Silva-Junior, E. A.; Koren, S.; Skaar, E. P.; Clardy, J.; Kolter, R.; et al. Amycomicin Is a Potent and Specific Antibiotic Discovered with a Targeted Interaction Screen. *Proc. Natl. Acad. Sci. U. S. A.* 2018, 115 (40), 10124–10129.
- (37) Świątek, M. A.; Gubbens, J.; Bucca, G.; Song, E.; Yang, Y.-H.; Laing, E.; Kim, B.-G.; Smith, C. P.; van Wezel, G. P. The ROK Family Regulator Rok7B7 Pleiotropically Affects Xylose Utilization, Carbon Catabolite Repression, and Antibiotic Production in Streptomyces Coelicolor. *J. Bacteriol.* **2013**, *195* (6), 1236–1248.
- (38) Rigali, S.; Titgemeyer, F.; Barends, S.; Mulder, S.; Thomae, A. W.; Hopwood, D. A.; van Wezel, G. P. Feast or Famine: The Global Regulator DasR Links Nutrient Stress to Antibiotic Production by Streptomyces. *EMBO Rep.* **2008**, *9* (7), 670–675.
- (39) Ken-ichi Harada\*, Kiyonaga Fujii, K. H. and M. S. Application of D,L-FDLA

  Derivatization to Determination of Absolute Configuration of Constituent Amino Acids in

  Peptide by Advanced Marfey's Method.
- (40) Marfey, P. Determination OfD-Amino Acids. II. Use of a Bifunctional Reagent, 1,5-Difluoro-2,4-Dinitrobenzene. *Carlsberg Res. Commun.* **1984**, *49* (6), 591–596.

# Chapter 4: Compounds from co-culture and mono-culture of Actinomycetes

# 4. 1 Introduction

The existing diversity of natural products is a testament to the innovation inherent to the biosynthetic machinery in microbes.<sup>1</sup> These complex systems, comprised of large multi-modular enzymes, have evolved to sequester resources so as to synthesize secondary metabolites for competitive advantage.<sup>2</sup> Using simple building blocks and combinatorial logic, bacteria are able to give rise to a plethora of novel scaffolds and activities. For this, concerted, multistep processes that include initiation, chain elongation, and subsequent tailoring are required. Common units such as malonyl-CoA and methylmalonyl-CoA are most frequently incorporated into polyketides during chain elongation, whereas proteinogenic and many non-proteinogenic amino acids go into producing non-ribosomal peptides.<sup>3</sup> The enzymatic orchestration of producing these specialized molecules has been studied for decades, and genomic analyses of the required enzymes have furthered our understanding of it. However, predicting the molecules that may eventually be isolated remains a challenging feat for two reasons: one, the prediction relies on homology with enzymatic pathways that have already been biochemically characterized,<sup>4</sup> and two, these enzymes have complex regulatory mechanisms in place that are difficult to predict *in silico*.<sup>5</sup>

The regulatory mechanisms are a major bottleneck when it comes to producing the natural products. Pleiotropic regulators affect many different genes and biosynthetic gene clusters simultaneously, like such as the ArpA in *Streptomyces coelicolor*. <sup>6–9</sup> Pathway specific regulators, on the other hand are usually grouped with the biosynthetic gene cluster (BGC) that it affects. <sup>10–12</sup> From chapters 2 and 3, it was evident that co-culture provides an excellent way to circumvent the

regulatory bottleneck that prevents an organism from producing certain secondary metabolites. Presumably, this is because in co-culture settings, the bacteria have the incentive to siphon the resources towards secondary metabolite production since it is in competition for survival.

Our lab has been a key player in the study of co-cultures among marine bacteria, particularly Micromonosporaceae, which is a relatively understudied family within Actinobacteria. Both co-culture and monoculture metabolomics studies had shown that there are many new and promising compounds to be discovered from this source. In addition, exploring new sources is not only important in order to find new molecules but also to understand how different environments and bacterial species result in the diversity of chemical structures produced. As discussed in chapter 2, secondary metabolite production of WMMB235 is greatly influenced by co-culture. Here, we investigate three aspects of WMMB235 and a closely related *Micromonospora* sp. WMMA2032: a) the impact of interspecies interaction on WMMA2032 and identification of the BGC that is activated as a result b) impact of WMMB235 co-culture with a *Microbulbifer* sp. and c) additional secondary metabolites produced by WMMB235.

## 4. 2 Results and Discussion:

# Co-culture results in increased metabolic profile in a Micromonospora sp.:

Previous work in the lab, conducted by Adnani *et al.*, demonstrated that there are various examples of bacterial co-culture combinations, where interspecies interaction influenced the metabolomic profile of bacterial species.<sup>13</sup> They designed microscale fermentations (500 µL) for evaluating the effects of co-culture in Micromonasporaceae including 47 *Micromonospora* spp., 11 *Verrucosispora* spp., and 7 *Solwaraspora* spp. with an improved inoculation method. Twelve out of the 65 strains showed distinctive differences in metabolite production and antibiotic activity

between the monocultures and their corresponding co-cultures with mycolic acid containing bacteria. By expanding this microscale study to include more strains within the Micromonasporaceae family, we discovered that *Micromonospora* sp. WMMA2032 showed antibiotic activity and a metabolomic profile significantly different when co-cultured with a *Dietzia* sp. WMMA184 versus when in monoculture. The co-culture also visibly showed different pigmentation compared to the mono-culture.

However, in order to feasibly study and extract the metabolites unique to the co-culture, it was crucial to replicate the impact of coculture on the production of secondary metabolites in a

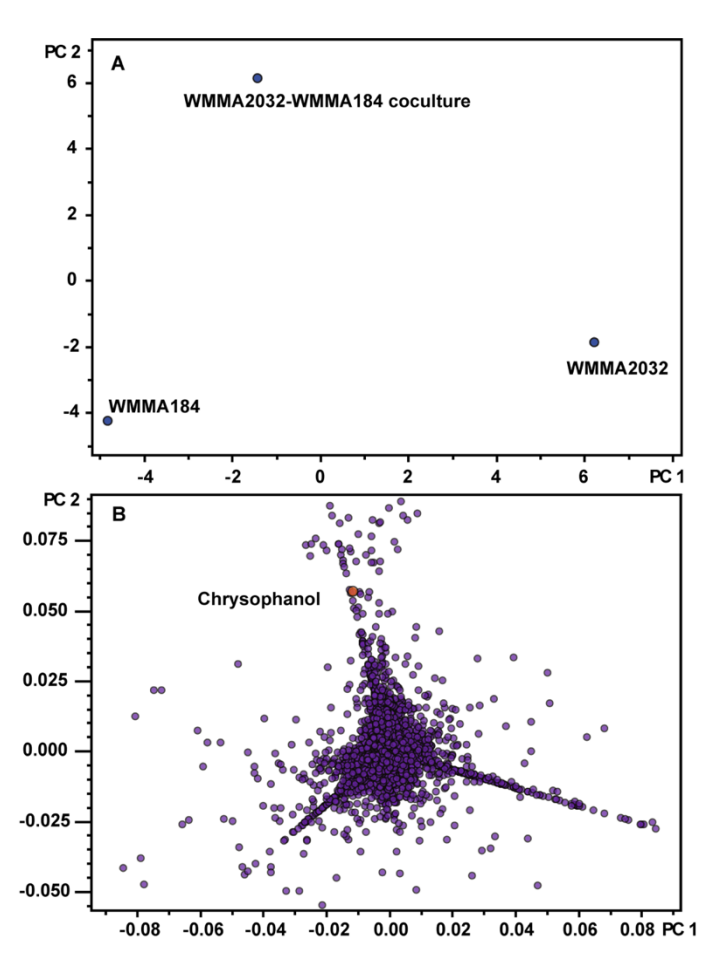


**Figure 4-1.** Principal component analysis of WMMA2032, WMMA184 and their co-culture. (A) Scores plot (B) Loadings plot showing the metabolites spatially correlated to the scores plot. Orange circle represent Chrysophanol, which is unique to the co-culture.

larger volume compared to the microscale. Hence, we grew the mono and co-cultures in 1-liter ASW-A cultures and re-evaluated the metabolite production in the larger scale. The cultures were extracted using acetone and subjected to liquid-liquid partition with hexanes/90% methanol in chloroform/70% water followed by methanol in water. LCMS analysis of the chloroform partition from each of the monocultures and their co-culture using LCMS clearly showed that the effect of coculture was reproducible and significant in large-scale and thus suitable for compound isolation. The LCMS files were analyzed

using principal component analysis (Figure 4-1). The scores plot showed the spatial separation of each of these samples, while the loadings plot showed the corresponding metabolites unique to the co-culture.

#### **Detection and isolation of co-culture specific compounds:**

LCMS and bioactivity guided fractionation led to the isolation of two compounds unique to the co-culture. The chloroform partition from 1 L each of WMMA2032, WMMA187 and their co-culture was subjected to Sephadex LH-20 column chromatography. Interestingly, at this stage, each of the three samples showed a drastic change in the complexity of metabolites produced, which was visually identifiable as shown in Figure 4-2. Of special note, was the orange band unique to co-culture (Figure 4-2), which was subsequently purified by RP-HPLC using a C-18 column, yielding

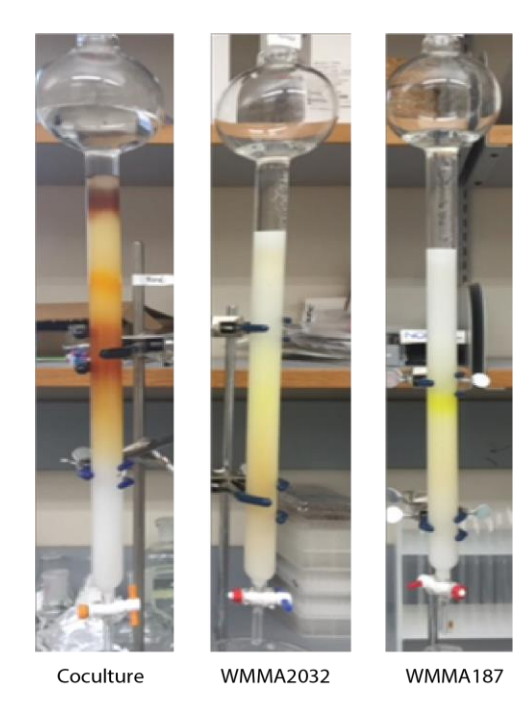


**Figure 4-2.** Sephadex LH-20 fractionation of cocultures and monocultures clearly showed the drastic increase in the metabolite production in co-culture.

16.5 mg and 4.6 mg of two bright orange compounds. LCMS analysis of these compounds showed their m/z ([M+H]<sup>+</sup>) values to be 255.051 and 235.25 respectively. Analysis of 1D and 2D NMR data (Appendix 3) showed that these were previously reported aromatic anthraquinone compounds, chrysophanol (Table 1) and GTRI-02<sup>15</sup>.

Figure 4-3. (A) Structure of Chrysophanol (B) Structure of GTRI-02

Table 4-1. NMR for 1 (600 MHz, CD<sub>3</sub>OD)

Position	δc, mult.	δ <sub>H</sub> (J in Hz)	HMBC
1	163.9 C		
2	125.6, CH	7.00, d (2.7)	1, 4, 13, 15
3	147.1, C		
4	113.3, CH	7.53, d (2.7)	1, 2, 10
5	119.4, CH	7.71, dd (7.5, 1.3)	7, 10, 12
6	136.5, CH	7.64, dd (8.3, 7.5)	8, 11,
7	125.3, CH	7.26, dd (8.3, 1.3)	5
8	163.4, C		
9	191.0, C		
10	184.2, C		
11	134.3, C		
12	118.0, C		
13	124.2, C		
14	138.6, C		
15	24.3, CH3	2.78, s	

## Biosynthetic gene clusters for unique co-culture compounds:

Bioinformatic analyses of the WMMA2032 and WMMA184 provided the evidence required to determine the producing organism of the aforementioned co-culture specific compounds. AntiSmash<sup>16</sup> analysis of the WMMA2032 genome revealed 59 clusters, while PRISM<sup>17</sup> showed 13 clusters (Table 2). Notably, BGC2, which is a type II PKS cluster had 63% similarity to actinorhodin BGC (MIBiG: BGC0000194) and 45% similarity granaticin BGC (MIBiG: BGC0000227) (Table 3). Both actinorhodin and granaticin share the core anthraquinone structure with that of **1** and **2**. In addition, analysis of the WMMA184 genome failed to show the

Figure 4-4. Structures of actinorhodin (left) and granaticin (right)

presence of any BGC that could produce a similar aromatic anthraquinone. Out of the 7 BGCs housed within WMMA184, there were two terpenes, one siderophore, one β-lactone, one NRPS, one type I PKS, and one ectoine. The data from both the genomes together suggested that **1** and **2** were likely produced by cluster 2 in WMMA2032, which was seemingly activated in the presence of WMMA187. Within cluster 2, the core biosynthetic genes were two ketosynthases (ctg1\_258,

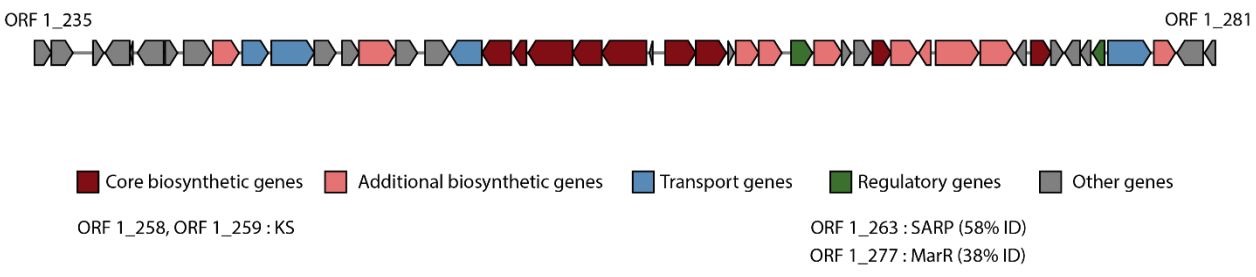


**Figure 4-5.** Putative BGC (Cluster 2) of Type II PKS, shows the core biosynthetic genes and the two regulatory genes.

ctg1\_259), acyl carrier protein (ctg1\_260), ketoacyl reductase (ctg1\_267) and a short chain dehydrogenase (ctg1\_273) (Figure 4-3). Interestingly, although chrysophanol had been isolated from various sources including fungi, plants and even insects and lichens, there was only one report in literature describing its isolation from bacteria, a *Streptomyces* sp. GW32/698. <sup>18,19</sup> Therefore, this study was the first report of production of this antibacterial compound by a *Micromonospora* sp.

Table 4-2. BGCs identified within WMMA2032

Cluster #	AntiSmash #	Туре	Homologous BGC
1	3	Siderophore	Desferrioxamine (80%)
2	4	Type 2 PKS	Actinorhodin (63%)
3	6	Type 2 PKS - fatty acid	Xanthiolipin (14%)
4	9	Terpene	Nocathiacin (4%)
5	13	Type 1 PKS	Rifamycin (38%)
6	16	Type 1 PKS - NRPS	
7	23	Type 1 PKS - NRPS	Tallysomycin (5%)
8	31	Terpene	Phosponoglycans (3%)
9	32	Terpene	Sioxanthin (100%)
10	39	Type 3 PKS	Hydroquinones (71%)
11	44		Pyrrolomycin
12	56	Terpene	
13	59	Bacteriocin-Terpene	Lymphostin (33%)

Since the chrysophanol gene cluster was active only in the co-culture conditions, it was crucial to investigate the regulatory genes in this cluster. The two regulatory genes annotated here were ctg1\_263, a SARP family regulator and ctg1\_277, a MarR regulator, both of which are transcriptional regulators found in myriad *Streptomyces* sp. and known to control expression of genes responsible for secondary metabolism<sup>20</sup>

**Table 4-3**. BGCs homologous to cluster 2 from WMMA2032, the putative BGC responsible for anthraquinone type compounds.

MIBiG Accession	Percent of Genes Similar to cluster 2
BGC0000194	63%
BGC0000227	45%
BGC0000221	36%
BGC0000225	31%
BGC0000195	31%
BGC0000228	27%
BGC0000245	36%
BGC0001409	27%
BGC0001061	27%
BGC0000223	27%
	BGC0000194  BGC0000227  BGC0000221  BGC0000225  BGC0000195  BGC0000228  BGC0000245  BGC0001409  BGC0001061

#### Coculture of WMMC694 with WMMB235

In chapter 3, we demonstrated that *Micromonospora* sp. WMMB235 interacted with certain marine-sponge-associated proteobacteria to produce keyicin. This study also revealed that

co-culture of WMMB235 and a *Microbulbifer* sp. WMMC694 resulted in the production of an antibiotic compound different from keyicin. Subsequent scale up and purification of these 1-L cultures, guided by activity against *S. Aureus* enabled the isolation of two known compounds, 3-(acetylamino) butyl paraben (3) and n-decyl paraben (4) that were only produced in the co-culture and not in the mono-cultures. Of these, only compound, 4, displayed activity against *S. Aureus*. The molecular formulae of compounds 3 and 4 were determined to be  $C_{13}H_{17}NO_4$  (m/z 274.1050; [M+Na]) and  $C_{17}H_{26}O_3$  (m/z 277.1785; [M-H]<sup>-</sup>) respectively. Analysis of 1D and 2D NMR data enabled the confirmation of these structures.

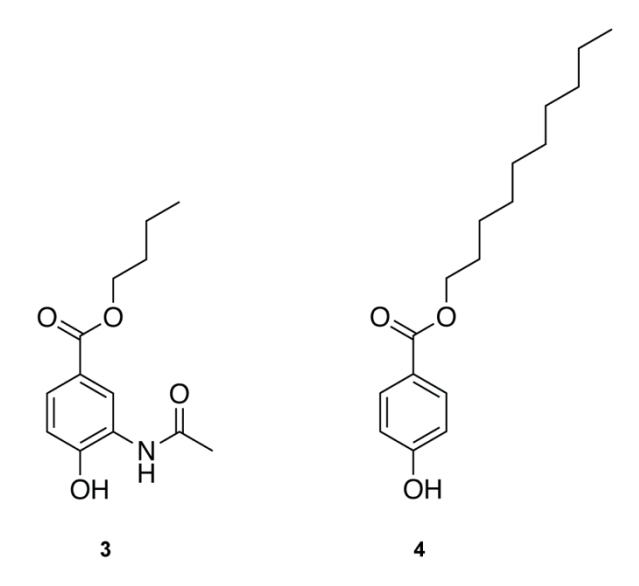


**Figure 4-6.** Structures of compounds isolated from Microbulbifer sp. WMMC694 co-culture with Micromonospora sp. WMMB235.

Interestingly, compound **4** was one of the series of parabens, that were isolated from a *Microbulbifer* sp. cultivated from a marine calcareous sponge and was found to have antimicrobial activity against marine *Leuconia nivea*-derived Gram positive strains *Bacillus* sp. L6-3e.<sup>21</sup> Compound **3** was also isolated from a *Microbulbifer* sp. derived from marine algae.<sup>22,23</sup> These reports suggested that the compounds isolated from the co-culture of WMMC694 and WMMB235 were in fact produced by *Microbulbifer* sp. WMMC694. This finding reiterated that bacteria often

have unpredictable regulatory mechanisms that could be activated in certain situations, but not in others. By understanding these differences, like we did in chapters 2 and 3, we may have better control over the compounds that we can access.

#### Other molecules isolated from WMMB235:

The genomic analysis of WMMB235 revealed tremendous untapped potential to produce new compounds (Chapter 2). As a result, we undertook large-scale purification and isolation of structurally interesting compounds. Following a protocol similar to the isolation of the compounds mentioned herein, the acetone extract was subjected to liquid – liquid partition and LH-20 fractionation using 1:1 ratio of CHCl<sub>3</sub> and MeOH. Although the products of the other BGCs, studied in chapter 2, remained elusive, perhaps due to a yet undiscovered regulatory gatekeeper, subsequent HPLC purification led us to compounds **5** (Table 4) and **6**, with molecular formulae of C<sub>10</sub>H<sub>10</sub>N<sub>2</sub>O<sub>2</sub> and C<sub>9</sub>H<sub>12</sub>N<sub>2</sub>O<sub>5</sub>, respectively. While compound **6** has been previously isolated and characterized from marine associated *Streptomyces microflavus*.<sup>24</sup>, compound **5** has only been reported to be synthetically derived.

Figure 4-7. Structures of compounds isolated from WMMB235 monoculture

Table 4-4. NMR for 5 (CD<sub>3</sub>OD, 600MHz)

Position	$\delta_{\rm C}$ , mult.	δ <sub>H</sub> (J in Hz)	HMBC
1	164.6, C		
2	150.6, CH	8.62, d (5.6)	3, 4, 7, 8
3	120.9, CH	7.59, d (5.6)	2, 6, 8
4	150.3, CH	9.34, s	1, 2, 3, 7, 8

5	153.0, C		
6	100.2, CH	6.65, s	5, 7, 8, 9
7	145.0, C		
8	120.9, C		
9	66.9, CH	4.77, q (6.6)	5, 6, 10
10	23.2, CH3	1.51, d (6.6)	5, 9

# 4.3 Conclusions

Actinobacteria have consistently served as a prolific source of bioactive natural products. However, the machinery required to produce these secondary metabolites are not always active. In this chapter, we showed that co-cultures are a consistent method of coaxing bacteria to produce more and different compounds than they do in monocultures. We reported the isolation of Chrysophanol from a *Micromonospora* sp. WMMA2032 and also found that a *Microbulbifer* sp. only produces antimicrobial parabens in the presence of *Micromonospora* sp. WMMB235.

#### 4.4 Materials and Methods

#### Strain collection and selection

*Micromonospora* sp. WMMA2032 was isolated from an unidentified ascidian collected on 8/6/2013 near the Stan Blum boat ramp in Fort Pierce, Florida (GPS 27.479262, -80311697). An approximately 1 cubic cm chunk of the ascidian was ground up in sterile ASW and plated onto various selective media. WMMA2032 was isolated on Gauze 1 medium supplemented with 50% ASW, cycloheximide (50 μg/mL) and nalidixic acid (25 μg/mL).

Dietzia sp. strain WMMA184 was isolated in 2011 from coral mucus of *Montastraea* faveolata collected off the coast of the Florida Keys. WMMA184 was isolated from a plate prepared using M1 medium supplemented with 50% artificial seawater (ASW).<sup>25</sup>

#### DNA extraction

Strains WMMA2032 (Micromonospora sp.) and WMMA184 (Dietzia sp.) were cultured in ASW-A media (20 g soluble starch, 10 g glucose, 5 g peptone, 5 g yeast extract, 5 g CaCO3 per liter of artificial seawater) at 28 °C and 200 rpm for 10 days. Packed cells of ~100 μL were yielded by centrifuging sufficient culture for 60 secs at 14,000 rpm. Supernatants were discarded and cells were washed with 1 mL of 10.3% sucrose solution. Centrifugation was repeated and cells were resuspended in 450 µL TSE containing lysozyme (5 mg/mL). The solution was incubated for one hour, with tubes inverted occasionally, at 37 °C. Proteinase k (20 mg/mL, 13 μL) was added and incubated for an additional 20 minutes at 37 °C. SDS (10%, 45 µL) and 180 µL of TE was added and tubes were inverted until cells became clear and viscous. Phenol:chloroform:isoamyl alcohol (25:24:1, 350 μL) were added and shaken until uniformly cloudy. Tubes were centrifuged at 14,000 rpm for 10 minutes and the top aqueous layer was collected. DNA was precipitated by addition of 1/10th volume of 5M NaCl and mixing, and then addition of an equal volume of 2propanol and inverting the tube until DNA precipitated. Precipitated DNA was removed using a glass hook and washed in 1 mL 70% EtOH. The solution was centrifuged and excess ethanol was removed. The DNA pellet was re-suspended in 500 μL TE and 10 μL of RNase A (10 mg/ml) prior to incubation at 37 °C for one hour. Afterwards, 350 µL of phenol:chloroform:isoamyl alcohol (25:24:1) were added, shaken, and subsequently centrifuged for 10 minutes at 14,000 rpm. The upper aqueous layer was removed. Extraction was performed using 300 µL chloroform and centrifuged at 14,000 rpm for 5 minutes. The upper aqueous layer was removed. NaCl (5 M, 1/10 volume) was added and tubes were inverted to mix. An equal volume isopropanol was added and tubes were inverted to mix until DNA precipitation was observed. DNA was removed with a glass hook and washed in 1 mL 70% ethanol. DNA was pelleted and excess ethanol was removed. The pellet was allowed to air dry until residual ethanol evaporated. The pellet was resuspended in appropriate volume of 10mM TRIS. DNA was then cleaned using PowerClean DNA Clean-Up Kit (MoBio, Carlsbad, CA 92010.) as per the manufacturer's protocol.

## **Genome sequencing of WMMA2032**

Complete genome of WMMA2032 (*Micromonospora* sp.) and WMMA184 (*Dietzia* sp.) were sequenced at the University of Washington using Pac Bio RS II (Pacific Biosciences) technology. Reads were assembled via the HGAP assembler into one contig of 6.4 Mb.

## **Genome sequencing of WMMA184**

The complete genome of *Dietzia* sp. WMMA184 was sequenced at the Duke Center for Genomic and Computational Biology (GCB) using Pac Bio RS II (Pacific Biosciences) technology. Reads were assembled using the HGAP assembler into six contigs.<sup>25</sup>

## **Bacterial large-scale culture:**

WMMA2032 and WMMA187 seed cultures were each inoculated into 5 x 10 mL cultures (25 × 150 mm tubes) of Artificial Sea Water-A medium (20 g soluble starch, 10 g glucose, 5 g peptone, 5 g yeast extract, 5 g CaCO3 per liter of artificial seawater), grown for 3 days and 2 days respectively. Separate salt solution I (415.2 g NaCl, 69.54 g Na<sub>2</sub>SO<sub>4</sub>, 11.74 g KCl, 3.40 g NaHCO<sub>3</sub>, 1.7 g KBr, 0.45 g H<sub>3</sub>BO<sub>3</sub>, 0.054 g NaF) and II (187.9 g MgCl<sub>2</sub>·6H<sub>2</sub>O, 22.72 g CaCl<sub>2</sub>·2H<sub>2</sub>O, 0.428 g SrCl<sub>2</sub>·6H<sub>2</sub>O) were made up and combined to give a total volume of 20 L. One liter monocultures of both the bacteria and their co-culture were also grown in ASW-A media with 70g/L of Diaion HP20 resin. To do this, 10 mL of WMMA2032 and WMMA187 were added to 1-liter each of ASW-A media for the monocultures, and 30mL of WMMA2032 and 10mL of WMMA187 were inoculated into 1-liter of ASW-A for co-culture fermentation. All three cultures were incubated in a shaker at 28 °C with 280 RPM for 7 days. The HP20 resin was filtered and washed and subsequently extracted with acetone. The acetone extracts for WMMA2032 (1.55g), WMMA187

(2.40g) and WMMA2032-WMMA187 co-culture (1.51g) were subjected to liquid-liquid partition, first using 10% aqueous MeOH and hexane (1:1) and then 30% aqueous MeOH and chloroform (1:1), resulting in 92 mg, 73 mg, and 140 mg of chloroform partition extracts respectively. Each of these was subjected to a Sephadex LH-20 column with MeOH:CHCl<sub>3</sub> (1:1), and 7 fractions were collected. The fraction containing 1 and 2 (36 mg) was partially subjected to RP HPLC (10/90% to 100/0% ACN-0.1% Acetic acid water in 42 mins) using Phenomenex Luna Phenylhexyl column (250 × 10 mm, 5μm).

#### Metabolomics of co-culture using UPLC/ESI-TOF-MS and PCA:

Aliquots of 1.5 mL from each culture was collected for metabolomic analyses. The collected samples were centrifuged at 3000RPM for 5 mins and the supernatant was processed using solid phase extraction and analyzed using UHPLC/UV/qTOF-HRESI-MS/MS. Briefly, solubilized extracts in 10:1 H<sub>2</sub>O: MeOH were subjected to automated SPE using a Gilson GX-271 liquid handling system. Extracts were loaded onto EVOLUTE ABN SPE cartridges (25 mg absorbent mass, 1 mL reservoir volume; Biotage, S4 Charlotte, NC), washed with water and eluted with MeOH (500 μL) directly into an LC/MS-certified vial. LC/MS data were acquired using a Bruker MaXis ESI-qTOF mass spectrometer (Bruker, Billerica, MA) coupled with a Waters Acquity UPLC system (Waters, Milford, MA) operated by Bruker Hystar software. Chromatographic separations were achieved with a gradient of MeOH and H<sub>2</sub>O (containing 0.1% formic acid) on an RP C-18 column (Phenomenex Kinetex 2.6 μm, 2.1 x 100 mm; Phenomenex, Torrance, CA) at a flow rate of 0.3 mL/min. The method was as follows: 1-12 min (10%-97% MeOH in H<sub>2</sub>O) and 12-14 min (97% MeOH). Full scan HRMS data (m/z 150–1550) were collected in positive ESI mode. The mass spectrometer was operated using the following parameters: capillary, 4.5 kV; nebulizer pressure, 1.2 bar; dry gas flow, 8.0 L/min; dry gas temperature, 205 °C; scan rate, 2 Hz. Tune mix

(ESI-L low concentration; Agilent, Santa Clara, CA) was introduced through a divert valve at the end of each chromatographic run for automated internal calibration.

#### PCA of LC/MS Data

Bucketing LC/MS data and PCA was performed using Bruker Profile Analysis 2.0 software. LC/MS bucketing was performed using the following parameters: data selection and processing, Find Molecular Features; spectrum type, line; spectrum polarity, positive; spectral range, 2–12 minutes and m/z=150–1500; advanced bucketing, 20 seconds and 20 mDa window; normalization: Sum of bucket values in analysis. PCA was performed on bucket tables using a Pareto scaling algorithm.

## Genomic analysis for biosynthetic gene cluster identification:

The WMMA2032 genome was analyzed using PRISM 3<sup>26</sup> and AntiSmash v4<sup>27</sup>. The parameters for AntiSmash included ClusterFinder with ClusterFinder algorithm for border prediction and the following features activated: KnownClusterBlast, ClusterBlast, SubClusterBlast, smCoG analysis, ActiveSiteFinder, Detect TTA codons, Whole-genome PFAM analysis. PRISM analysis was conducted using default parameters which uses Prodigal for gene prediction and 10000bp as the maximum length between open reading frame to consider them part of the same BGC. All of the optional search options were enabled.

## **Antibiotic Activity Screening:**

For testing activity against Methicillin-sensitive *S. aureus* (MSSA) an agar-based antibiotic assay was used as reported before.<sup>13</sup> Seed cultures of the strain to be screened were grown overnight in 10 mL of LB media (10g Tryptone, 5 g Yeast extract, 10 g NaCl into 1 L ddH<sub>2</sub>O)(25 x 150 mm tubes). To prepare uniform lawns for screening, 400 µL of overnight culture was inoculated into

200 mL of cation-adjusted Mueller-Hinton agar (CAMHA) (1.5 g soluble starch, 17.5 g casein, 3 g beef extract, 15 g agar, 12.5 mg Mg<sup>2+</sup> and 25 mg Ca<sup>2+</sup> in 1 L milli-Q H2O) and maintained at 50–55 °C. For each screening plate, 30 mL of inoculated agar was poured into OmniTray (Thermo Scientific, Waltham, MA) and cooled for 30 min. The extract tested at each stage of fractionation was dissolved in MeOH to a final concentration of 20  $\mu$ g/ $\mu$ L, and 5  $\mu$ L was spotted onto the agar. Screening plates were incubated at 37 °C overnight and subsequently visually observed for zones of inhibition.

# 4.5 References

- (1) Cimermancic, P.; Medema, M. H.; Claesen, J.; Kurita, K.; Wieland Brown, L. C.; Mavrommatis, K.; Pati, A.; Godfrey, P. A.; Koehrsen, M.; Clardy, J.; et al. Insights into Secondary Metabolism from a Global Analysis of Prokaryotic Biosynthetic Gene Clusters. Cell 2014, 158 (2), 412–421.
- (2) Stone, M. J.; Williams, D. H. On the Evolution of Functional Secondary Metabolites (Natural Products). *Mol. Microbiol.* **1992**, *6* (1), 29–34.
- (3) Michael A. Fischbach, A.; Walsh, C. T. Assembly-Line Enzymology for Polyketide and Nonribosomal Peptide Antibiotics: Logic, Machinery, and Mechanisms. **2006**.
- (4) Bachmann, B. O.; Ravel, J. Chapter 8 Methods for In Silico Prediction of Microbial Polyketide and Nonribosomal Peptide Biosynthetic Pathways from DNA Sequence Data. *Methods in Enzymology*. 2009.
- (5) Hertweck, C. Hidden Biosynthetic Treasures Brought to Light. *Nat. Chem. Biol.* **2009**, *5* (7), 450–452.
- (6) Swiątek, M. A.; Gubbens, J.; Bucca, G.; Song, E.; Yang, Y.-H.; Laing, E.; Kim, B.-G.; Smith, C. P.; van Wezel, G. P. The ROK Family Regulator Rok7B7 Pleiotropically Affects Xylose Utilization, Carbon Catabolite Repression, and Antibiotic Production in Streptomyces Coelicolor. *J. Bacteriol.* 2013, 195 (6), 1236–1248.
- (7) Rigali, S.; Titgemeyer, F.; Barends, S.; Mulder, S.; Thomae, A. W.; Hopwood, D. A.; van Wezel, G. P. Feast or Famine: The Global Regulator DasR Links Nutrient Stress to Antibiotic Production by Streptomyces. *EMBO Rep.* **2008**, *9* (7), 670–675.
- (8) Brakhage, A. A.; Schroeckh, V. Fungal Secondary Metabolites Strategies to Activate Silent Gene Clusters. *Fungal Genet. Biol.* **2011**, *48* (1), 15–22.
- (9) Ohnishi, Y.; Kameyama, S.; Onaka, H.; Horinouchi, S. The A-Factor Regulatory Cascade Leading to Streptomycin Biosynthesis in Streptomyces Griseus: Identification of a Target Gene of the A-Factor Receptor. *Mol. Microbiol.* **1999**, *34* (1), 102–111.
- (10) Chater, K. F.; Bir??, S.; Lee, K. J.; Palmer, T.; Schrempf, H. The Complex Extracellular Biology of Streptomyces: REVIEW ARTICLE. *FEMS Microbiol. Rev.* **2010**, *34* (2), 171–198.
- (11) Laureti, L.; Song, L.; Huang, S.; Corre, C.; Leblond, P.; Challis, G. L.; Aigle, B. Identification of a Bioactive 51-Membered Macrolide Complex by Activation of a Silent

- Polyketide Synthase in Streptomyces Ambofaciens. *Proc. Natl. Acad. Sci. U. S. A.* **2011**, *108* (15), 6258–6263.
- (12) Takano, E.; Kinoshita, H.; Mersinias, V.; Bucca, G.; Hotchkiss, G.; Nihira, T.; Smith, C. P.; Bibb, M.; Wohlleben, W.; Chater, K. A Bacterial Hormone (the SCB1) Directly Controls the Expression of a Pathway-Specific Regulatory Gene in the Cryptic Type I Polyketide Biosynthetic Gene Cluster of Streptomyces Coelicolor. *Mol. Microbiol.* 2005, 56 (2), 465–479.
- (13) Adnani, N.; Vazquez-Rivera, E.; Adibhatla, S.; Ellis, G.; Braun, D.; Bugni, T. Investigation of Interspecies Interactions within Marine Micromonosporaceae Using an Improved Co-Culture Approach. *Mar. Drugs* 2015, *13* (10), 6082–6098.
- (14) Adnani, N.; Chevrette, M. G.; Adibhatla, S. N.; Zhang, F.; Yu, Q.; Braun, D. R.; Nelson, J.; Simpkins, S. W.; McDonald, B. R.; Myers, C. L.; et al. Coculture of Marine Invertebrate-Associated Bacteria and Interdisciplinary Technologies Enable Biosynthesis and Discovery of a New Antibiotic, Keyicin. ACS Chem. Biol. 2017, 12 (12), 3093–3102.
- (15) YEO, W.-H.; YUN, B.-S.; KIM, S.-S.; PARK, E.-K.; KIM, Y.-H.; YOO, I.-D.; YU, S.-H. GTRI-02, a New Lipid Peroxidation Inhibitor from Micromonospora Sp. SA246. *J. Antibiot. (Tokyo).* **1998**, *51* (10), 952–953.
- (16) Weber, T.; Blin, K.; Duddela, S.; Krug, D.; Kim, H. U.; Bruccoleri, R.; Lee, S. Y.; Fischbach, M. A.; Müller, R.; Wohlleben, W.; et al. AntiSMASH 3.0—a Comprehensive Resource for the Genome Mining of Biosynthetic Gene Clusters. *Nucleic Acids Res.* **2015**, 43 (W1), W237–W243.
- (17) Skinnider, M. A.; Dejong, C. A.; Rees, P. N.; Johnston, C. W.; Li, H.; Webster, A. L. H.; Wyatt, M. A.; Magarvey, N. A. Genomes to Natural Products PRediction Informatics for Secondary Metabolomes (PRISM). *Nucleic Acids Res.* 2015, 43 (20), gkv1012.
- (18) Fotsoa, S.; Maskeya, R. P.; Grun-Wollnyb, I.; Schulzc, K.-P.; Munkc, M.; Laatscha, H. Bhimamycin A-E and Bhimanone: Isolation, Structure Elucidation and Biological Activity of Novel Quinone Antibiotics from a Terrestrial Streptomycete; 2003; Vol. 56.
- (19) Bringmann, G.; Noll, T. F.; Gulder, T. A. M.; Grüne, M.; Dreyer, M.; Wilde, C.; Pankewitz, F.; Hilker, M.; Payne, G. D.; Jones, A. L.; et al. Different Polyketide Folding Modes Converge to an Identical Molecular Architecture. *Nat. Chem. Biol.* 2006, 2 (8), 429–433.

- (20) Romero-Rodríguez, A.; Robledo-Casados, I.; Sánchez, S. An Overview on Transcriptional Regulators in Streptomyces. *BBA Gene Regul. Mech.* **2015**, *1849*, 1017–1039.
- (21) Quévrain, E.; Domart-Coulon, I.; Pernice, M.; Bourguet-Kondracki, M.-L. Novel Natural Parabens Produced by a Microbulbifer Bacterium in Its Calcareous Sponge Host Leuconia Niveae Mi\_1880 1527..1539. **2009**.
- (22) Miyuki Nishijima; Takadera, Takahide; Imamura, Nobutaka; Kasai, Hiroaki; An, Kwang-Deuk; Adachi, Kyoko; Nagao, Tomokazu; Sano, Hiroshi; Yamasato, K. Microbulbifer Variabilis Sp. Nov. and Microbulbifer Epialgicus Sp. Nov., Isolated from Pacific Marine Algae, Possess a Rod–coccus Cell Cycle in Association with the Growth Phase. *Int. J. Syst. Evol. Microbiol.* **2009**, *59*, 1696–1707.
- (23) Nagao, T., Adachi, K., Nishida, F., Nishijima, M. & Mochida, K. Butyl and Octyl 3-Acetamido-4-Hydroxybenzoate as Fat-Soluble UV Absorbers, and Their Manufacture with Pelagiobacter Species. 2000016976, 2000.
- (24) Li, K.; Li, Q.-L.; Ji, N.-Y.; Liu, B.; Zhang, W.; Cao, X.-P.; Li, K.; Li, Q.-L.; Ji, N.-Y.; Liu, B.; et al. Deoxyuridines from the Marine Sponge Associated Actinomycete Streptomyces Microflavus. *Mar. Drugs* **2011**, *9* (5), 690–695.
- (25) Braun, D. R.; Chevrette, M. G.; Acharya, D.; Currie, C. R.; Rajski, S. R.; Ritchie, K. B.; Bugni, T. S. Complete Genome Sequence OfDietziasp. Strain WMMA184, a Marine Coral-Associated Bacterium. *Genome Announc.* **2018**, *6* (5), e01582-17.
- (26) Skinnider, M. A.; Merwin, N. J.; Johnston, C. W.; Magarvey, N. A. PRISM 3: Expanded Prediction of Natural Product Chemical Structures from Microbial Genomes. *Nucleic Acids Res.* **2017**, *45* (W1), W49–W54.
- (27) Blin, K.; Wolf, T.; Chevrette, M. G.; Lu, X.; Schwalen, C. J.; Kautsar, S. A.; Suarez Duran, H. G.; de los Santos, E. L. C.; Kim, H. U.; Nave, M.; et al. AntiSMASH 4.0—improvements in Chemistry Prediction and Gene Cluster Boundary Identification. *Nucleic Acids Res.* **2017**, *45* (W1), W36–W41.

# Chapter 5: Mechanistic insight into interspecies interaction of gut symbionts

# 5.1 Introduction

From the studies described in Chapters 2-4 of this thesis, and the literature surveyed therein, it is clear that bacterial communication has a significant impact on the behavior of microbes. Not only do bacteria sense the presence of other species or strains around them, they regulate the production of their biosynthetic arsenal accordingly. Unsurprisingly, the phenomenon of bacterial interaction is not limited to terrestrial or marine bacteria, and is in fact ubiquitous in nature. The mammalian gastrointestinal tract, in particular, serves as the ideal milieu for these interactions to take place, considering trillions of bacteria co-exist there. Recent focus on these commensal bacteria has led to increased understanding of their composition, metabolism and impact on the host's health. Although the genomes of these bacteria lack the extensive scope of secondary biosynthetic machinery that exists in Actinobacteria, heir close association with the host makes the study of gut microbiome crucial. Nutrient metabolism, drug metabolism, immunomodulation, immunomodulation, and maintaining the structure and function of the gastrointestinal tract.

Lactobacillus reuteri inhabits the gut of a diverse range of mammals, such as pigs, mice and rats, and also some species of birds, <sup>18</sup> and is a model organism to study different interactions within the host's body. <sup>19,20</sup> In this chapter, we report a collaborative study with M. Ozcam and J. P. Van Pijkeren to understand the dynamics between two gut bacterial strains of Lactobacillus reuteri: L. reuteri R2lc and L. reuteri 100-23. The first of these two strains, inhibits the other in

mixed fermentations. The overarching goal for the project described here was to discover how R2lc outcompetes 100-23 in their co-cultures.

In a previous study, Ozcam *et al.* identified two polyketide synthase (PKS) clusters (designated pks1 and pks2) in *L. reuteri* R2lc with unknown products. They also reported the development of PKS mutants R2lcΔpks1 or R2lcΔpks2.<sup>21</sup> For this study, they hypothesized that one of the PKS clusters may be conferring competitive advantage over *L. reuteri* 100-23, since PKS products can often have antimicrobial properties. Several biological assays conducted by Ozcam and coworkers helped verify this hypothesis; some of these experiments will be described briefly here. We conducted complimentary chemical experiments, utilizing our expertise in metabolomics of co-cultures, to elucidate the mechanism of interaction between the strains and to discover the PKS product.

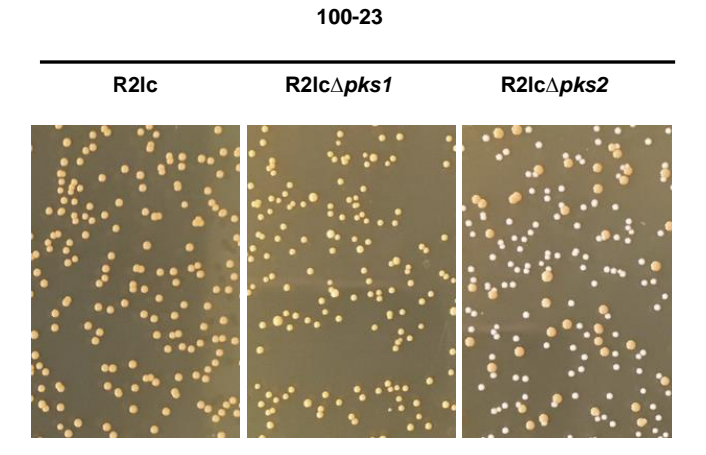


**Figure 5-1.** A polyketide synthase cluster in *L. reuteri* R2lc provides competitive advantage. *L. reuteri* R2lc, R2lc∆pks1 but not R2lc∆pks2 suppress 100-23 in vitro. Unpublished data, printed with permission of Mustafa Özçam and JP van Pijkeren (Dept. of Food Science, UW-Madison)

Using the PKS deletion mutants and the wild-type strains, our collaborators performed an *in vitro* competition experiment by mixing each of these strains with 100-23. They found that both wild-type R2lc and R2lcΔpks1, but not R2lcΔpks2, inhibited 100-23, suggesting that the product of cluster pks2 is required for the competitive advantage (Figure 5-1, unpublished data). Subsequent *in vivo* experiments in germ-free mice with 1:1 mixture of R2lc and 100-23 in one

group and R2lcΔpks2 and 100-23 in another confirmed this finding. Over a period of six days, R2lc/100-23 competition ratio was 980-fold, whereas R2lcΔpks2/100-23 competition ratio was 3.6-fold (p=0.05) (unpublished data).<sup>22</sup>

Our aims for understanding the chemical interaction between R2lc and 100-23 were two-fold: i) comparative metabolomics analysis of R2lc and R2lcΔpks2 to delineate the impact of the Δpks2 cluster and, ii) determine the impact of cell-cell contact on inhibition of 100-23 growth.

## **5.2 Results and Discussion:**

#### R2lc pks2 product determined using comparative metabolomics

*In vitro* and *in vivo* experiments where *L. reuteri* strains R2lc (wild type and Δpks2) and 100-23 were grown together, showed clear inhibition of 100-23 in the presence of R2lc and not R2lcΔpks2 (Figure 5-1). These results directed us to evaluate the metabolomic output of these strains in the presence of 100-23 in a time dependent manner, in an effort to better understand the secondary metabolite output of cluster pks2. Simultaneously, we performed a time-course analysis of the *in vitro* competition to better corroborate the metabolite profile with biological activity.

Bacterial cultures of R2lc and R2lcΔpks2 were grown co-cultured with 100-23 in liquid media in 500 mL flasks, in a one-to-one ratio. Monocultures of all three strains were also similarly grown. Aliquots from each of these cultures were collected every two hours for 12 hours, and then at 24 hours. The collected samples were first incubated with MeOH for cell lysis, to ensure that our successive analyses included not only the extracellular metabolites secreted into the medium, but also intra-cellular metabolites. Subsequently, these samples were processed and analyzed using UPLC-PDA-MS. This data showed that R2lc, in both co-culture and mono-culture produced unique compounds, which were not produced by the mutant R2lcΔpks2. These compounds had a

maximum absorption wavelength of 380nm (Figure 5-2A) and eluted towards the end of the gradient run where the solvent composition was close to 100% MeOH, indicating hydrophobic characteristics. The large retention time of the compounds on the C18 column and the maximum absorption wavelength of 380 nm was consistent with the putative product of the R2lc pks2 cluster, which was predicted to produce polyene compounds. Extracted UV chromatogram of R2lc over time at 380 nm showed an increase in the production of these compounds up to 12 hours of incubation, after which the intensity reduced as shown in samples at 24 hours. Together these data suggested that putative polyene compounds were produced in a time-dependent manner (Figure 5-2A) and were not contingent on the presence of 100-23. The bacterial strains were similarly grown in a parallel study to evaluate the competitive interaction over time. Samples taken at the same time points of every two hours for 12 hours for each of three monocultures and two co-cultures were plated on culture plates and incubated. The colony forming units (CFU)/mL were estimated for each of the time points. The results confirmed that PKS-mediated 100-23 inhibition was time dependent and started at 6-hour after R2lc and 100-23 were co-cultured at one-to-one ratio. After ten hours, 4-log fewer 100-23 were recovered compared to R2lc (Figure 5-2B). As a result, we concluded that the R2lc exhibited inhibitory activity in tandem with the production of the polyene.

We subsequently analyzed the LCMS data of the monoculture and co-culture samples collected above to identify the polyene products produced by R2lc. LCMS data for samples with the highest concentration of the polyene (at 12 hours of incubation) for each of the conditions were processed using Bruker Profile Analysis, as described previously.<sup>23</sup> The molecule feature finding algorithm with advanced bucketing was used to generate the spectral table consisting of retention time (RT) and m/z pairs; each of these RT-m/z pairs represent a compound. To identify the molecules exclusive to R2lc or R2lc co-culture, the ions which are also present in R2lc  $\Delta$ pks2 or R2lc  $\Delta$ pks2 co-culture were filtered out. Subsequently, only the compounds eluting between the retention times 10.20 min and 10.90 min were analyzed to find the molecules consistent with the

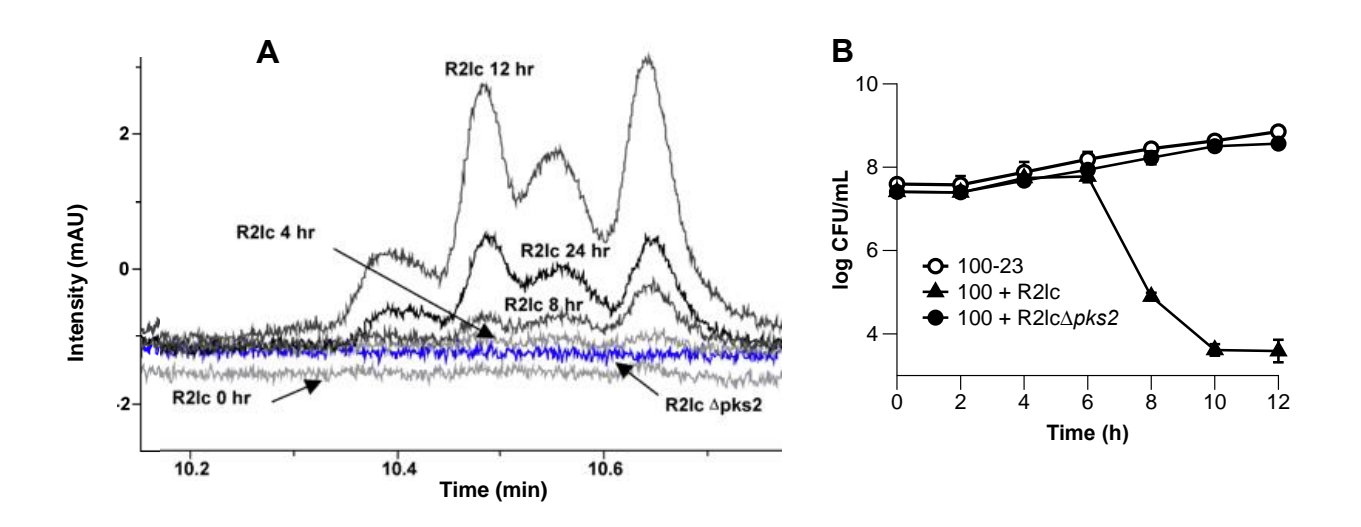


**Figure 5-2.** *L. reuteri*-pks inhibits 100-23 in a time dependent manner. A) UPLC-PDA-MS analysis of R2lc and Δpks2 mutant. R2lc but not Δpks2 produces unique compounds with a maximum absorption of 380nm (Black: R2lc, blue: Δpks2) B). R2lc has bactericidal effect against 100-23. Single culture (OD600=0.1) or co-cultures (OD600=0.05 from each strain) were mixed and incubated in MRS broth (pH: 4.0, 37°C) and samples were collected every two hours for up to 12 hours. The data represents the average of three independent experiments. Error bars represents standard deviation. Figure 5-2b shows unpublished data, printed with permission of Mustafa Özçam and JP van Pijkeren (Dept. of Food Science, UW-Madison)

UV absorption at 380 nm (Fig. 3B). Through this approach several compounds were identified as putative molecules of interest, unique to R2lc.

The mass spectrum of the peak between 10.52 min – 10.58 min in the R2lc chromatogram at 12 hours clearly showed an ion with m/z [M+H]<sup>+</sup> value of 257.1172 and corresponding m/z [M+Na]<sup>+</sup> value of 279.0092, which were absent in the 12-hour culture of R2lc  $\Delta$ pks2 (Figure 5-

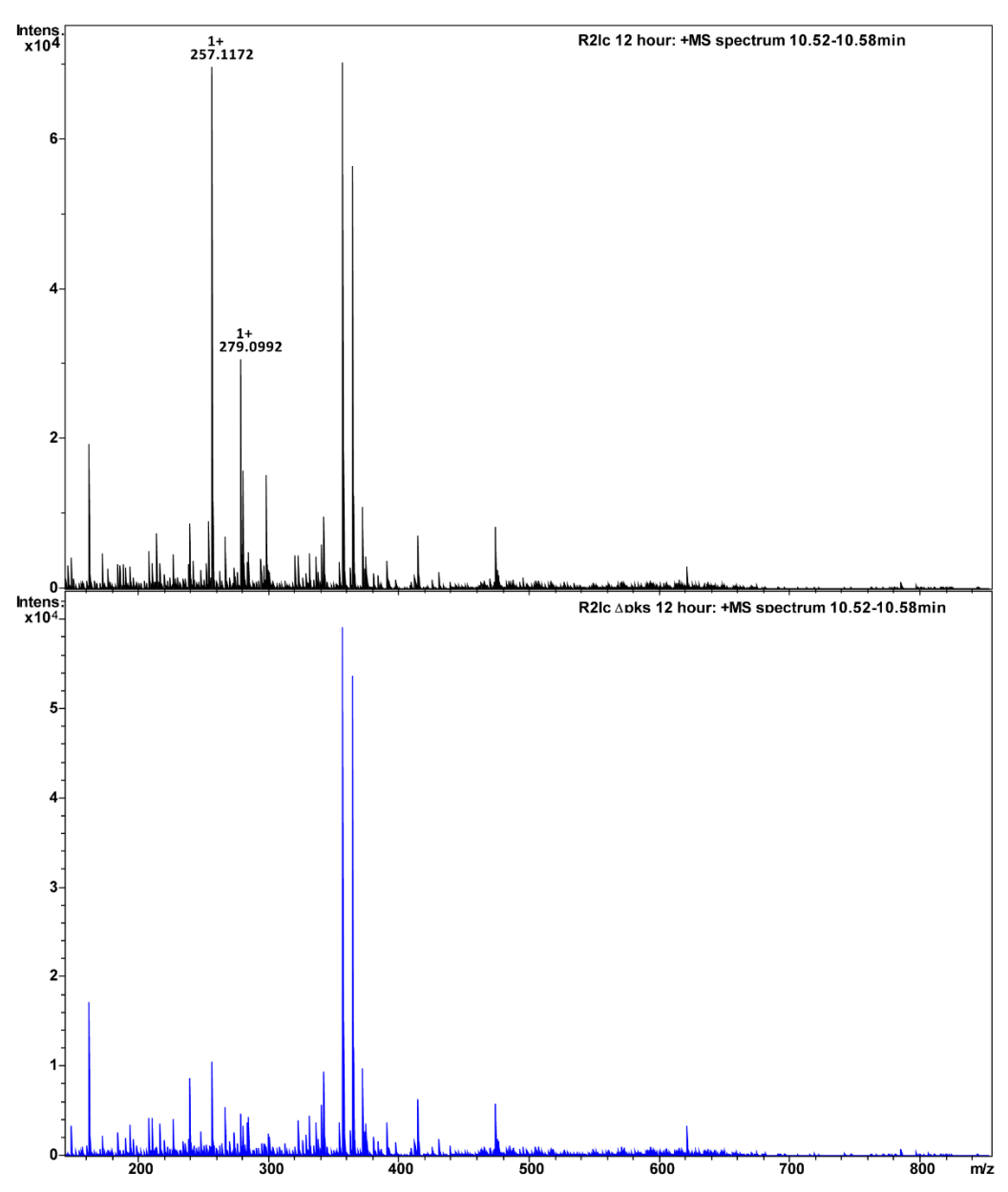


**Figure 5-3.** Mass spectra of R2lc and R2lc  $\triangle$ pks2-PKS between 1052-10.58 min corresponding to a peak found only in R2lc (black) but not R2lc  $\triangle$ pks2-PKS (blue). The R2lc spectra shows presence of m/z 257.1172 and m/z 279.0992, not found in the other.

3). This ion was one of the molecules of interest found in the bucket table (Appendix). Bruker SmartFormula algorithm, which uses both the exact mass of the molecular ion and the isotopic pattern allowed accurate determination of the molecular formula as  $C_{16}H_{16}O_3$ . Antibase, a comprehensive database of natural compounds from bacteria and fungi allowed for swift dereplication of this compound, which was identified as Calostomal,<sup>24</sup> a polyene pigment from *Gasteromycete Calostoma cinnabarinum*.

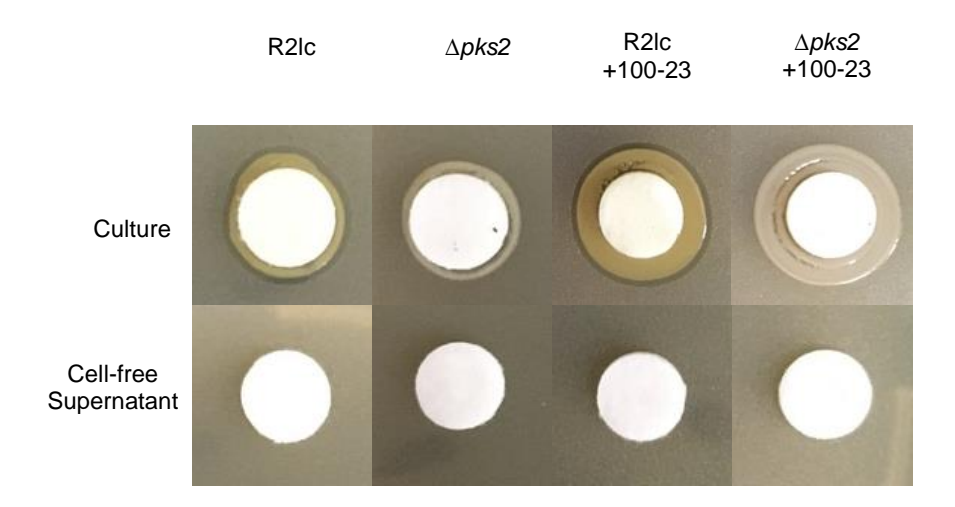


**Figure 5-4.** R2lc-PKS inhibits 100-23 in a cell-to-cell contact dependent manner. *L. reuteri* 100-23 culture was diluted 100-fold, mixed with MRS top agarose and poured on MRS agar plates. Represented strains were added on discs and placed on 100-23 top agarose followed by incubation for 24 hours. Unpublished data, printed with permission of Mustafa Özçam and JP van Pijkeren (Dept. of Food Science, UW-Madison).

## Mechanistic insight into R2lc and 100-23 interaction

Since a small molecule product of the pks2 cluster from R2lc was implicated in the inhibition of 100-23, we set out to understand if cell-cell interaction was required for the inhibition, or if cell-free supernatant from R2lc was sufficient. Our collaborators performed a disc-diffusion assay where R2lc cell-culture and its cell-free supernatant were separately tested against 100-23. It was clear from this experiment that that R2lc culture but not R2lc cell-free supernatant yielded a zone of inhibition. Importantly, R2lc and 100-23 co-culture yielded a similar size zone of

inhibition to R2lc culture whereas the cell-free supernatant of co-culture was not effective against 100-23 (Figure 5-4), suggesting that R2lc-mediated inhibition might be contact dependent.

To confirm that cell-cell contact was indeed necessary for 100-23 inhibition, we conducted the connected flask assay as described by our lab before. Here, the R2lc and 100-23 monocultures were grown in flasks separated by a 0.2 µm diffusible membrane that allowed free movement of small molecules. Additionally, R2lc and 100-23 co-cultures were also grown together on one side of the flask, separated from 100-23 monoculture on the other side of the membrane. By plating these cultures after 16 hours of incubation, we found that only in the flasks where cell-cell contact was allowed (the co-culture), was the growth of 100-23 inhibited. There was no reduction in 100-23 growth when R2lc was separated through a 0.2 µm diffusible membrane. These results strongly suggested that even though the pkk2 product was necessary for inhibition of 100-23, cell-cell contact was also required.

## 5.3 Conclusion

Intercellular communication, be it microbe-microbe or microbe-host, has myriad causes and outcomes, ranging from nutrient acquisition and antibiosis to biofilm formation and pathogenesis. In the case of the gut microbiome, where a complex group of bacteria have access to the same limited resources, having a competitive advantage is crucial. The preliminary studies found that *Lactobacillus reuteri* R2lc had higher fitness compared to other strains. Our subsequent metabolomics studies proved that R2lc indeed produced a polyene that was the direct product of the polyketide cluster (pks2). We further demonstrated that inhibition of *Lactobacillus reuteri* 100-23 is cell contact dependent. These results together provided a clearer understanding of bacterial interaction in the gut microbiome, which is crucial to elucidating the ecological and evolutionary relationships and also exploiting them for better health outcome for the host.

#### **5.4 Materials and Methods**

#### **Bacterial strains and culture conditions**

*L. reuteri* strains were cultured in De Man Rogosa Sharpe (MRS) medium (Difco, BD BioSciences). Unless stated otherwise, we prepared bacterial cultures as follows: *L. reuteri* strains were incubated at 37 °C under hypoxic conditions (5% CO<sub>2</sub>, 2% O<sub>2</sub>).

#### **Disc-diffusion assay**

*L. reuteri* 100-23 cells ( $10^6$  CFU) were mixed with 2 mL MRS containing 0.3% agarose and poured on MRS plates and dried for 10 min at room temperature. Sterile Whatman paper (Buckinghamshire, UK) discs were dipped into *L. reuteri* R2lc, R2lc $\Delta pks2$ , R2lc+100-23 and R2lc $\Delta pks2$ +100-23 cultures (OD<sub>600</sub>:2.0) for 5 seconds. Then cultures were filter sterilized and sterile discs were dipped into cell-free supernatants. Plates were incubated overnight.

## Mechanism of interaction using connected flask study:

Customized connected flasks were used to grow R2lc and 100-23, wherein a 0.2  $\mu$ m diffusible membrane separated each of the cultures, allowing exchange of metabolites but eliminating cell-cell contact<sup>25</sup>. The culture volume in each flask was 200 ml and the flasks were incubated with a platform shaker at 50 RPM at 37  $^{\circ}$ C.

## LC/MS Sample preparation

An aliquot of 1.5 ml from each of the cultures were collected in Eppendorf tubes and centrifuged at 5000 RPM for 5 min. The supernatants were collected and transferred to 1-dram vials and the cell pellets were incubated with 100  $\mu$ L of methanol for 1 hr. After the incubation period, the samples were centrifuged again, and the methanol extracts of the cells were added to the respective 1-dram vials. A Gilson GX-271 liquid handling system was used to subject 900  $\mu$ L

of the samples to automated solid phase extraction (SPE). Extracts were loaded onto preconditioned (1 mL MeOH followed by 1 mL H2O) EVOLUTE ABN SPE cartridges (25 mg absorbent mass, 1 mL reservoir volume; Biotage, S4 Charlotte, NC). Samples were subsequently washed using H<sub>2</sub>O (1 mL) to remove media components and eluted with MeOH (500 μL) directly into an LC/MS-certified vial.

## **UHPLC/HRESI-qTOF-MS** Analysis of Extracts

LC/MS data were acquired using a Bruker MaXis ESI-qTOF mass spectrometer (Bruker, Billerica, MA) coupled with a Waters Acquity UPLC system (Waters, Milford, MA) with a PDA detector operated by Bruker Hystar software, as previously described <sup>23</sup>. Briefly, a solvent system of MeOH and H<sub>2</sub>O (containing 0.1% formic acid) was used on an RP C-18 column (Phenomenex Kinetex 2.6µm, 2.1 x 100 mm; Phenomenex, Torrance, CA) at a flow rate of 0.3 mL/min. The chromatogram method started with a linear gradient from MeOH/H2O (10%/90%) to MeOH/H<sub>2</sub>O (97%/3%) in 12 min, then held for 2 min at MeOH/H<sub>2</sub>O (97%/3%). Full scan mass spectra (*m/z* 150–1550) were measured in positive ESI mode. The mass spectrometer was operated using the following parameters: capillary, 4.5 kV; nebulizer pressure, 1.2 bar; dry gas flow, 8.0 L/min; dry gas temperature, 205 °C; scan rate, 2 Hz. Tune mix (ESI-L low concentration; Agilent, Santa Clara, CA) was introduced through a divert valve at the end of each chromatographic run for automated internal calibration. Bruker Data Analysis 4.2 software was used for analysis of chromatograms.

# **5.5 References**

- (1) Shank, E. A.; Kolter, R. New Developments in Microbial Interspecies Signaling. *Curr. Opin. Microbiol.* **2009**, *12* (2), 205–214.
- (2) Scherlach, K.; Hertweck, C. Mediators of Mutualistic Microbe–Microbe Interactions. *Nat. Prod. Rep.* **2018**.
- (3) Vogt, S. L.; Peña-Díaz, J.; Finlay, B. B. Chemical Communication in the Gut: Effects of Microbiota-Generated Metabolites on Gastrointestinal Bacterial Pathogens. *Anaerobe* 2015, 34, 106–115.
- (4) Bäckhed, F.; Ley, R. E.; Sonnenburg, J. L.; Peterson, D. A.; Gordon, J. I. Host-Bacterial Mutualism in the Human Intestine. *Science* (80). **2005**, 307, 1915–1920.
- (5) Sender, R.; Fuchs, S.; Milo, R. Revised Estimates for the Number of Human and Bacteria Cells in the Body. *PLoS Biol.* **2016**, *14* (8), e1002533.
- (6) Zhang, F.; Braun, D. R.; Ananiev, G. E.; Hoffmann, F. M.; Tsai, I.-W.; Rajski, S. R.; Bugni, T. S. Biemamides A–E, Inhibitors of the TGF-β Pathway That Block the Epithelial to Mesenchymal Transition. *Org. Lett.* **2018**, *20* (18), 5529–5532.
- (7) Wyche, T. P.; Piotrowski, J. S.; Hou, Y.; Braun, D.; Deshpande, R.; McIlwain, S.; Ong, I. M.; Myers, C. L.; Guzei, I. a.; Westler, W. M.; et al. Forazoline A: Marine-Derived Polyketide with Antifungal in Vivo Efficacy. *Angew. Chemie Int. Ed.* 2014, 53 (43), 11583–11586.
- (8) Zhang, F.; Barns, K.; Hoffmann, F. M.; Braun, D. R.; Andes, D. R.; Bugni, T. S. Thalassosamide, a Siderophore Discovered from the Marine-Derived Bacterium *Thalassospira Profundimaris. J. Nat. Prod.* 2017, 80 (9), 2551–2555.
- (9) Macfarlane, S.; Macfarlane, G. T. Regulation of Short-Chain Fatty Acid Production. *Proc. Nutr. Soc.* **2003**, *62* (01), 67–72.
- (10) Winter, J.; Moore, L. H.; Dowell, V. R.; Bokkenheuser, V. D. C-Ring Cleavage of Flavonoids by Human Intestinal Bacteria. *Appl. Environ. Microbiol.* **1989**, *55* (5), 1203–1208.
- (11) Wallace, B. D.; Wang, H.; Lane, K. T.; Scott, J. E.; Orans, J.; Koo, J. S.; Venkatesh, M.; Jobin, C.; Yeh, L.-A.; Mani, S.; et al. Alleviating Cancer Drug Toxicity by Inhibiting a Bacterial Enzyme. *Science* (80-. ). **2010**, 330 (6005), 831–835.

- (12) Clayton, T. A.; Baker, D.; Lindon, J. C.; Everett, J. R.; Nicholson, J. K. Pharmacometabonomic Identification of a Significant Host-Microbiome Metabolic Interaction Affecting Human Drug Metabolism. *Proc. Natl. Acad. Sci.* 2009, 106 (34), 14728–14733.
- (13) Hooper, L. V. Do Symbiotic Bacteria Subvert Host Immunity? *Nat. Rev. Microbiol.* **2009**, 7 (5), 367–374.
- (14) Hasegawa, M.; Osaka, T.; Tawaratsumida, K.; Yamazaki, T.; Tada, H.; Chen, G. Y.; Tsuneda, S.; Nunez, G.; Inohara, N. Transitions in Oral and Intestinal Microflora Composition and Innate Immune Receptor-Dependent Stimulation during Mouse Development. *Infect. Immun.* 2010, 78 (2), 639–650.
- (15) Lutgendorff, F.; Akkermans, L. M. A.; Söderholm, J. D. The Role of Microbiota and Probiotics in Stress-Induced Gastro-Intestinal Damage. *Curr. Mol. Med.* **2008**, *8* (4), 282–298.
- (16) Stappenbeck, T. S.; Hooper, L. V.; Gordon, J. I. Nonlinear Partial Differential Equations and Applications: Developmental Regulation of Intestinal Angiogenesis by Indigenous Microbes via Paneth Cells. *Proc. Natl. Acad. Sci.* 2002, 99 (24), 15451–15455.
- (17) Jandhyala, S. M.; Talukdar, R.; Subramanyam, C.; Vuyyuru, H.; Sasikala, M.; Nageshwar Reddy, D. Role of the Normal Gut Microbiota. *World J. Gastroenterol.* **2015**, *21* (29), 8787–8803.
- (18) Duar, R. M.; Frese, S. A.; Lin, X. B.; Fernando, S. C.; Burkey, T. E.; Tasseva, G.; Peterson, D. A.; Blom, J.; Wenzel, C. Q.; Szymanski, C. M.; et al. Experimental Evaluation of Host Adaptation of Lactobacillus Reuteri to Different Vertebrate Species. *Appl. Environ. Microbiol.* **2017**, *83* (12), e00132-17.
- (19) Martínez, I.; Maldonado-Gomez, M. X.; Gomes-Neto, J. C.; Kittana, H.; Ding, H.; Schmaltz, R.; Joglekar, P.; Cardona, R. J.; Marsteller, N. L.; Kembel, S. W.; et al. Experimental Evaluation of the Importance of Colonization History in Early-Life Gut Microbiota Assembly. *Elife* **2018**, *7*.
- (20) Walter, J.; Britton, R. A.; Roos, S. Host-Microbial Symbiosis in the Vertebrate
   Gastrointestinal Tract and the Lactobacillus Reuteri Paradigm. *Proc. Natl. Acad. Sci.* 
   2011, 108 (Supplement\_1), 4645–4652.
- (21) Özçam, M.; Tocmo, R.; Oh, J.-H.; Afrazi, A.; Mezrich, J. D.; Roos, S.; Claesen, J.; van

- Pijkeren, J.-P. The Gut Symbionts *Lactobacillus Reuteri* R2lc and 2010 Encode a Polyketide Synthase Cluster That Activates the Mammalian Aryl-Hydrocarbon Receptor. *Appl. Environ. Microbiol.* **2018**.
- (22) Özçam, M. Chapter 4: R2lc Ecology, University of Wisconsin Madison, 2018.
- (23) Hou, Y.; Braun, D. R.; Michel, C. R.; Klassen, J. L.; Adnani, N.; Wyche, T. P.; Bugni, T. S. Microbial Strain Prioritization Using Metabolomics Tools for the Discovery of Natural Products. *Anal. Chem.* 2012, 84 (10), 4277–4283.
- (24) Gruber, G.; Steglich, W. Calostomal, a Polyene Pigment from the Gasteromycete Calostoma Cinnabarinum (Boletales). *Z. Naturforsch.* **2007**, *62*, 129–131.
- (25) Adnani, N.; Chevrette, M. G.; Adibhatla, S. N.; Zhang, F.; Yu, Q.; Braun, D. R.; Nelson, J.; Simpkins, S. W.; McDonald, B. R.; Myers, C. L.; et al. Coculture of Marine Invertebrate-Associated Bacteria and Interdisciplinary Technologies Enable Biosynthesis and Discovery of a New Antibiotic, Keyicin. ACS Chem. Biol. 2017, 12 (12), 3093–3102.

## **Chapter 6: Conclusions and Future Work**

## 6.1 Concluding remarks

Natural products in the form of secondary metabolites from bacteria were made possible through elegant enzymology. The genes were clustered in the genomes in the form of biosynthetic gene clusters (BGCs). Recent advances in bioinformatics have equipped natural product chemists with *a priori* information on the probability of a bacterium to produce unique molecules. However, the discovery that most of these BGCs were inactive in the laboratory setting led to tremendous efforts in accessing these silent molecules. Although techniques like genetic modifications and heterologous expression led to the activation of certain silent BGCs and isolation of their corresponding secondary metabolites, <sup>2-4</sup> they required that the organism was amenable to genetic modifications and that their regulatory circuits were contained in the heterologous host known (chapter 1). As such, a simple but useful means of activating silent BGCs developed by various research groups was co-culturing of microbes.

The pivotal studies in bacterial cocultures conducted by Adnani *et al.* in our lab inspired further exploration into utilizing interspecies interaction to activate silent BGCs.<sup>5,6</sup> Most importantly, the discovery that *Micromonospora* sp. WMMB235, in the presence of *Rhodococcus* sp. WMMA185 produced a novel antibiotic, keyicin, was the foundation for in-depth analysis into the mode of interaction between these bacteria and the regulation of the BGC *kyc*. By elucidating the pathway that led to the BGC activation, we might be able to find a universal method for activating similarly regulated BGCs in other Actinobacteria.

In chapter 2, we employed multi-omics analyses to understand the regulatory bottleneck in WMMB235 monoculture and to investigate what caused the production of keyicin only in co-

culture. Comparative transcriptomics analysis made it clear that most genes within *kyc* were significantly upregulated in co-culture, indicating that the regulation was at the transcription level. Quantitative proteomics confirmed increased translation in co-culture for certain key genes, in particular the glycosyltransferases (GTs). LCMSMS-based molecular networking of the co-cultured bacteria at different time points showed the presence of analogs that had the same aglycone core but different glycosylation pattern. This hinted that GTs added the sugars on the keyicin aglycone as a tailoring step. We also found several other BGCs that were transcriptionally activated during co-culture.

Equipped with the knowledge gained in the multi-omics study, in chapter 3 we analyzed the mechanism of small molecule activation of *kyc*. We found the quorum sensing regulator *luxR* upstream of the biosynthetic genes upon surveying the BGC for transcriptional regulators. Accordingly, we screened a library of *luxR* ligands (acyl homoserine lactones) and discovered six compounds that activated production of keyicin. This showed that regulation of *kyc* was, at least in part, through the unprecedented mechanism of interspecies quorum sensing. In addition, serial fractionation of the WMMA185 extracts led to the isolation of three compounds that also activated production of keyicin, two of which were diketopiperazines.

While the coculture between WMMB235 and WMMA185 provided an excellent platform for mechanistic studies of interspecies interaction, newer co-culture systems also warranted further investigation. In chapter 4, we explored the unique metabolites produced when *Micromonospora* sp. WMMA2032 was co-cultured with *Dietzia* sp. WMMA184 and WMMB235 with *Microbulbifer* sp. WMMC694. These findings reiterated the idea that bacteria do not produce all the secondary metabolites that are encoded in their genome in every setting and require certain environmental cues to stimulate production.

Finally, in chapter 5 we performed metabolomics analysis of a *Lactobacillus reuteri* strain R2lc, which outcompetes another strain 100-23 in a mixed culture. In the process, a polyene that led to the inhibition of 100-23 was discovered. Further studies to elucidate the mechanism of interaction between these strains were undertaken. Through these we found that the inhibition of 100-23 only occurred when cell-cell contact between the two strains was allowed.

Thus, multiple techniques spanning several disciplines were used to study different types of co-cultures, adding to the growing body of knowledge in regulation of biosynthesis and interspecies communication.

### **6.2 Future Work**

The results outlined in chapters 2 and 3 form a framework to explore mechanisms of activating silent BGCs via interspecies interaction and small molecule induction. The process of integrating genomics, transcriptomics, proteomics and metabolomics demonstrated for *Micromonospora* sp. WMMB235 and *Rhodococcus* sp. WMMA185 can be applied to other bacterial co-culture combinations. Furthermore, similar comparative analyses can also be made for bacteria with silent BGCs that are activated via other means, such as addition of non-native chemical elicitors. Taking these analyses into account, we can then begin to find patterns for regulatory mechanisms by surveying a large number of bacteria with silent BGCs, and eventually strategize how best to access silent molecules from a strain not studied before.

Since the molecules isolated from WMMA185 were unable to completely recapitulate the effect of the co-culture, further analyses into the different small molecule activators for keyicin is required. In addition, additional efforts into isolating the products of other BGCs within WMMB235 can be made. Initial screening of the WMMB235 extracts in monoculture and

coculture with WMMA185 failed to show the presence of these putative products, and perhaps different methods are needed to improve their production and subsequent isolation.

The ultimate aim of these interdisciplinary studies is the discovery of new molecules for potential clinical use. To this end, better understanding of how compounds are biosynthesized is crucial. Therefore, by extrapolating the findings and techniques discussed in this thesis to newer systems, we can improve our ability to discover new bioactive molecules.

## **6.3 References**

- (1) Rutledge, P. J.; Challis, G. L. Discovery of Microbial Natural Products by Activation of Silent Biosynthetic Gene Clusters. *Nat. Rev. Microbiol.* **2015**, *13* (8), 509–523.
- (2) Ishida, K.; Lincke, T.; Behnken, S.; Hertweck, C. Induced Biosynthesis of Cryptic Polyketide Metabolites in a Burkholderia Thailandensis Quorum Sensing Mutant. **2010**.
- (3) Laureti, L.; Song, L.; Huang, S.; Corre, C.; Leblond, P.; Challis, G. L.; Aigle, B. Identification of a Bioactive 51-Membered Macrolide Complex by Activation of a Silent Polyketide Synthase in Streptomyces Ambofaciens. *Proc. Natl. Acad. Sci. U. S. A.* 2011, 108 (15), 6258–6263.
- (4) Lin, X.; Hopson, R.; Cane, D. E. Genome Mining in Streptomyces Coelicolor: Molecular Cloning and Characterization of a New Sesquiterpene Synthase. **2006**.
- (5) Hou, Y.; Braun, D. R.; Michel, C. R.; Klassen, J. L.; Adnani, N.; Wyche, T. P.; Bugni, T. S. Microbial Strain Prioritization Using Metabolomics Tools for the Discovery of Natural Products. *Anal. Chem.* 2012, 84 (10), 4277–4283.
- (6) Adnani, N.; Chevrette, M. G.; Adibhatla, S. N.; Zhang, F.; Yu, Q.; Braun, D. R.; Nelson, J.; Simpkins, S. W.; McDonald, B. R.; Myers, C. L.; et al. Coculture of Marine Invertebrate-Associated Bacteria and Interdisciplinary Technologies Enable Biosynthesis and Discovery of a New Antibiotic, Keyicin. ACS Chem. Biol. 2017, 12 (12), 3093–3102.

# Appendix 1 Supplementary data for Chapter 2

Parameters for AntiSmash	102
Transcriptomics details	102
Table A1.1 The total RNA concentrations	103
Table A1.2 DiLeu reporter tags used	104
Figure A1.1 Sample quality control report of the RNA-Seq reads	105
Figure A1.2 Schematic for labeled proteomics using DiLeu	106
Figure A1.3 Structural analysis of keyicin-like compounds	107
Figure A1.4 Keyicin and two of its analogs with temporal changes	108

#### Parameters for AntiSmash

The fasta nucleotide sequence was uploaded on AntiSmash v3.0 with ClusterFinder on, "Use ClusterFinder algorithm for BGC border prediction" on, Minimum cluster size in CDS 5, Minimum number of biosynthetic-related PFAM domains 5, Minimum ClusterFinder probability at 60% and using the "All on" for extra features which uses the following programs: KnownClusterBlast, ClusterBlast, SubClusterBlast, smCoG analysis, Active Site Finder, Detect TTA codons, Whole genome PFAM analysis.

### **Transcriptomics details**

Read filtering done by removing low abundance genes defined as those with an average read count below a threshold of 1.0 in two or more samples. Samples in RNASeq experiment were normalized by the method of trimmed mean of M-values (TMM), resulting in more uniform distributions centered on a common median.

**Table A1.1:** The total RNA concentrations yielded after the RNAeasy Plus Mini Kit extraction were all between 300-500 ng/ml concentration and had  $A_{260}/A_{280}$  values ~ 2 suggesting good quality RNA. The values of the secondary measure of RNA purity  $A_{260}/A_{230}$  are also around the expected ~1.8.

Entry	Sample name	A <sub>260</sub> (10mM)	A260/280	A260/230	Concentration(ng/ml)
1	185D21	12.851	2.09	2.13	514
2	185D21	9.636	2.05	1.98	385
3	185D23	5.839	2.08	1.95	233
4	235D21	9.833	2.03	2.22	393
5	235D22	6.3	2.07	1.82	252
6	235D23	12.14	2.05	2.02	485
7	CoD21	10.005	2.02	2.2	400
8	CoD22	12.039	2.04	2.09	481
9	CoD23	11.127	1.97	2.2	445
10	185D51	8.344	2.06	2.11	333
11	185D52	10.453	1.94	1.98	418
12	185D53	11.641	2.03	1.99	465
13	235D51	12.334	2.05	2.2	493
14	235D52	10.832	2	2.15	433
15	235D53	12.221	1.99	2.05	489
16	CoD51	12.187	2.05	2.05	487
17	CoD52	12.631	2.04	2.13	505
18	CoD53	11.802	1.98	2.04	472

**Table A1.2:** DiLeu reporter tags used to label each sample in the multiplex for Day 5 and Day 8 protein samples before analysis on LC-MS/MS for quantitative proteomics.

DiLeu Tag	Day 5 or Day 8 Sample	Reporter ion
115a	WMMB235 Mono rep1	115.12476m/z
116a	WMMB235 with WMMA185 extract rep1	116.12812m/z
117a	WMMB235 Mono rep2	117.13147m/z
118a	WMMB235 with WMMA185 extract rep2	118.13483m/z
117c	WMMB235 Mono rep3	117.14363m/z
118c	WMMB235 with WMMA185 extract rep3	118.14699m/z

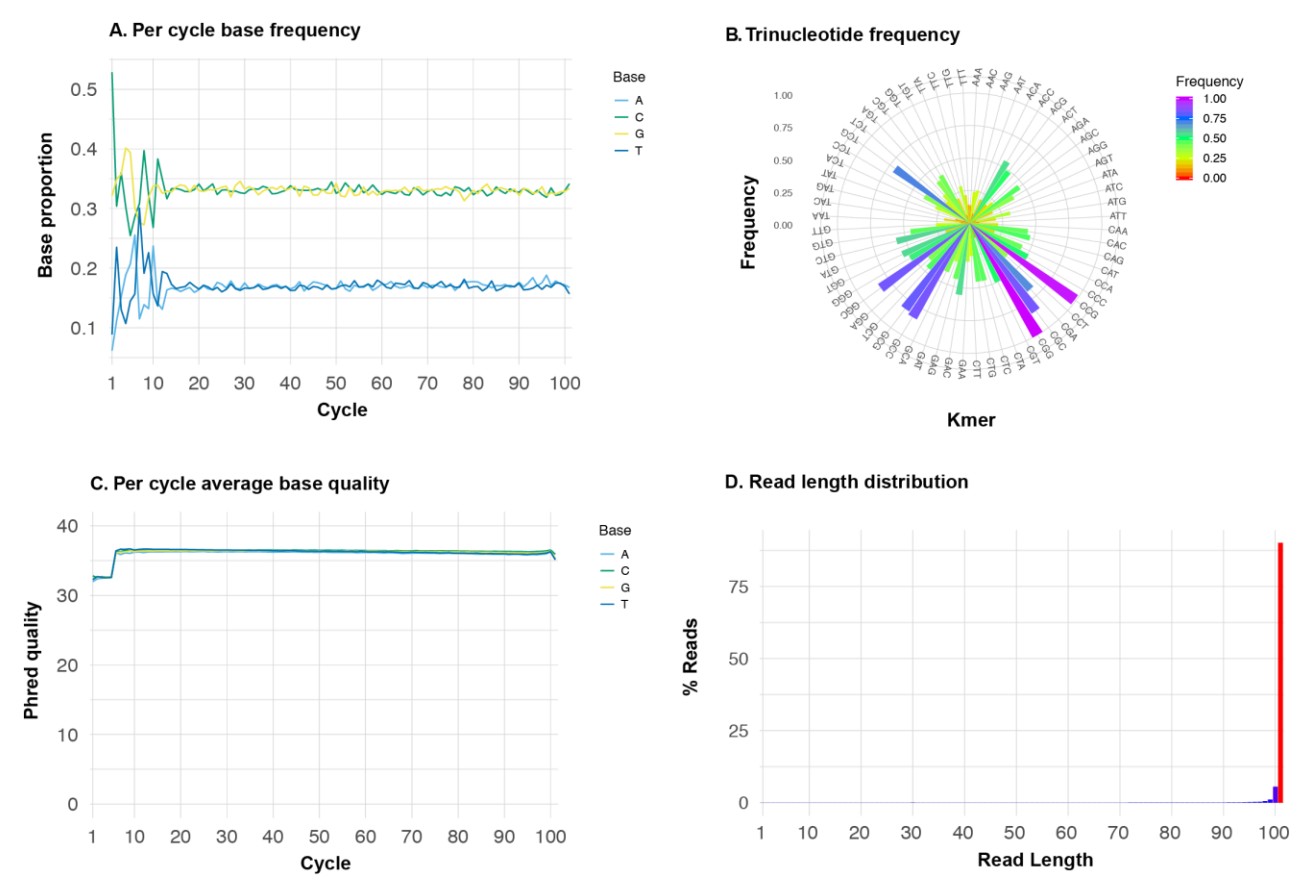


**Figure A1.1**. Sample quality control report of the RNA-Seq reads for sample – co-culture day 2, Replicate 2. Similar results were obtained for all the nine samples, and suggested high quality reads. **A)** Per cycle base frequency. The frequency of each nucleotide base position across the length of the read shows the absence of any sequence bias. The effect on the base composition in the early sequences (cycles 1–10) is known and does not affect the base content of the read. **B)** Trinucleotide frequency. The relative frequency of trinucleotides (3-mer) shows relatively uniform representation. If one or more 3-mers dominate the remaining 3-mers, it may indicate the presence of a contaminating sequence, which is not the case here. **C)** Per cycle average base quality. The Phred scaled quality scores are > 30 which is equivalent to 99.9% base call accuracy. **D)** Read length distribution. Expected value of 100 bp (target read length) observed for majority of reads during RNASeq experiment.

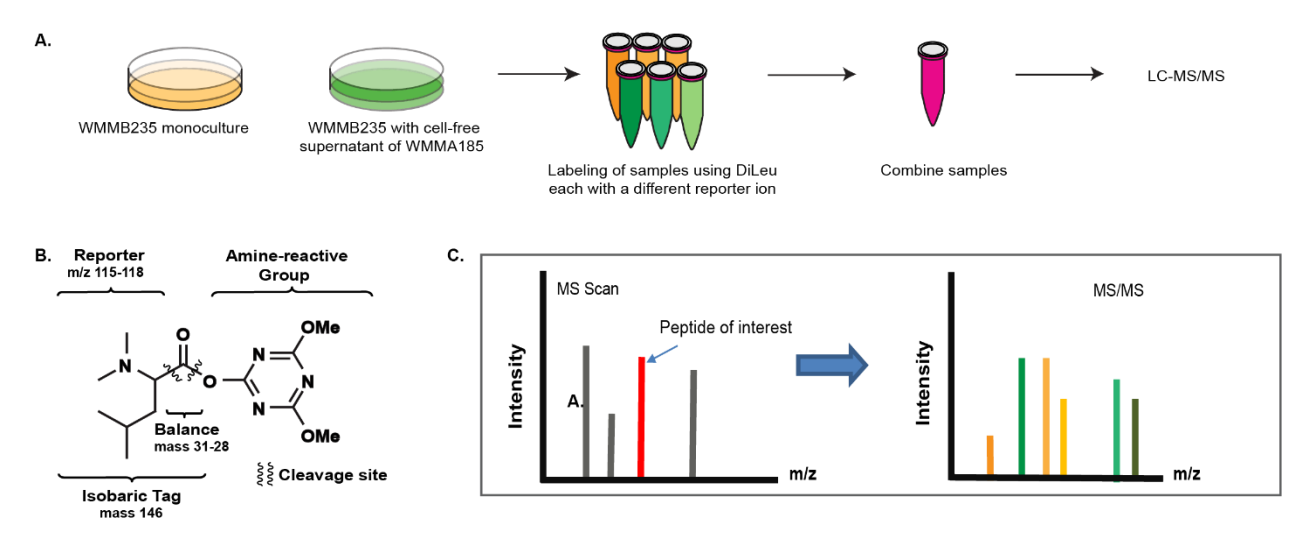
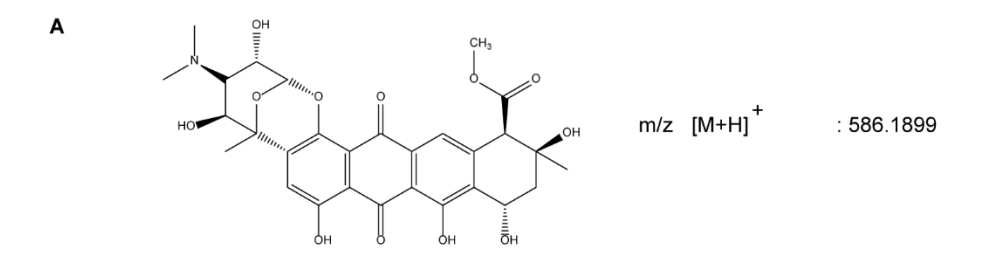


**Figure A1.2.** Schematic for labeled proteomics using DiLeu. **A)** Triplicates of WMMB235 monoculture and WMMB235 cultured in the supernatant of WMMA185 were labeled individually and combined according day of sampling (day 5 or day 8). **B)** DiLeu reporter showing the range in reporter ion mass and the amine reactive group, allowing the same mass of the modified peptide in MS1 scan but different MS2 ions after fragmentation at the cleavage site. **C)** Schematic showing a common peptide of interest in the MS1 scan fragmenting to 6 different reporter ions, each from a different sample on a particular day. This allows for quantification in the peptide present in each sample.



В

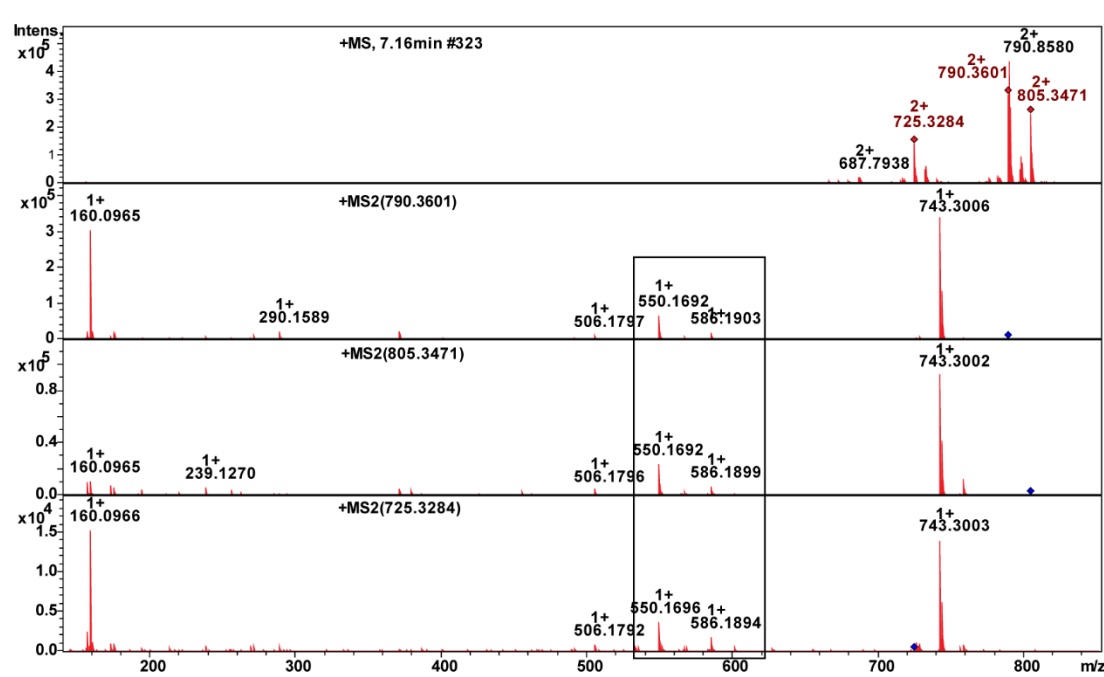


**Figure A1.3.** Structural analysis of keyicin-like compounds. (**A**) Aglycone core of keyicin. (**B**) Analogs of keyicin all share the anthracycline core as reflected by m/z signals at 550.1696, as well as m/z = 790.3601, 805.3471 (keyicin) and 725.3284 amu.

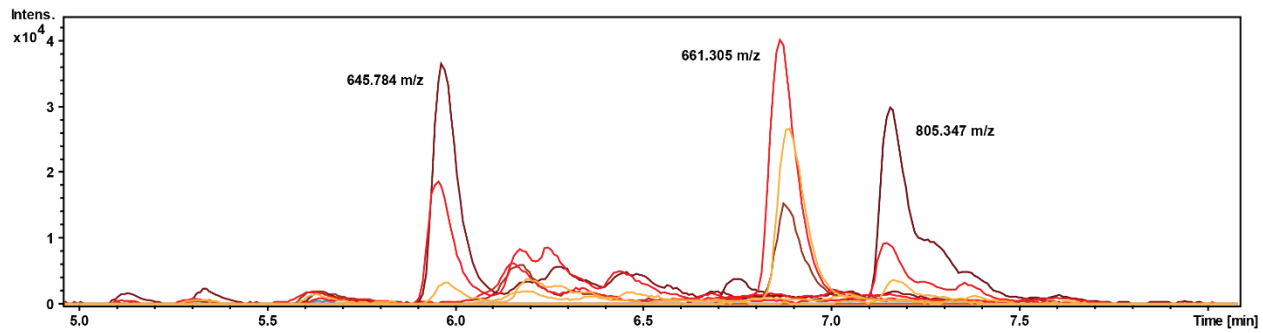


**Figure A1.4.** Keyicin and two of its analogs with temporal changes in intensity over time. Yellow: day 2, orange: day 5, Red: day 8 and Maroon: day 14. Keyicin (m/z = 805.347) increases in intensity over time; m/z = 645.784 follows a similar pattern, suggesting it is an analog; m/z = 661.305 first increases in intensity, but then is reduced by day 14, suggesting its intermediacy *en route* to keyicin or related analogs.

# Appendix 2 Supplementary data for Chapter 2

<b>Figure A2.1.</b> 1H NMR of <b>8</b> , 600MHz, CD <sub>3</sub> OD	110
Figure A2.2. HSQC NMR of 8, 600MHz, CD <sub>3</sub> OD	111
Figure A2.3. <sup>1</sup> H COSY NMR of 8, 600MHz, CD <sub>3</sub> OD	112
Figure A2.4. HMBC NMR of 8, 600MHz, CD <sub>3</sub> OD	113
Figure A2.5. HRMS spectra of 8 taken in positive ion mode using ESI	114
Figure A2.6. 1H NMR of 9, 600MHz, CD <sub>3</sub> OD	115
Figure A2.7. <sup>1</sup> H COSY NMR of 9, 600MHz, CD <sub>3</sub> OD	116
Figure A2.8. HRMS spectra of 9 taken in positive ion mode using ESI	117
Figure A2.9. <sup>1</sup> H NMR of 9 and 10, 600MHz, CD <sub>3</sub> OD	118
Figure A2.10. HRMS spectra of 10 taken in positive ion mode using ESI	119
Figure A2.11 Marfey's analysis for 9	120
Figure A2.12 Marfey's analysis for 10	121
Figure A2.13. <sup>1</sup> H NMR of commercial <b>8</b> , 500MHz, CD <sub>3</sub> OD	122
Figure A2.14. <sup>1</sup> H NMR of commercial <b>9</b> , 500MHz, CD <sub>3</sub> OD	123
Figure A2.15. <sup>1</sup> H NMR of commercial 10, 500MHz, CD <sub>3</sub> OD	124

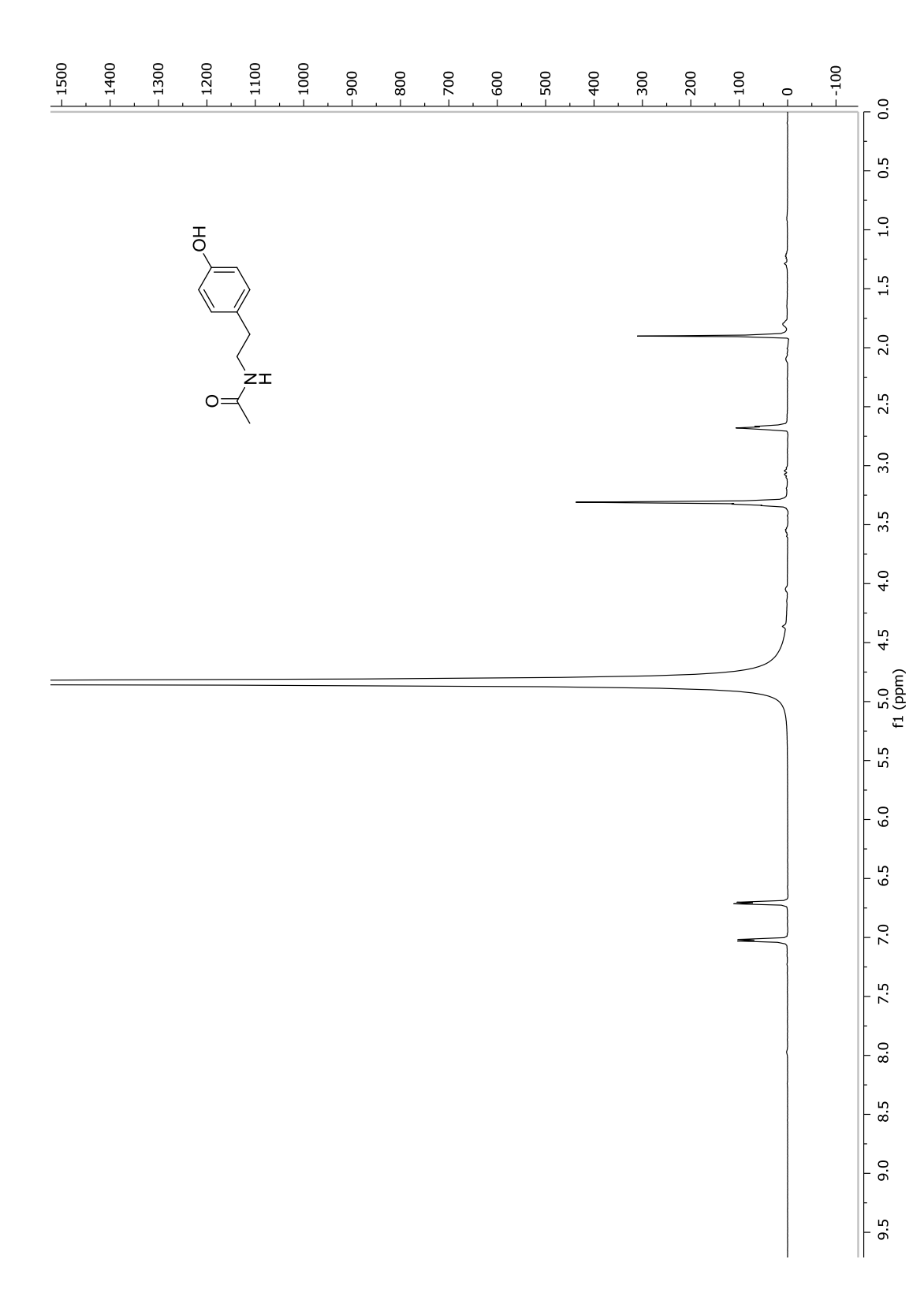


Figure A2.1. 1H NMR of 8, 600MHz, CD<sub>3</sub>OD

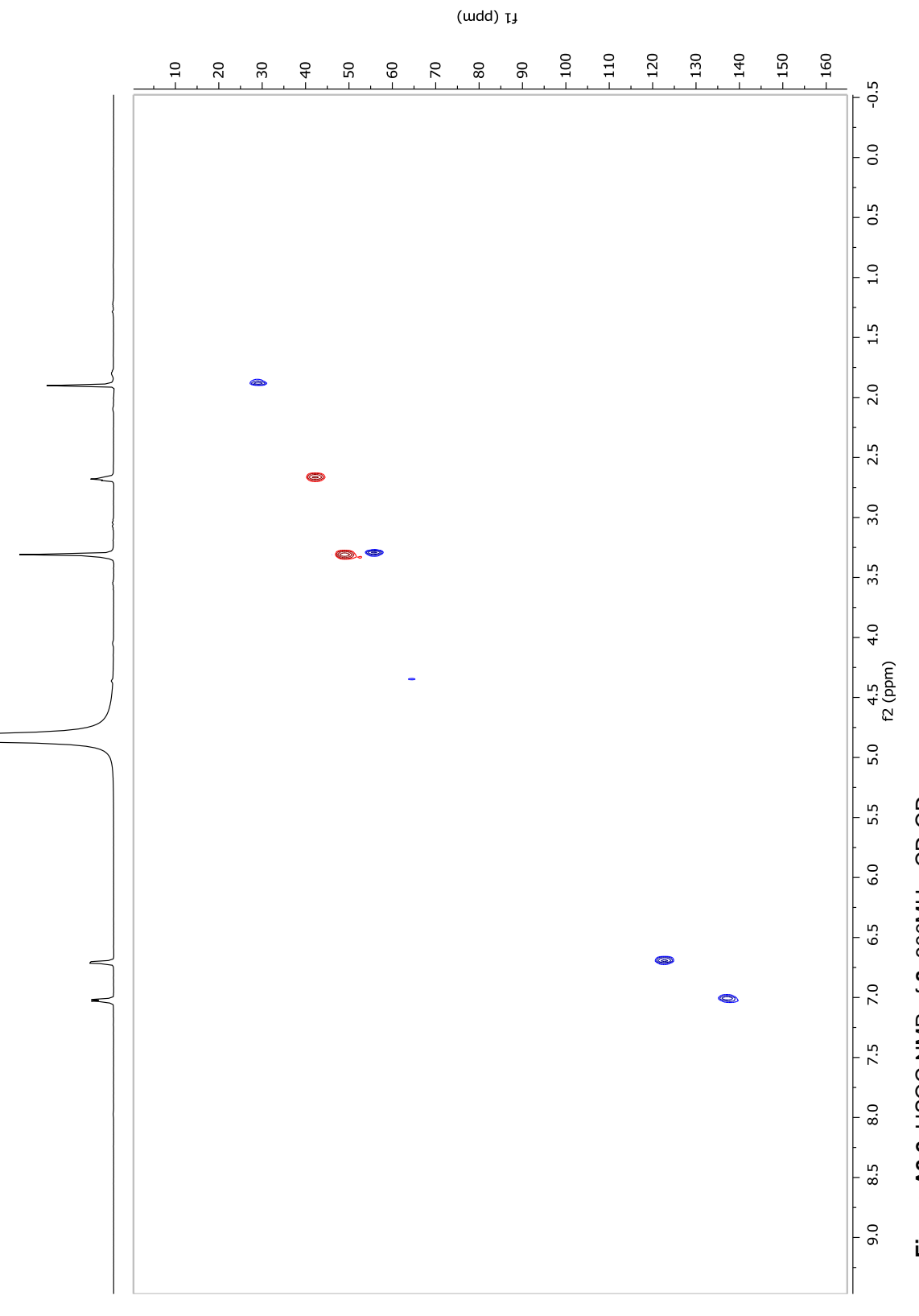


Figure A2.2. HSQC NMR of 8, 600MHz,  $CD_3OD$ 

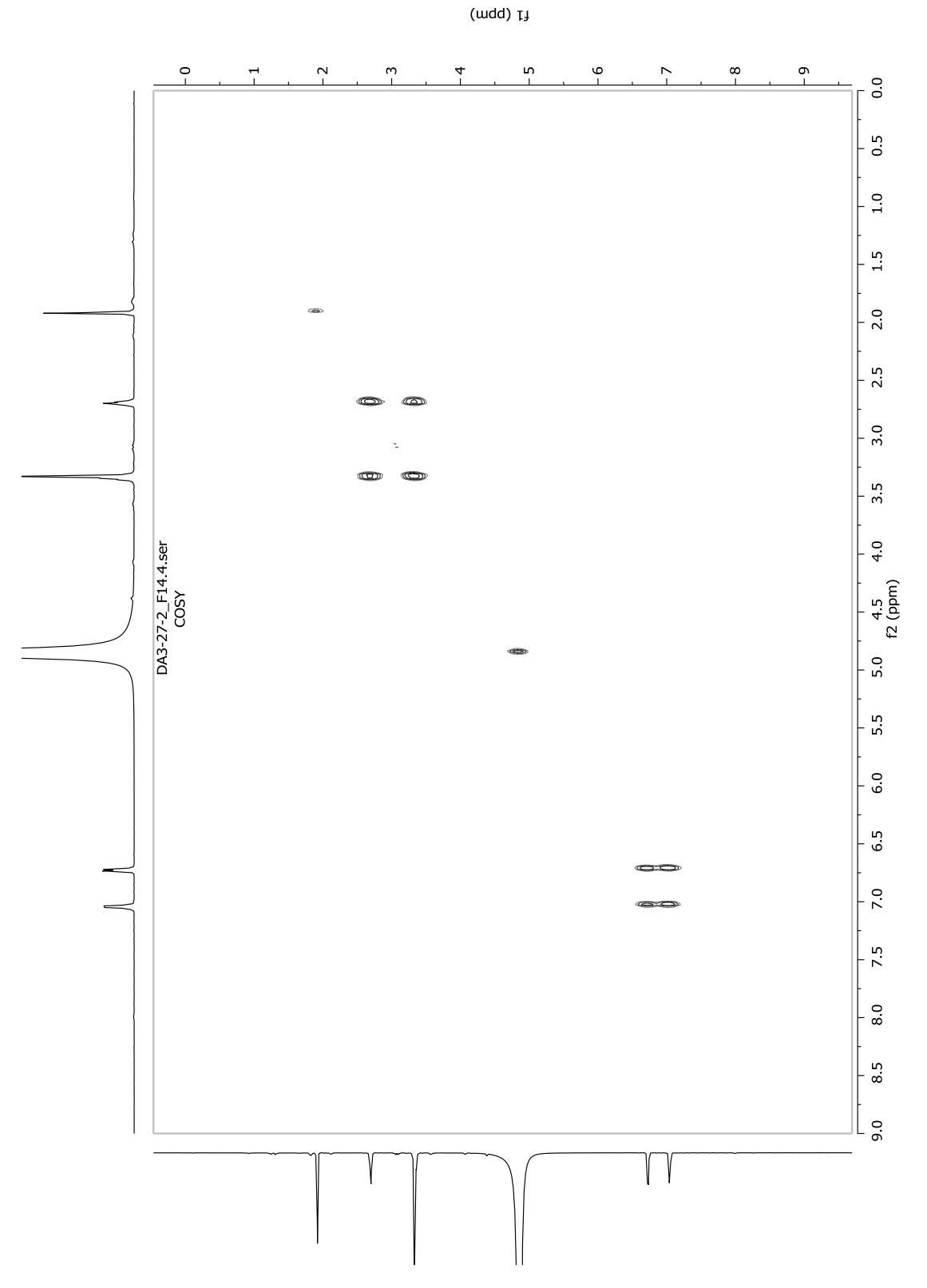


Figure A2.3. <sup>1</sup>H COSY NMR of 8, 600MHz, CD<sub>3</sub>OD

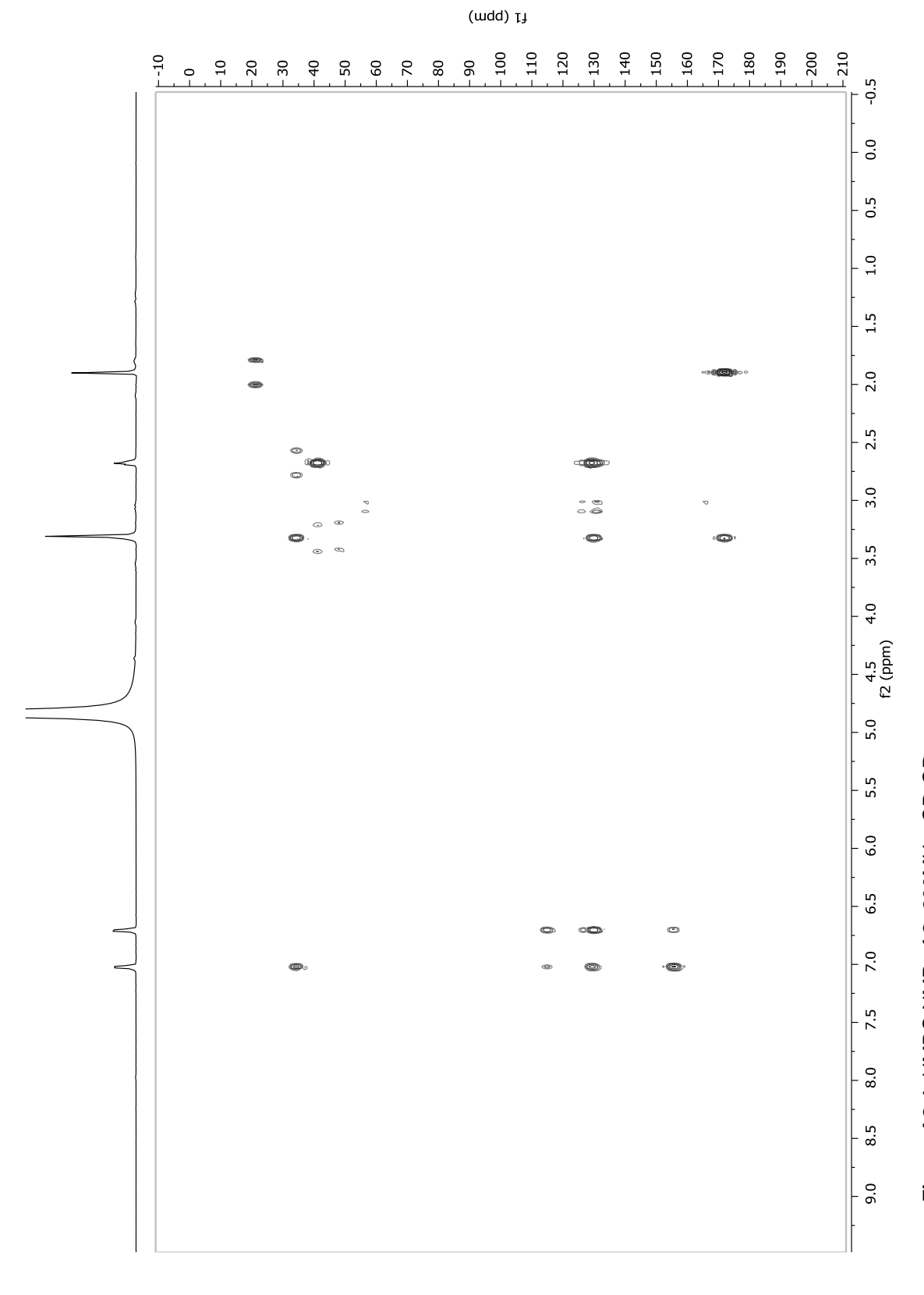


Figure A2.4. HMBC NMR of 8, 600MHz, CD<sub>3</sub>OD

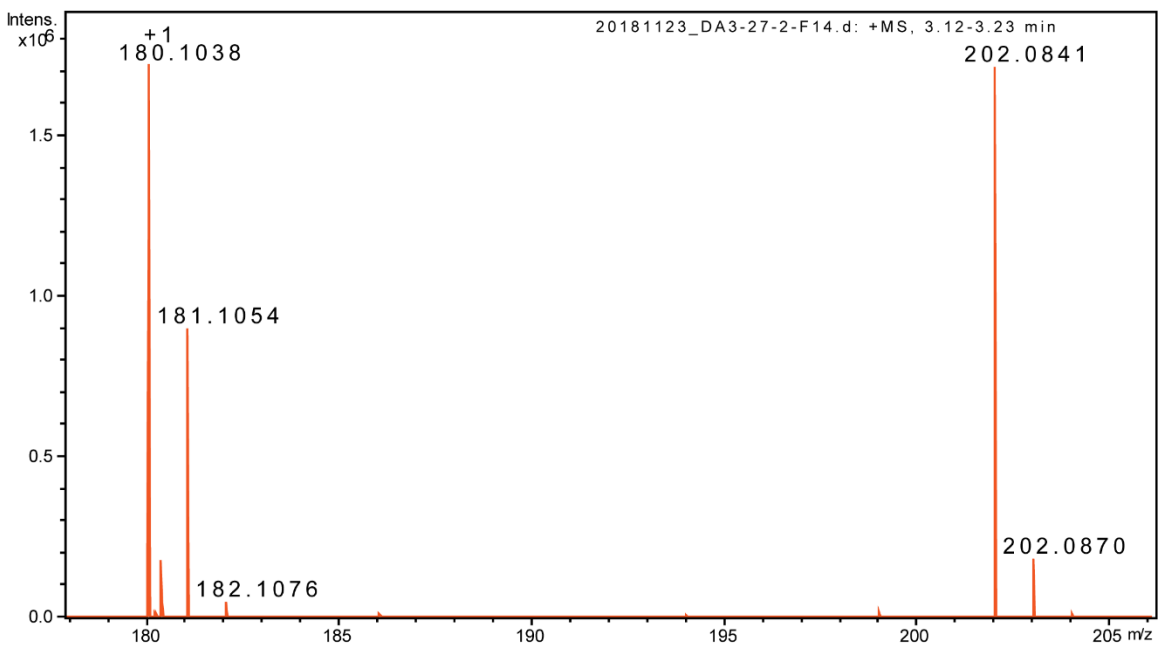


Figure A2.5. HRMS spectra of 8 taken in positive ion mode using ESI.

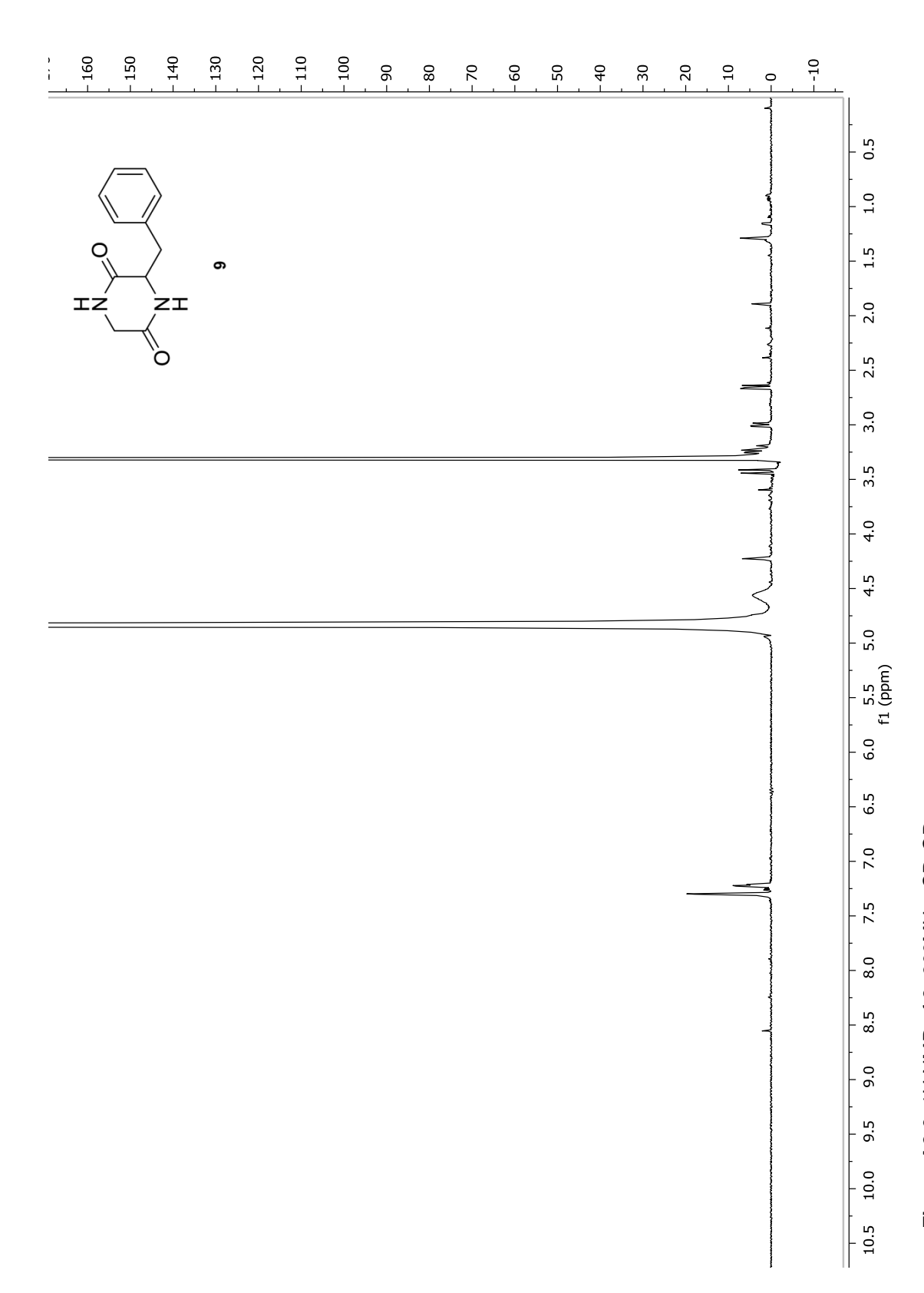
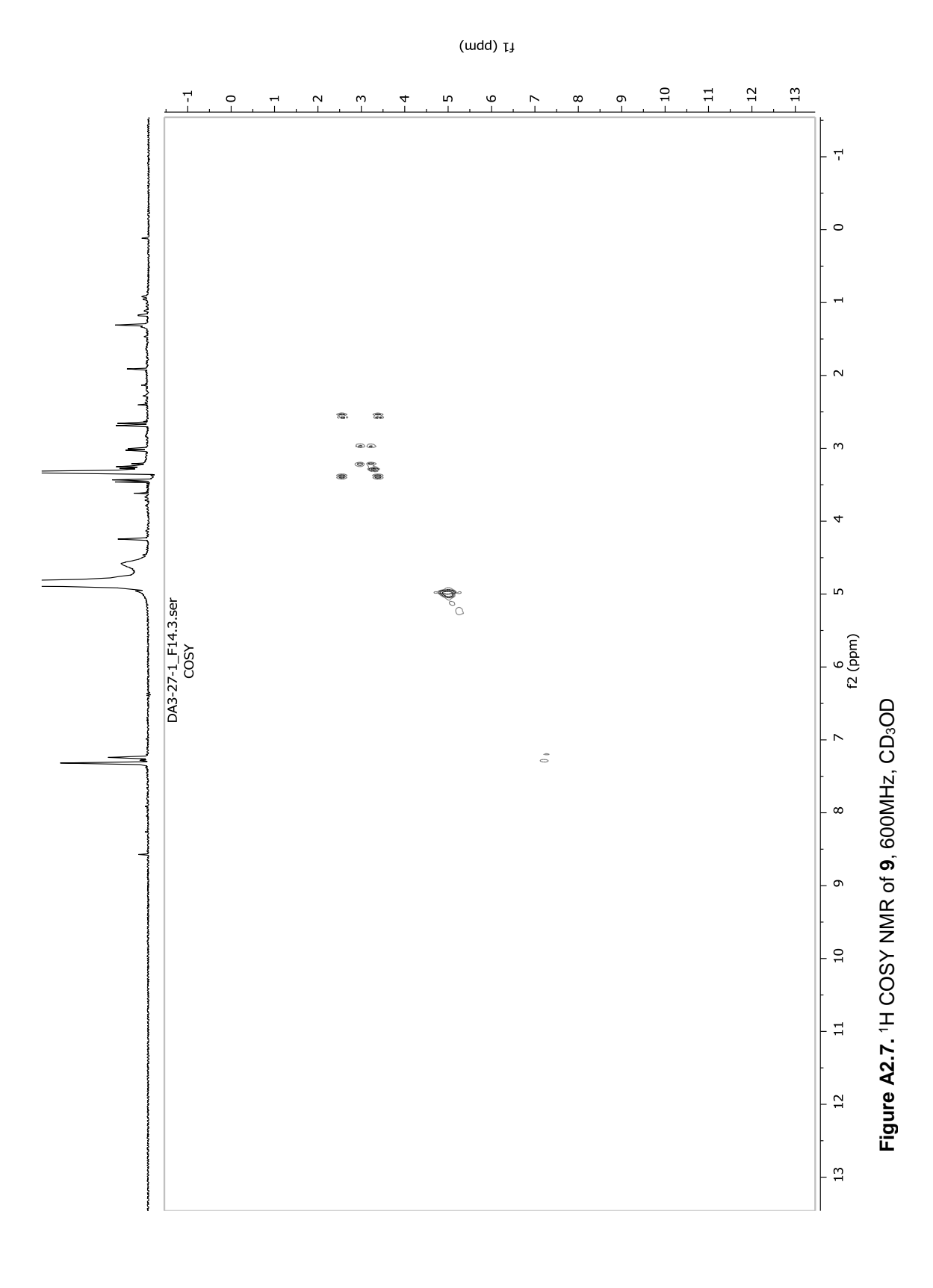


Figure A2.6. 1H NMR of 9, 600MHz,  $CD_3OD$ 



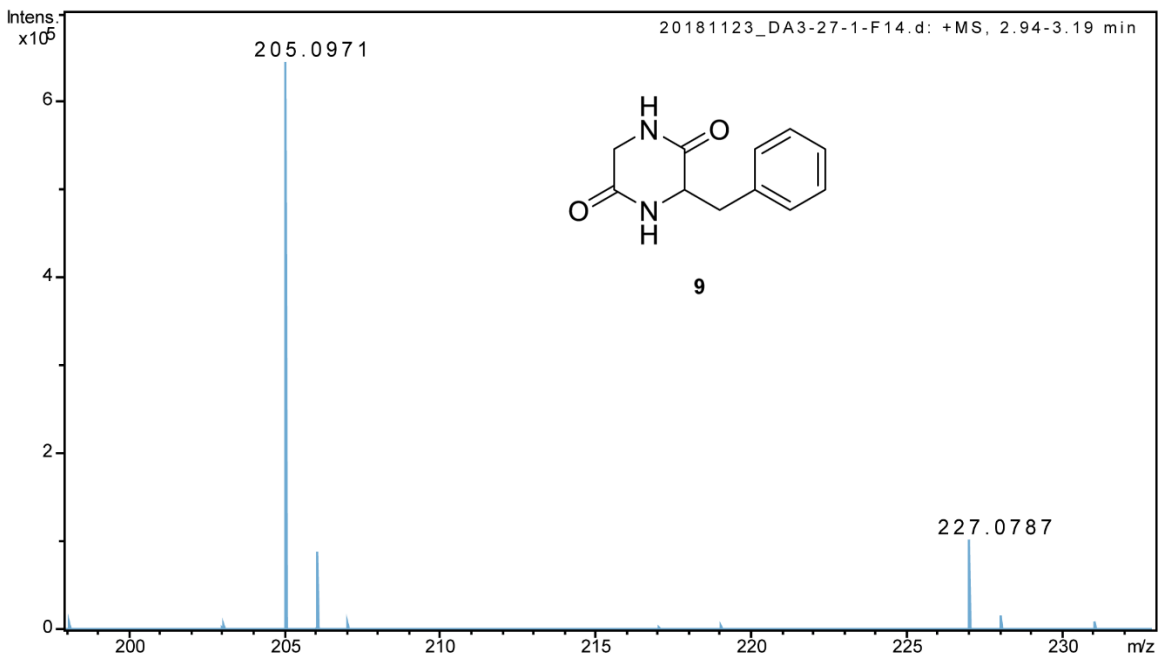


Figure A2.8. HRMS spectra of 9 taken in positive ion mode using ESI.

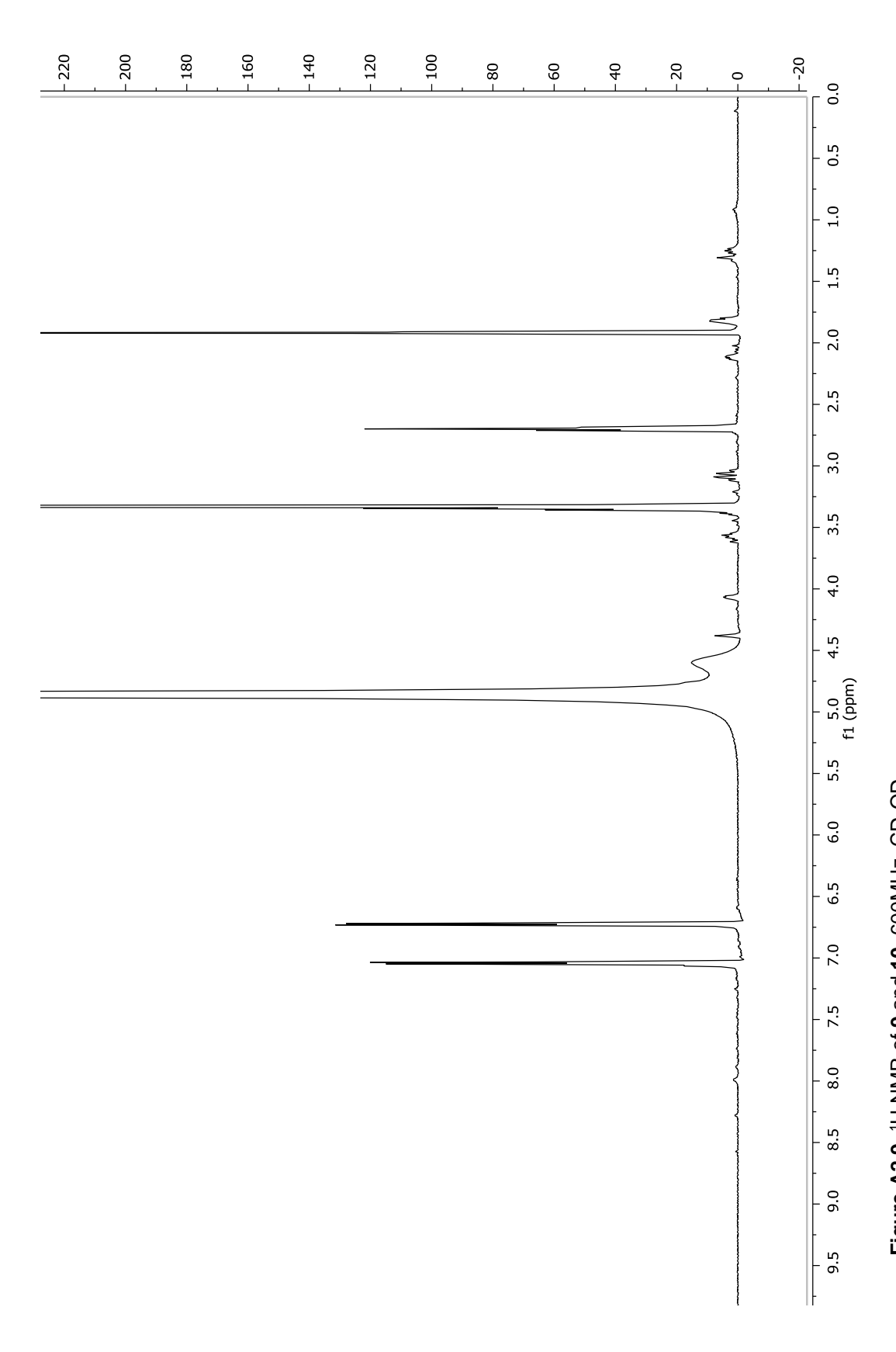
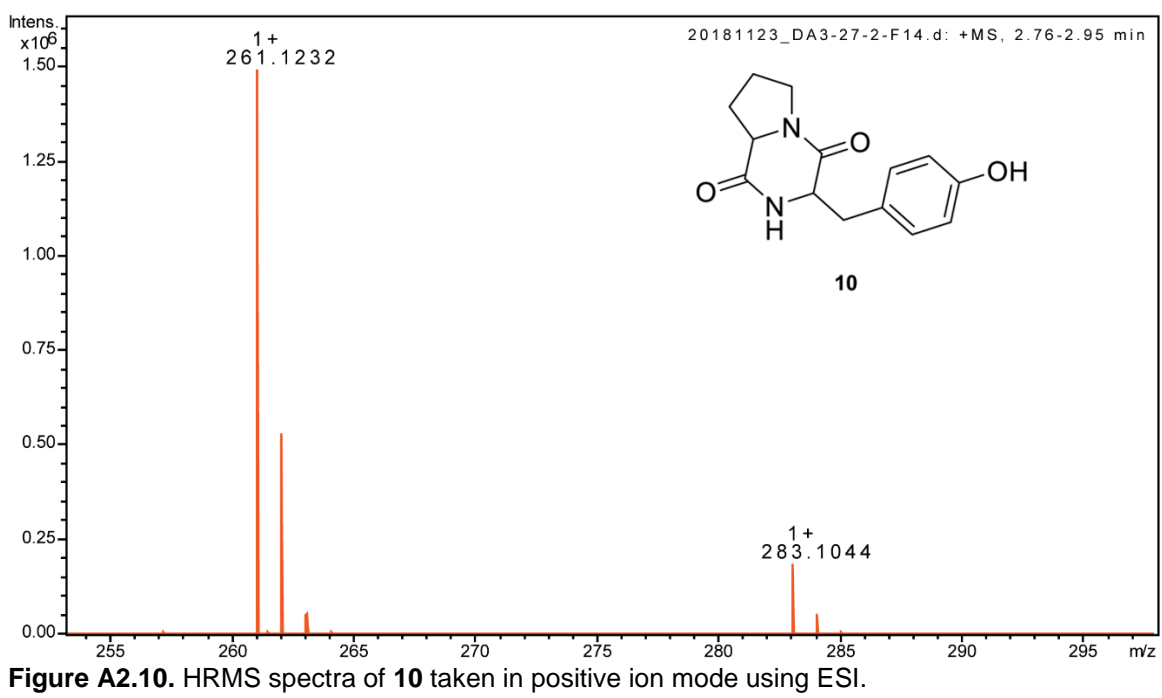


Figure A2.9.  $^1\text{H}$  NMR of 9 and 10, 600MHz, CD $^3\text{OD}$ 



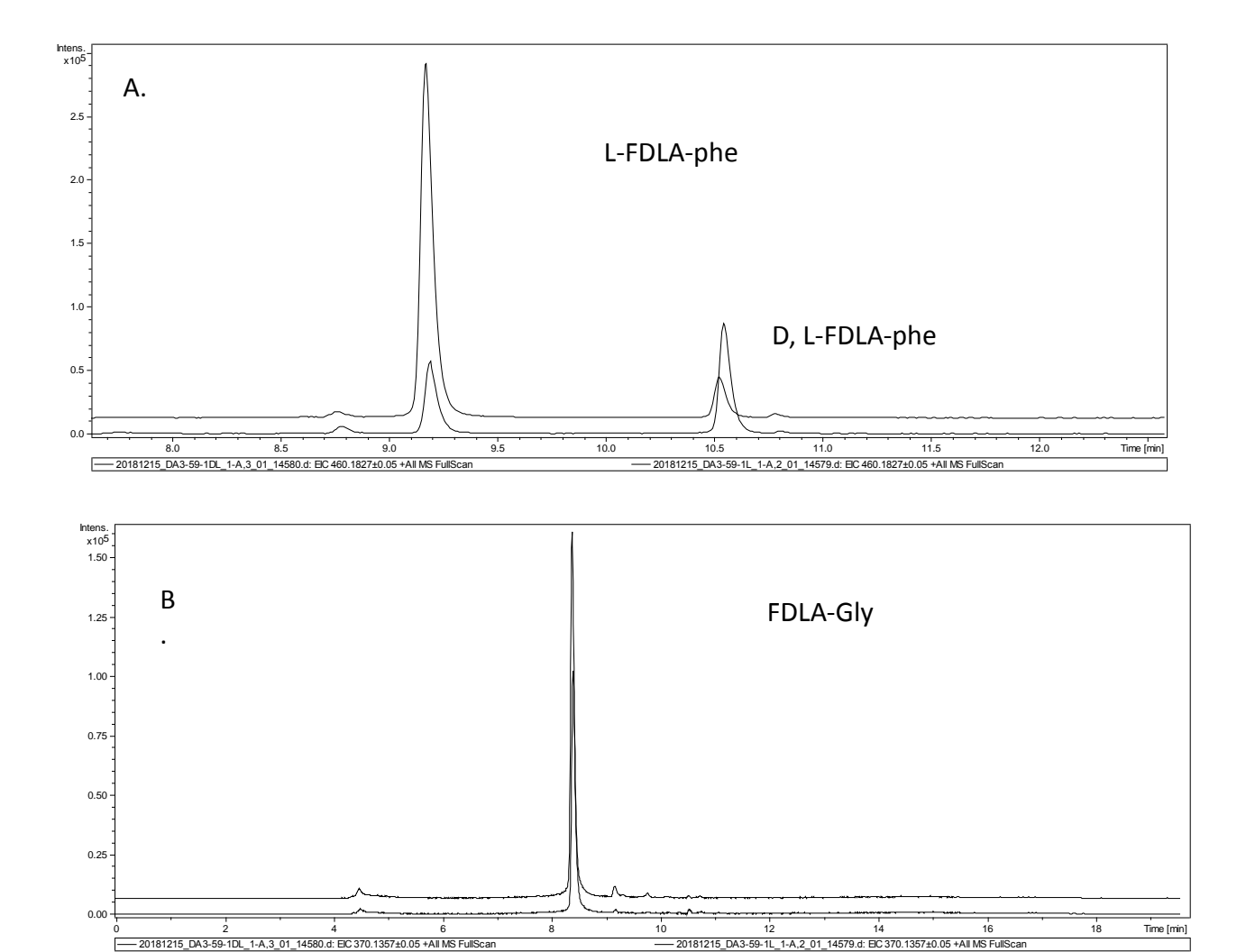
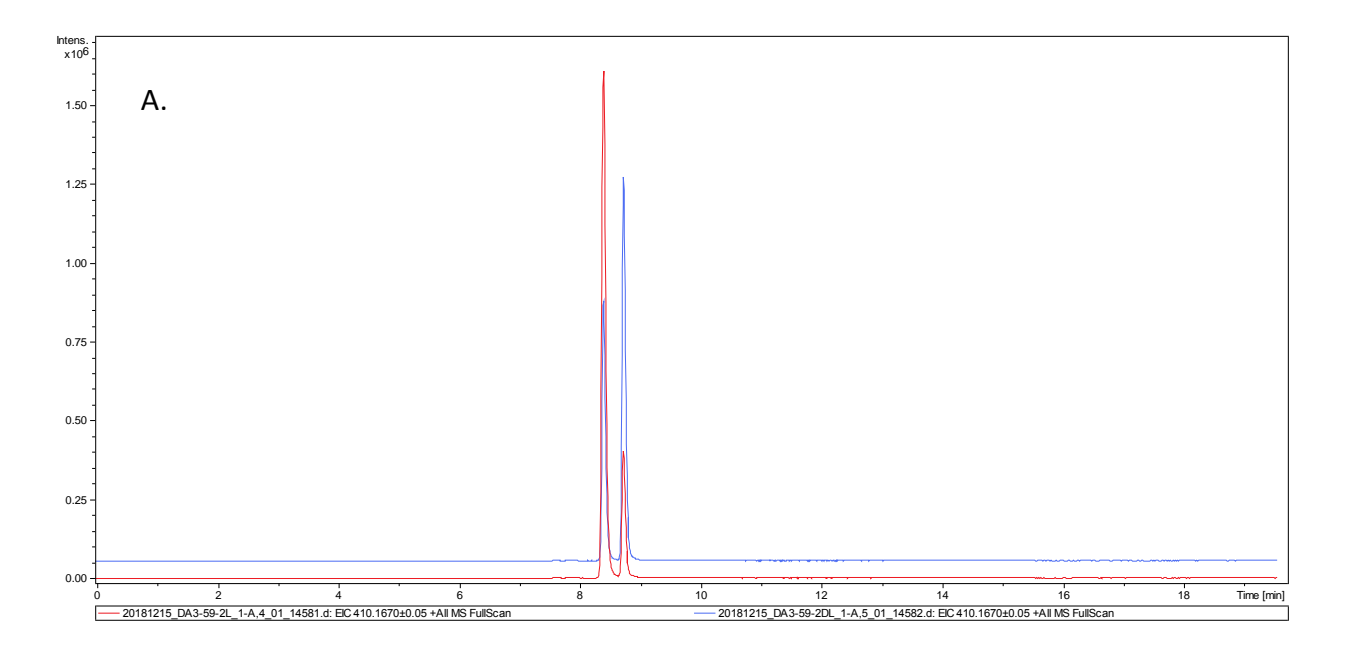


Figure A2.11 Marfey's analysis for 9

A) EIC for Phe at m/z 460.1827 B) EIC for Gly at m/z 370.1357



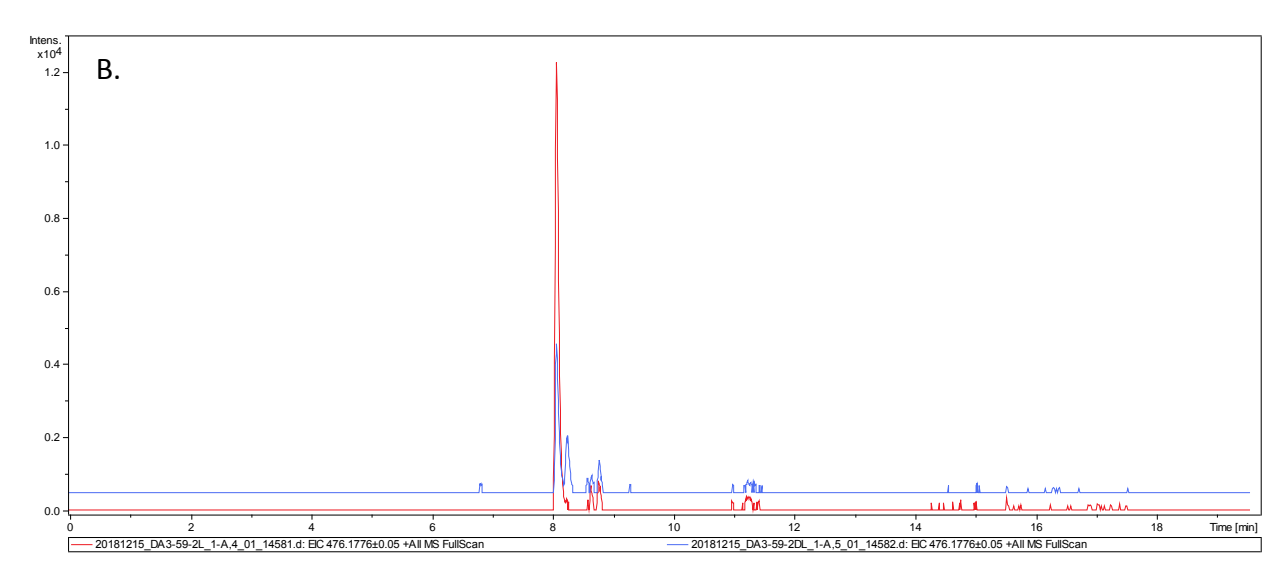
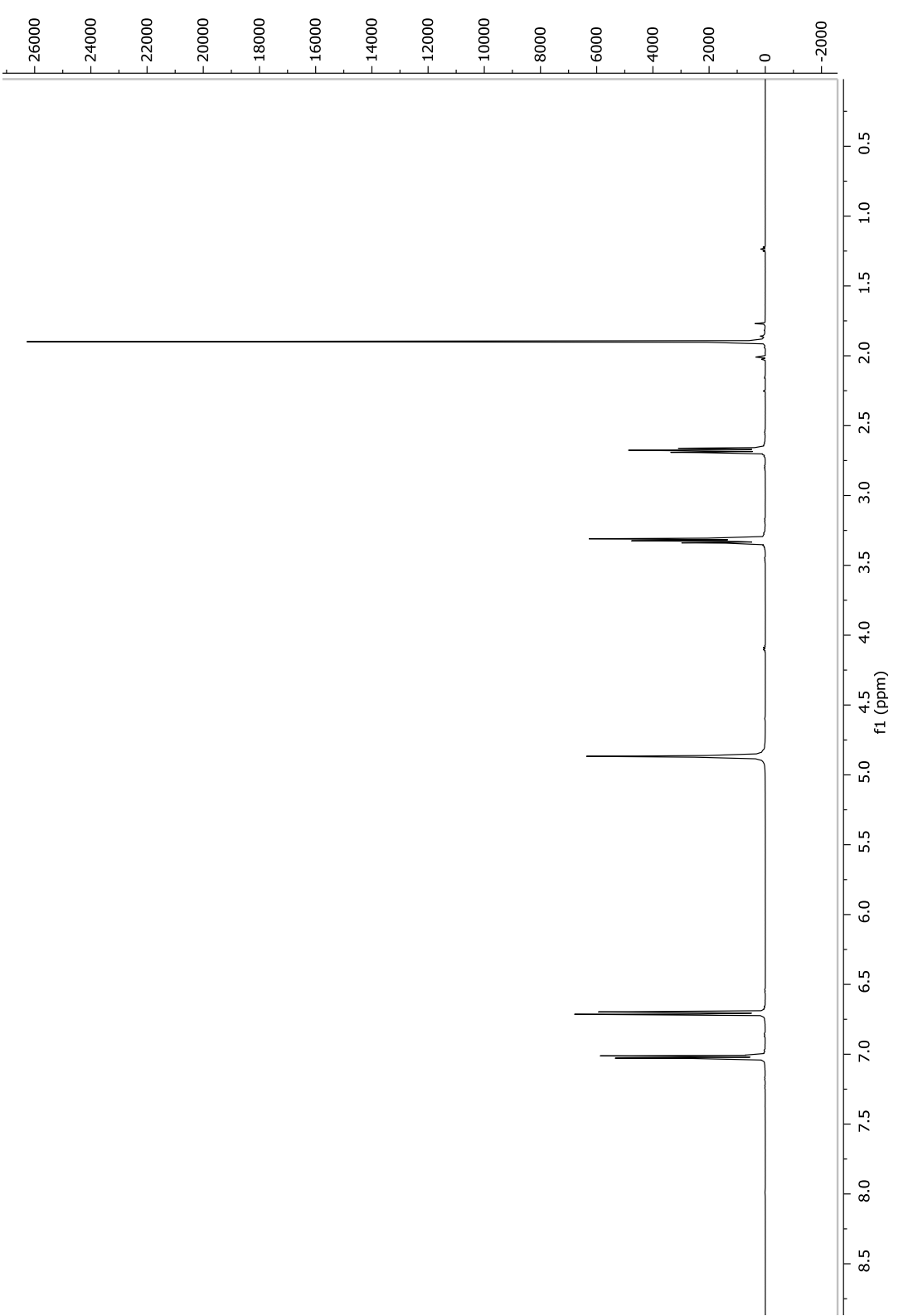


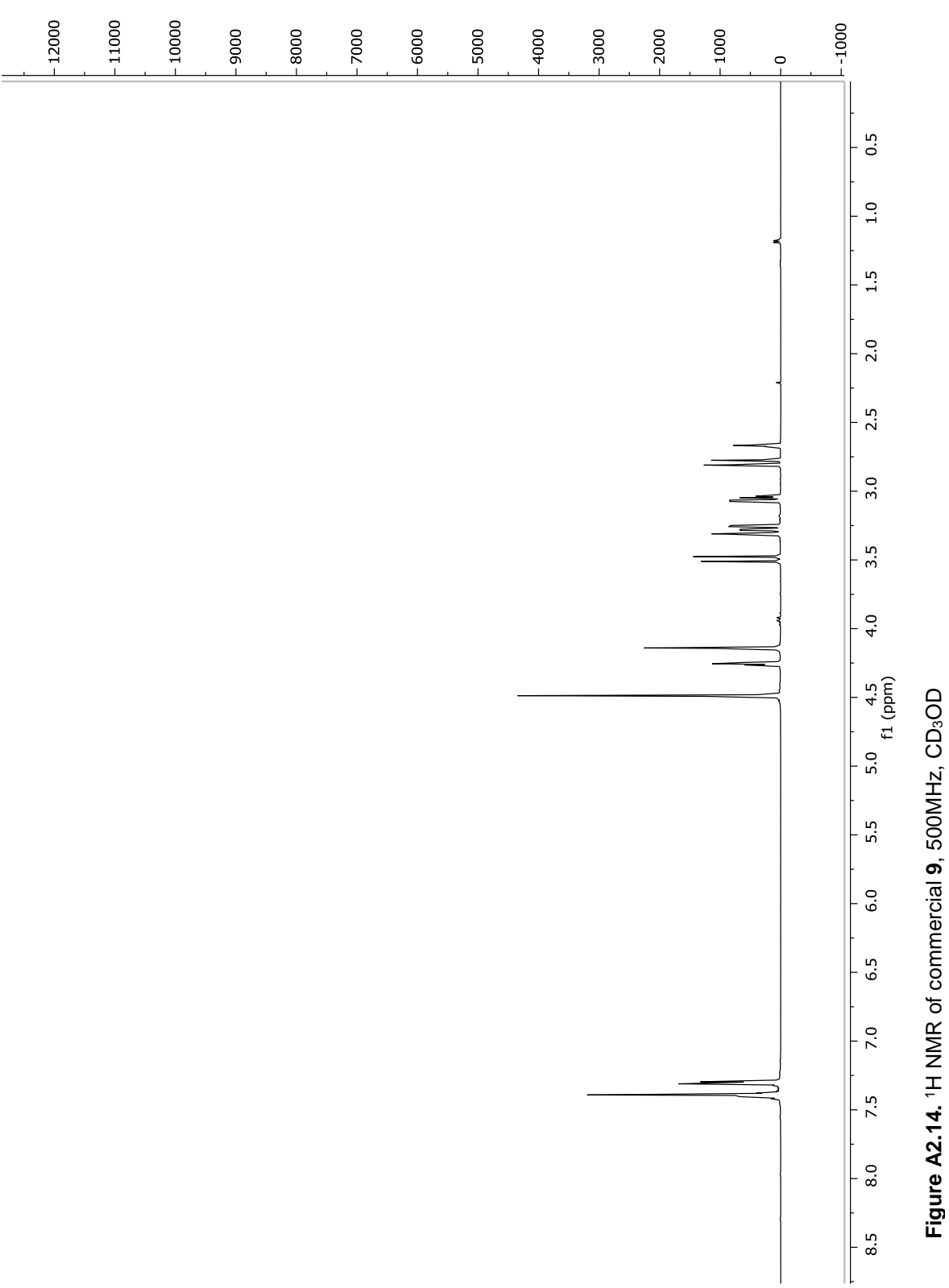
Figure A2.12 Marfey's analysis for 10

A) EIC for Pro at *m/z* 410.1670 B) EIC for Tyr at *m/z* 476.1776

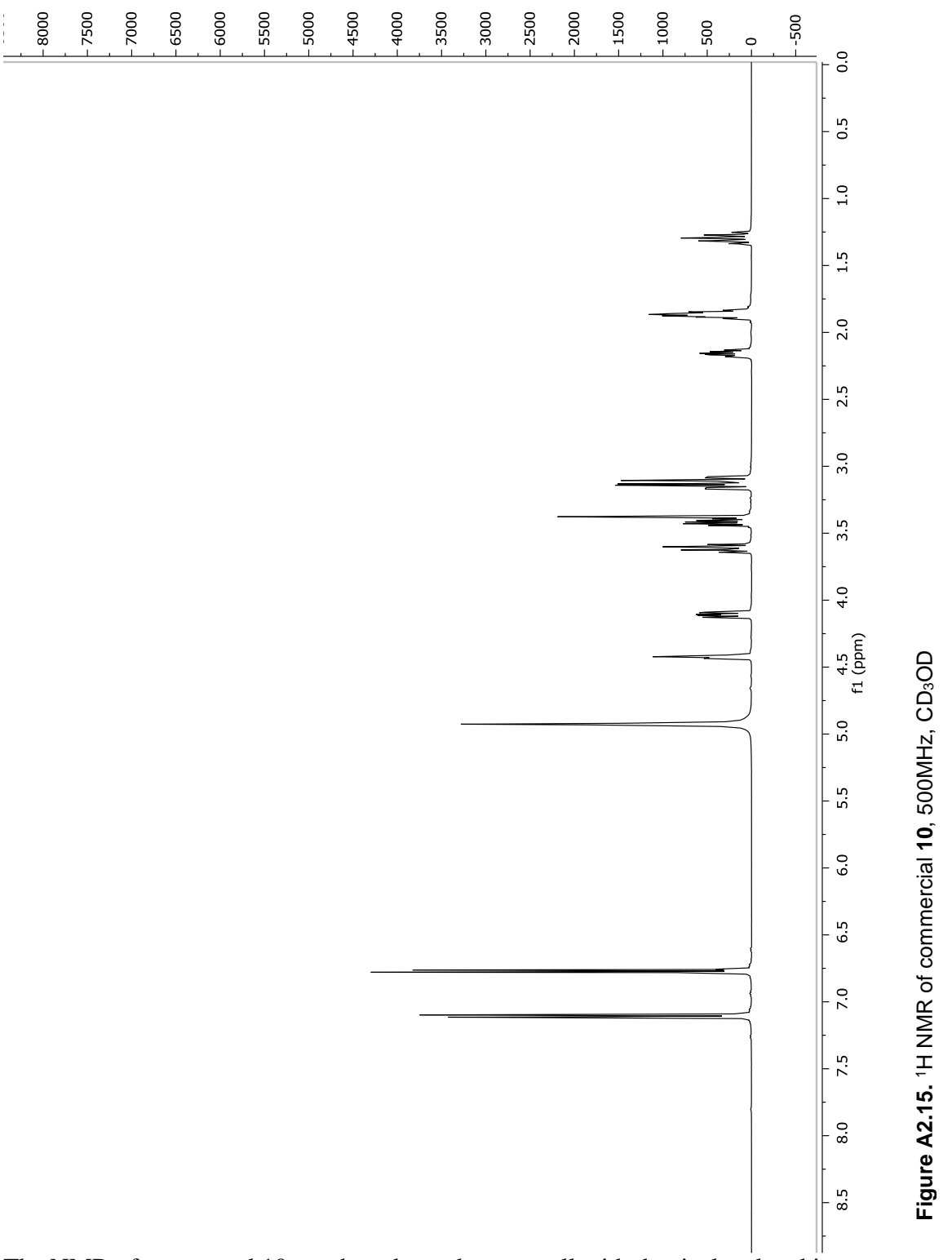
Figure A2.13. <sup>1</sup>H NMR of commercial 8, 500MHz, CD<sub>3</sub>OD



The NMR of compound 8 purchased matches up well with that isolated.



The NMR of compound 9 purchased matches up well with that isolated



The NMR of compound 10 purchased matches up well with that isolated and increases our confidence in the structure.

# **Appendix 3 Supplementary data for Chapter 4**

Figure A3.1. <sup>1</sup> H NMR of 1, 600MHz, CD₃OD	1106
Figure A3.2. <sup>13</sup> C NMR of <b>1</b> , 125 MHz, CD <sub>3</sub> OD	
Figure A3.3. <sup>1</sup> H COSY NMR of 1, 600MHz, CD <sub>3</sub> OD	128
Figure A3.4. HSQC NMR of 1, 600MHz, CD₃OD	129
Figure A3.5. HMBC NMR of 1, 600MHz, CD <sub>3</sub> OD	130
Table A3.1. NMR data for 2 (CD3OD, 600 MHz)	131
Figure A3.6. <sup>1</sup> H NMR of <b>2</b> , 600MHz, CD <sub>3</sub> OD	132
Figure A3.7. <sup>1</sup> H COSY NMR of <b>2</b> , 600MHz, CD <sub>3</sub> OD	133
Figure A3.8. HSQC NMR of 2, 600MHz, CD₃OD	134
Figure A3.9. HMBC NMR of 2, 600MHz, CD <sub>3</sub> OD	135
Figure A3.10. HRMS spectra of 3 taken in positive ion mode using ESI	114
Figure A3.11. <sup>1</sup> H NMR of 3, 600MHz, CD <sub>3</sub> OD	137
<b>Figure A3.12.</b> <sup>13</sup> C NMR of <b>3</b> , 125 MHz, CD₃OD	138
Figure A3.13. HSQC NMR of 3, 600 MHz, CD₃OD	139
Figure A3.14. <sup>1</sup> H COSY NMR of 3, 600 MHz, CD <sub>3</sub> OD	140
Figure A3.15. HMBC NMR of 3, 600 MHz, CD₃OD	141
Figure A3.16. HRMS of 4 in negative ESI mode	142
<b>Figure A3.17.</b> ¹H NMR of <b>4</b> , 600 MHz, CD₃OD	143
Figure A3.18. <sup>13</sup> C NMR of 4, 125 MHz, CD <sub>3</sub> OD	144
Figure A3.19. HSQC NMR of 4, 600 MHz, CD₃OD	145
Figure A3.20. COSY NMR of 4, 600 MHz, CD₃OD	146
Figure A3.21. HMBC NMR of 4, 600 MHz, CD <sub>3</sub> OD	147
<b>Figure A3.22.</b> ¹H NMR of <b>5</b> , 600 MHz, CD₃OD	148
Figure A3.23. HSQC NMR of 5, 600 MHz, CD₃OD	149
Figure A3.24. ¹H COSY NMR of 5, 600 MHz, CD₃OD	150
Figure A3.25. HMBC NMR of 5, 600 MHz, CD <sub>3</sub> OD	151
Figure A3.26. HRMS spectra of 6 taken in positive ion mode using ESI	152
Figure A3.27. <sup>1</sup> H NMR of 6, 600 MHz, CD <sub>3</sub> OD/CDCl <sub>3</sub>	153
Figure A3.28. HSQC NMR of 6, 600 MHz, CD <sub>3</sub> OD/CDCl <sub>3</sub>	154
Figure A3.29. HMBC NMR of 6, 600 MHz, CD <sub>2</sub> OD/CDCl <sub>2</sub>	155

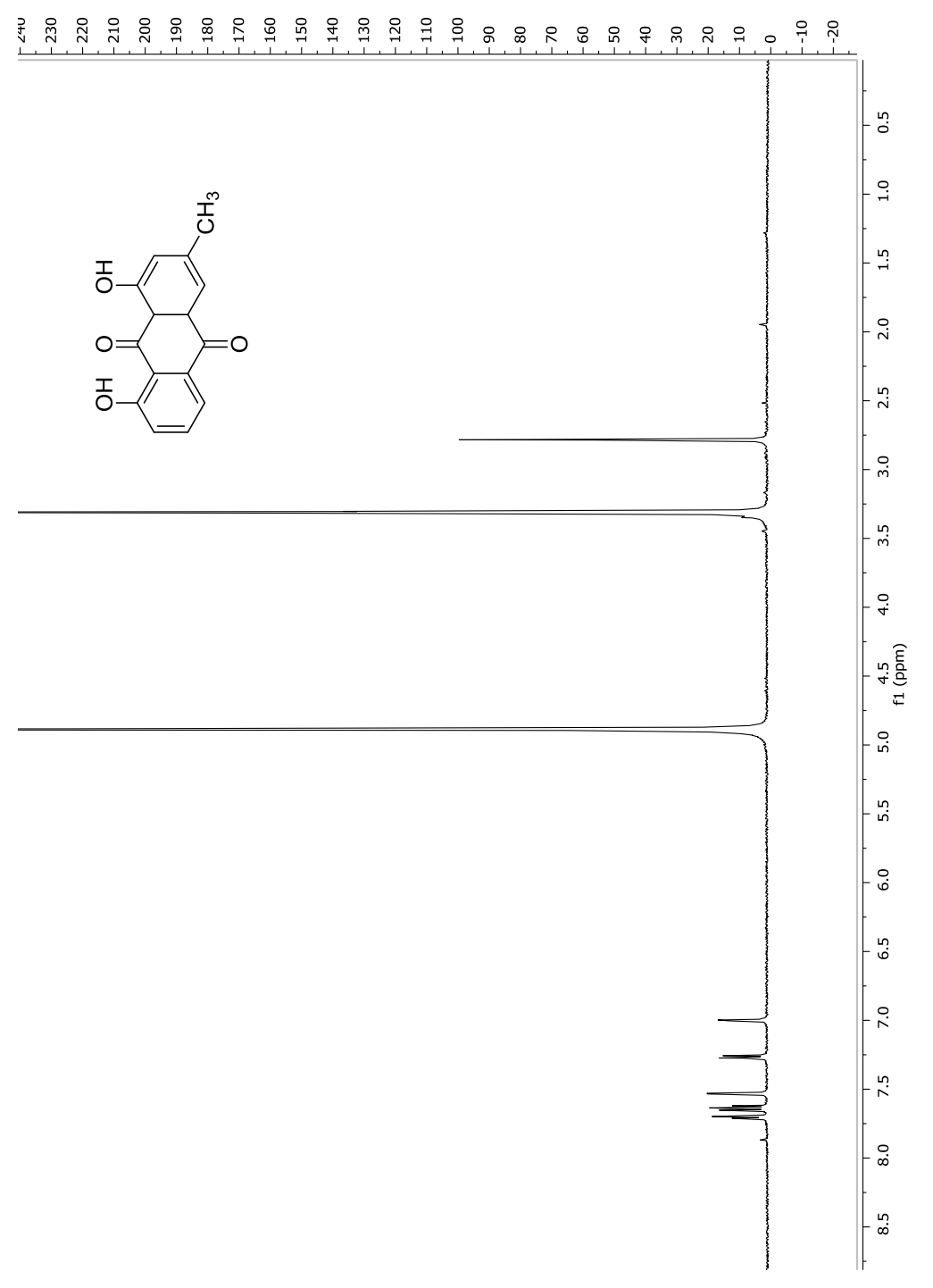


Figure A3.1.  $^1\text{H}$  NMR of 1, 600MHz, CD $_3$ OD

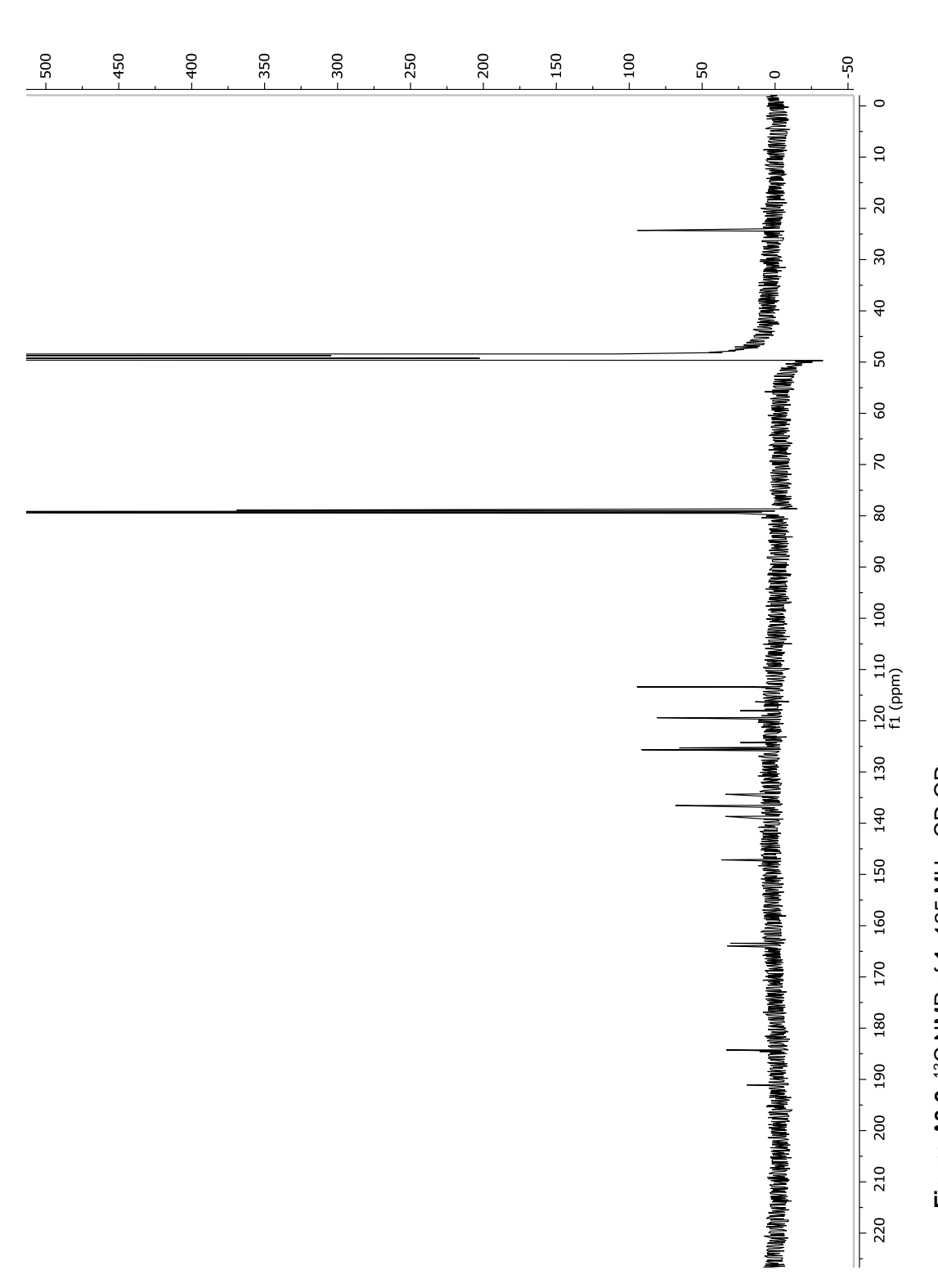


Figure A3.2.  $^{13}\text{C}$  NMR of 1, 125 MHz, CD $_3\text{OD}$ 

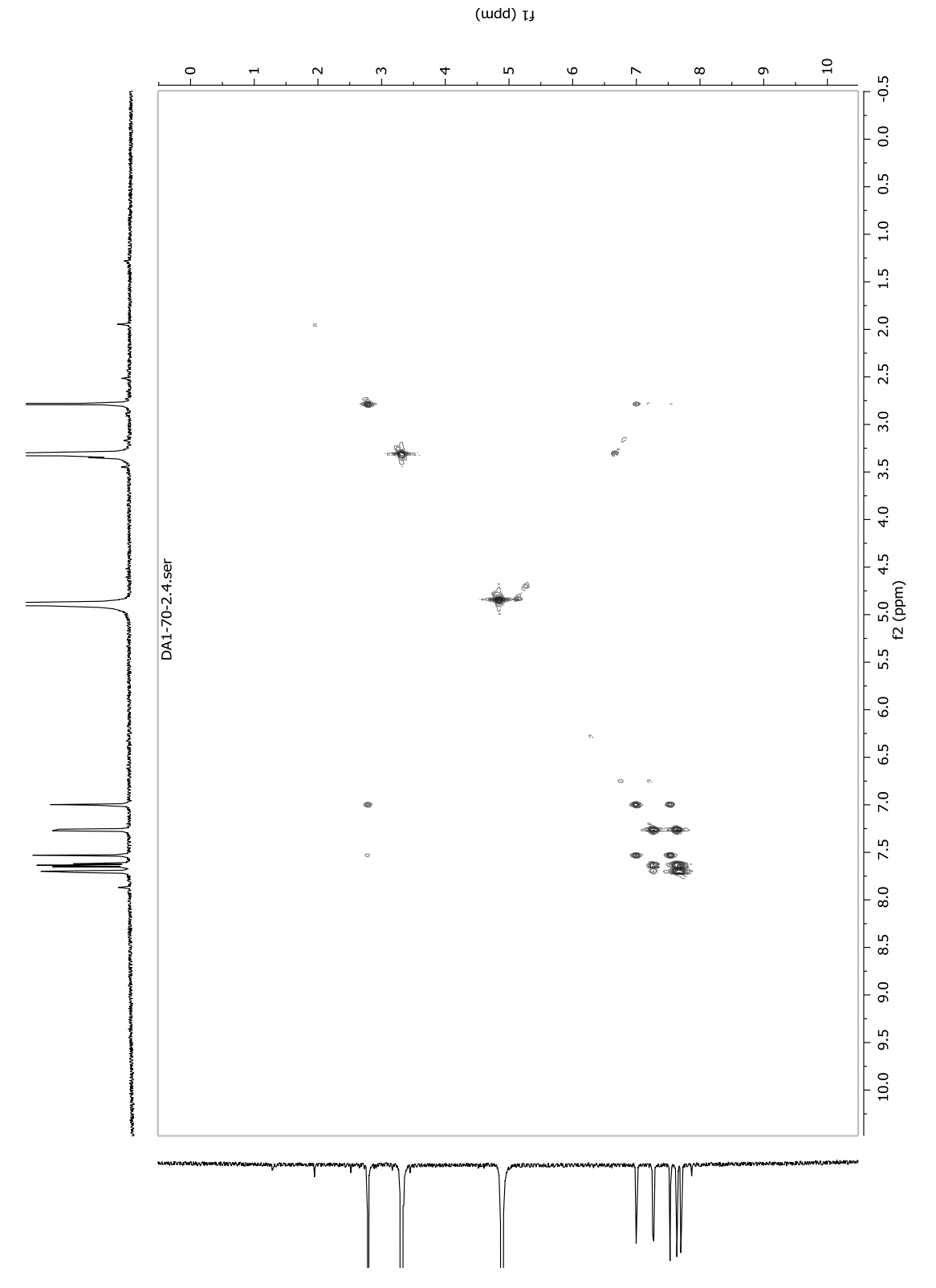
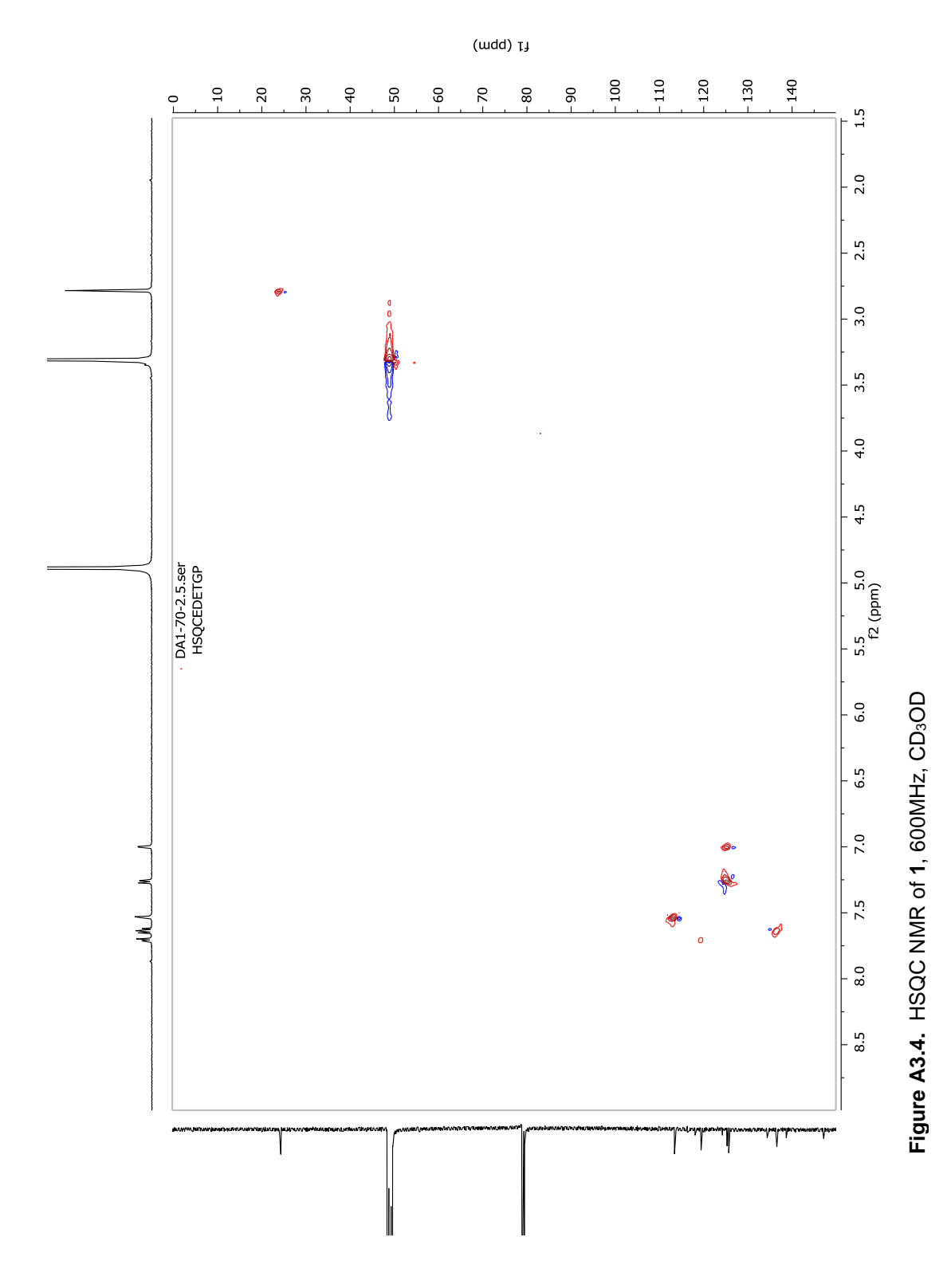


Figure A3.3. <sup>1</sup>H COSY NMR of 1, 600MHz, CD<sub>3</sub>OD



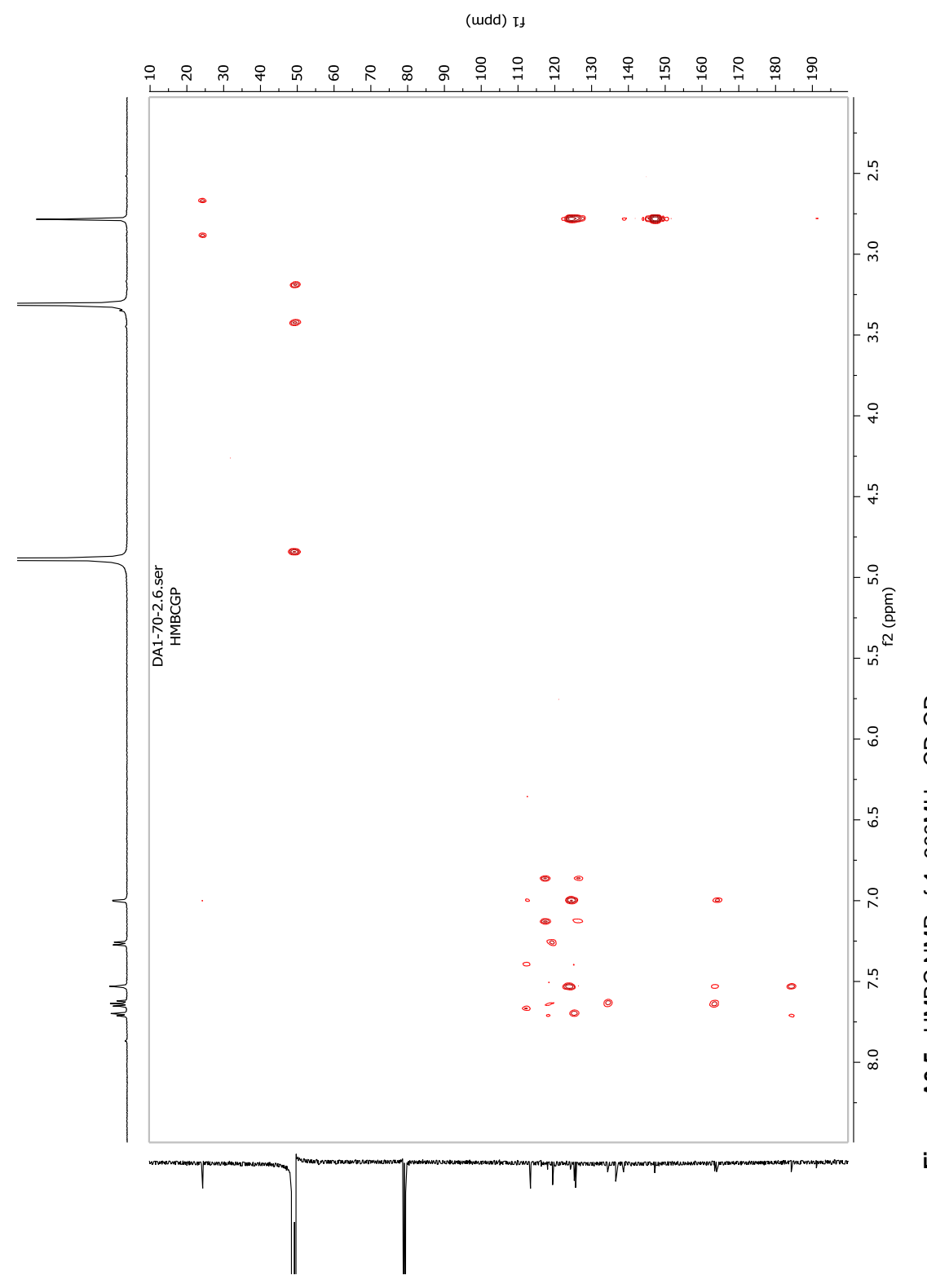


Figure A3.5. HMBC NMR of 1, 600MHz, CD<sub>3</sub>OD

Table A3.4. NMR data for 2 (CD3OD, 600 MHz)

Position	$\delta_{\rm C}$ , mult.	δ <sub>H</sub> (J in Hz)	HMBC
1	197.31, C		
2	48.94, CH	2.53, m	1, 3, 4, 9
		2.77, dd (16.3, 3.8)	1, 3, 4
3	65.63, CH	4.22, tt (7.4, 3.6)	1, 10
4	39.1, CH2	2.85, dd (16.1, 7.2)	2, 3, 5, 9, 10
		3.09, dd (16.1, 3.6)	2, 3, 5, 9, 10
5	114.09, CH	6.67, s	1, 4, 8, 9, 6, 7, 11
6	157.95, C		
7	139.01, C		
8	131.31, C		
9	124.04, C		
10	145.86, C		
11	205.98, C		
12	31.72, CH3	2.43, s	5, 11
13	18.46, CH3	2.41, s	1, 7, 8, 9

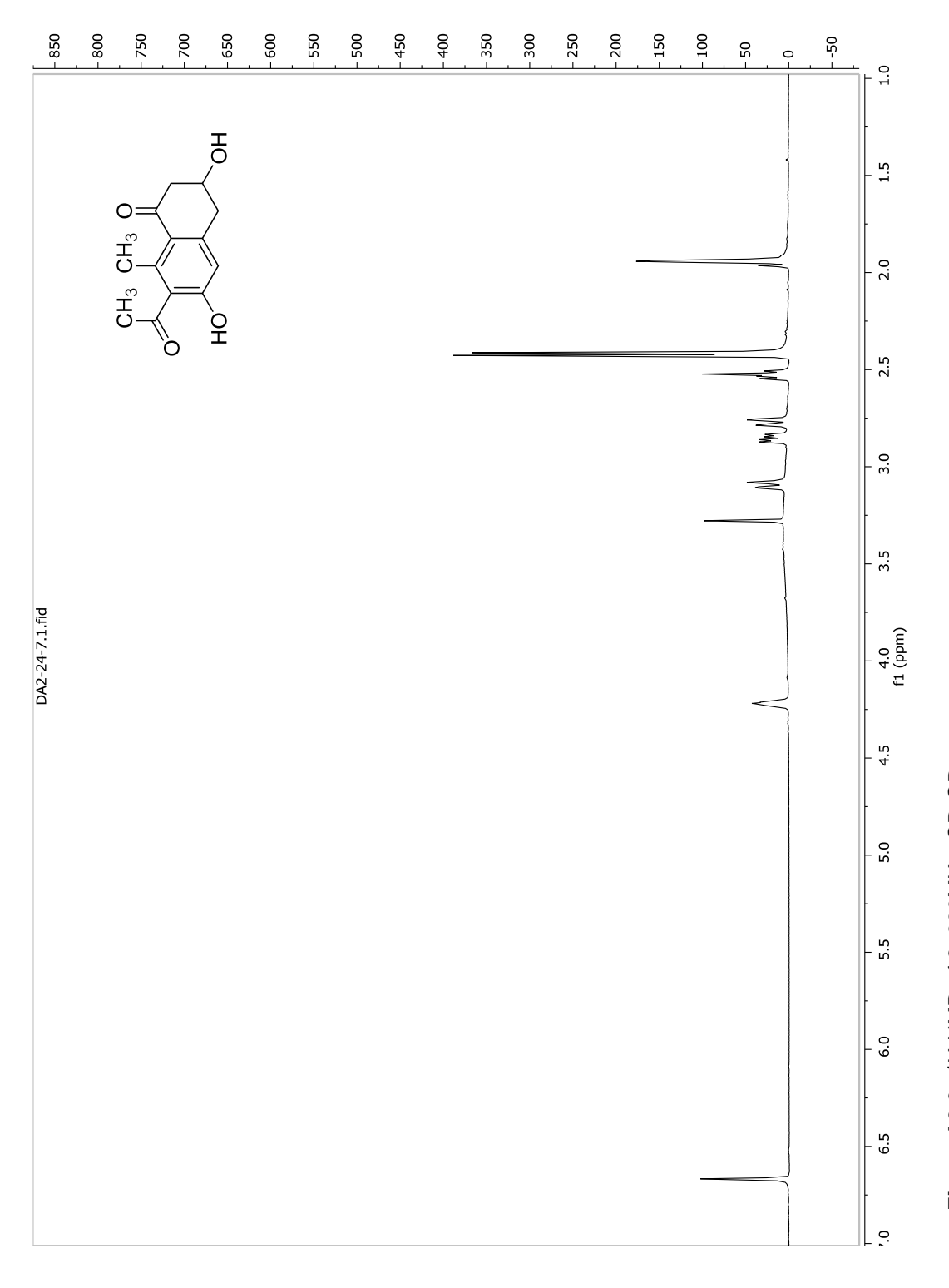


Figure A3.6. <sup>1</sup>H NMR of 2, 600MHz, CD<sub>3</sub>OD

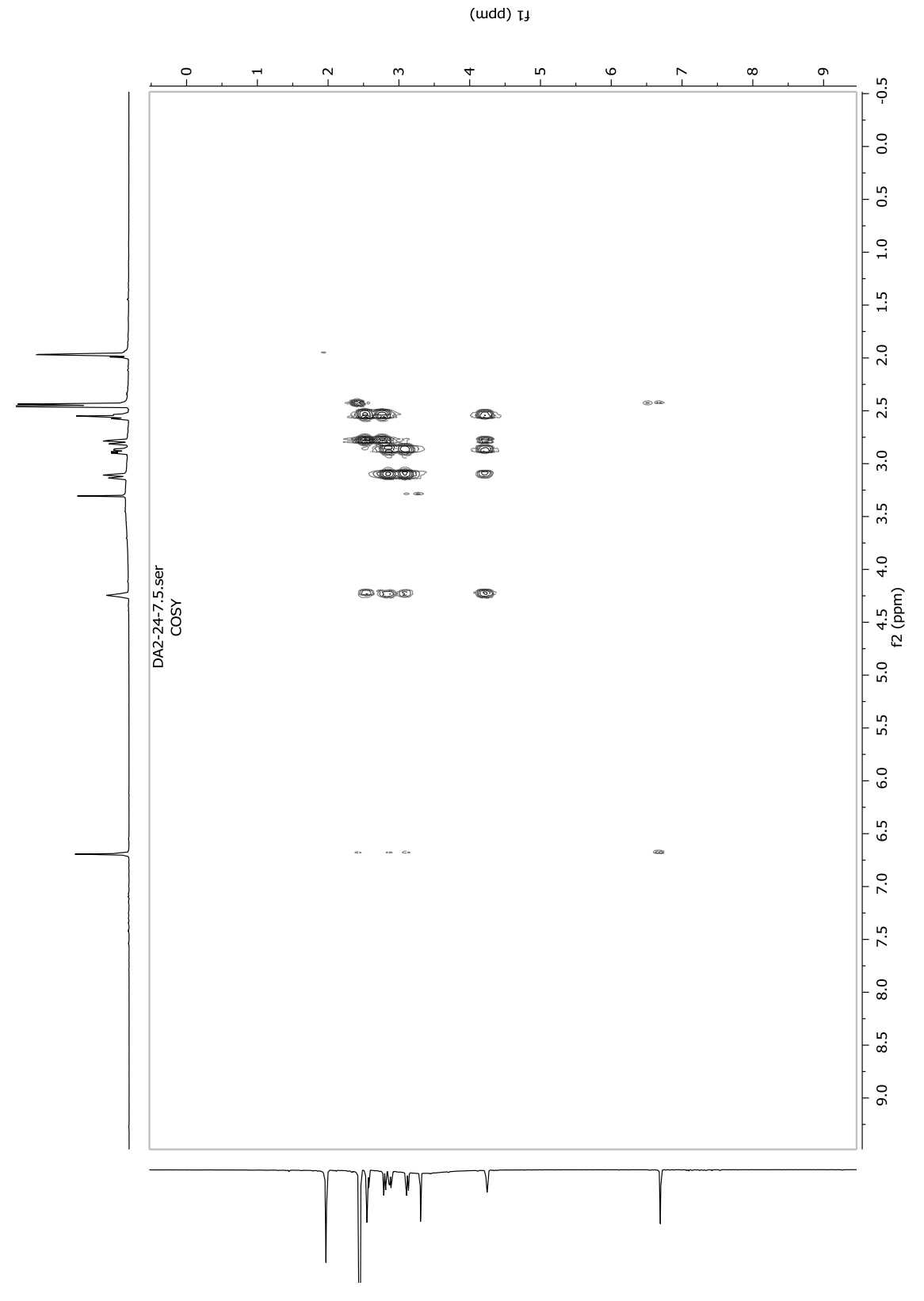


Figure A3.7. <sup>1</sup>H COSY NMR of 2, 600MHz, CD<sub>3</sub>OD

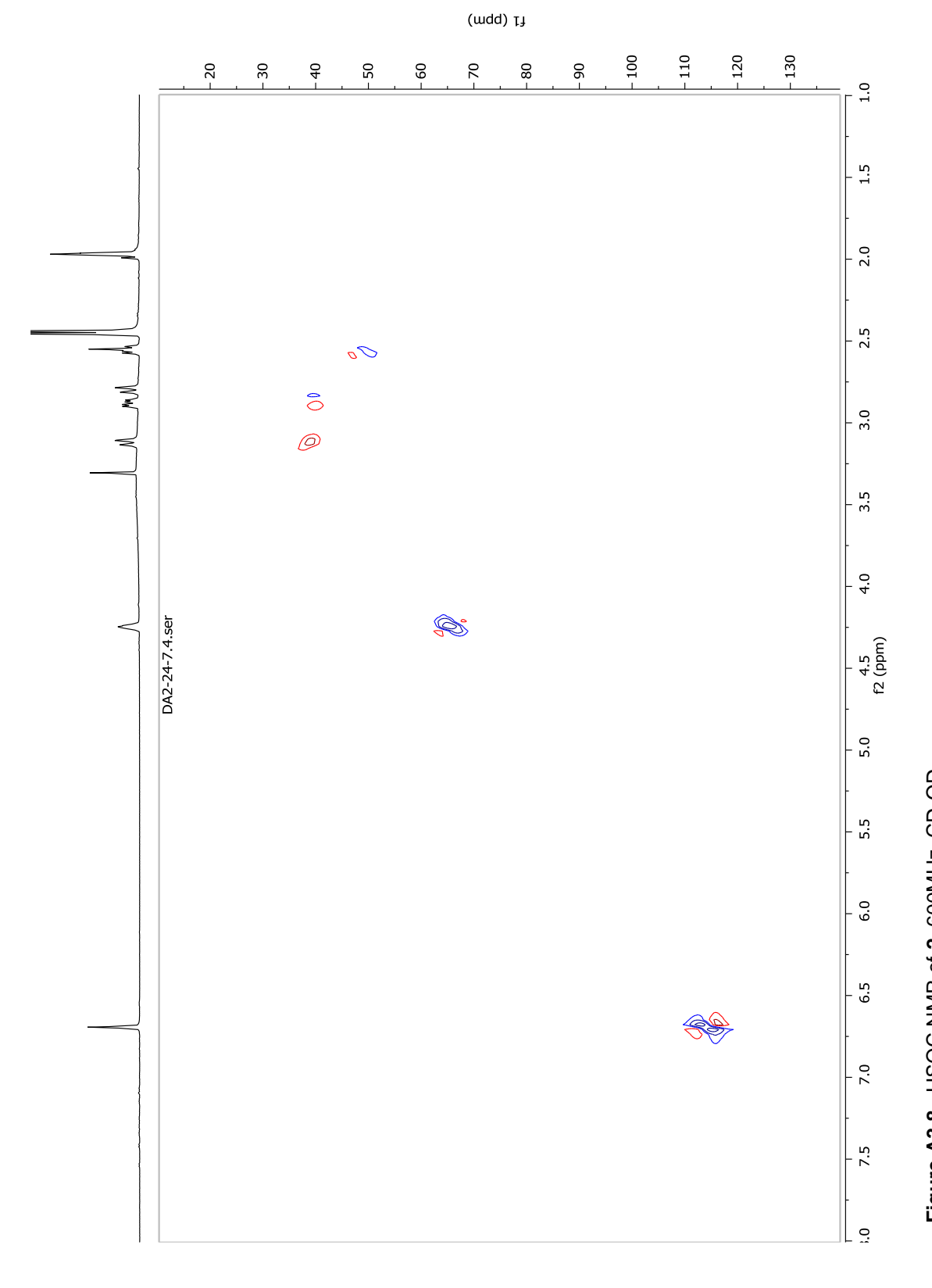


Figure A3.8. HSQC NMR of 2, 600MHz,  $CD_3OD$ 

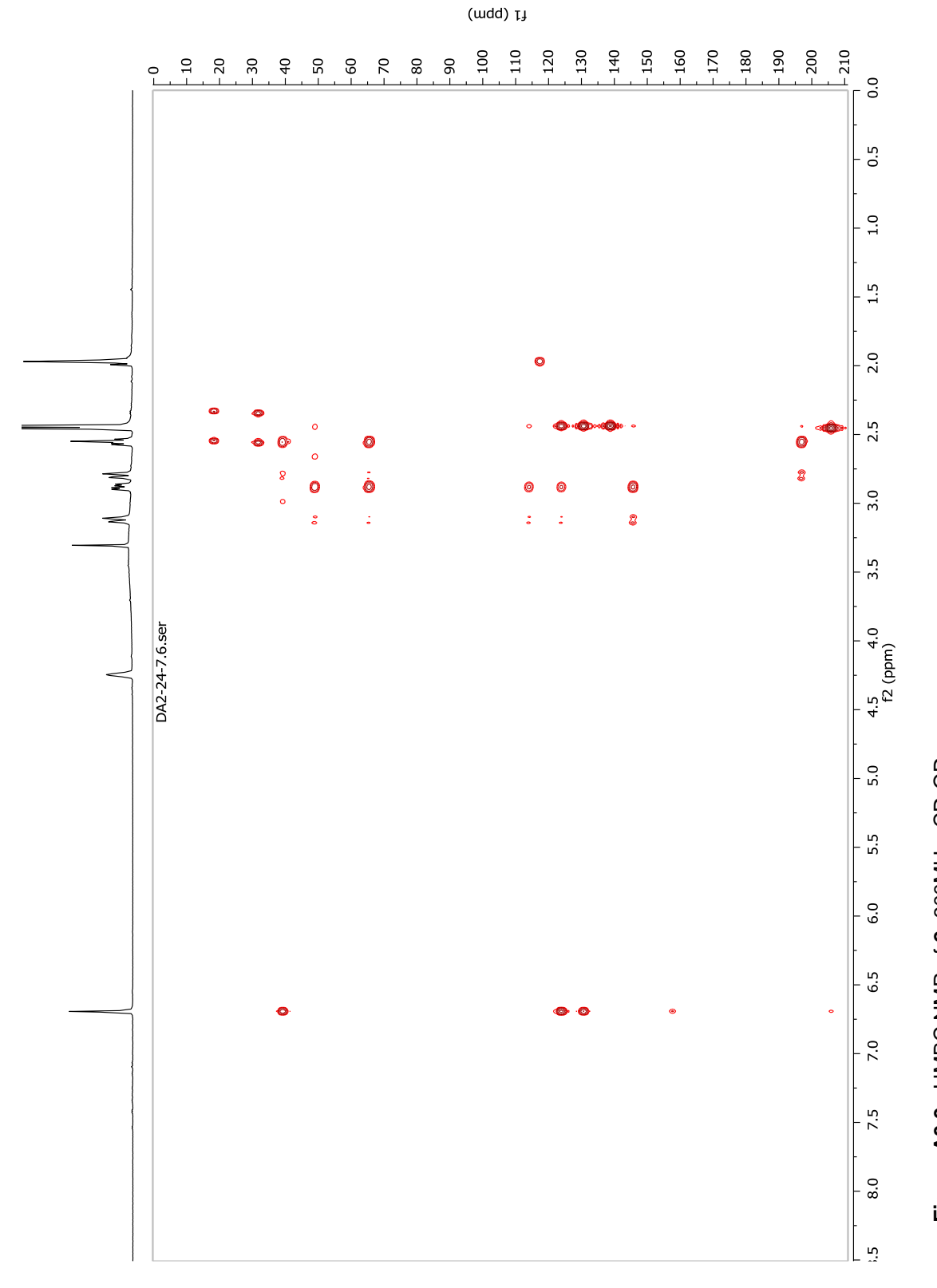


Figure A3.9. HMBC NMR of 2, 600MHz,  $CD_3OD$ 

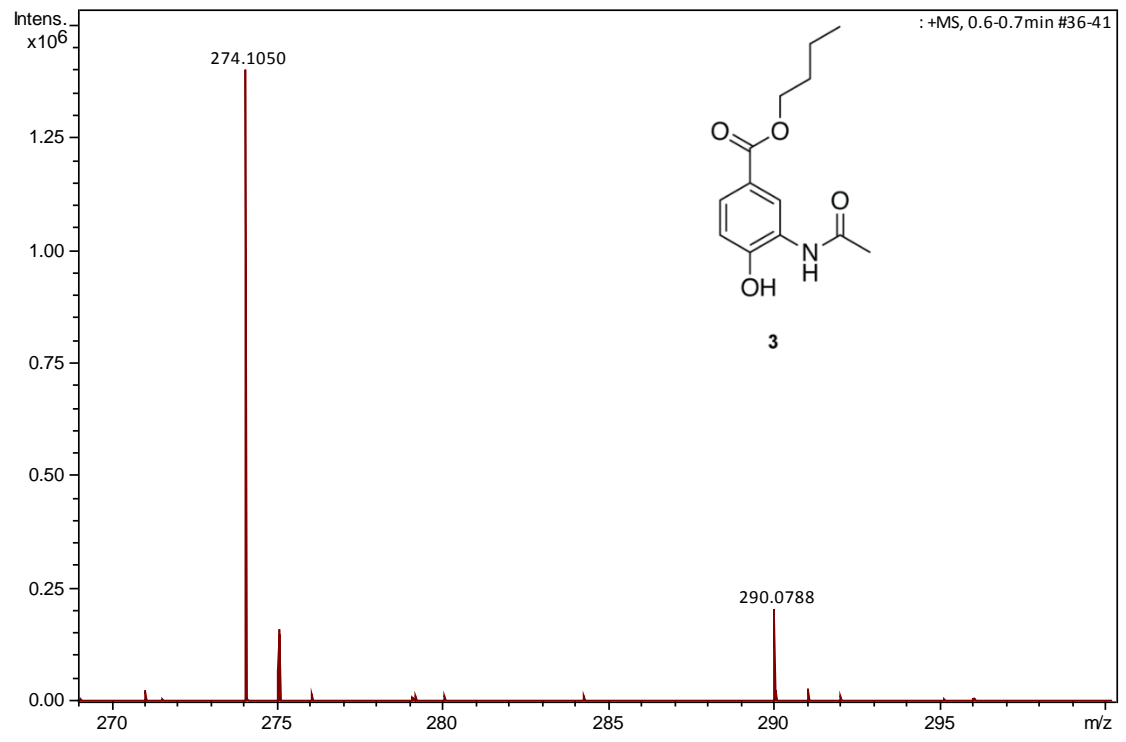


Figure A3.10. HRMS spectra of 3 taken in positive ion mode using ESI.

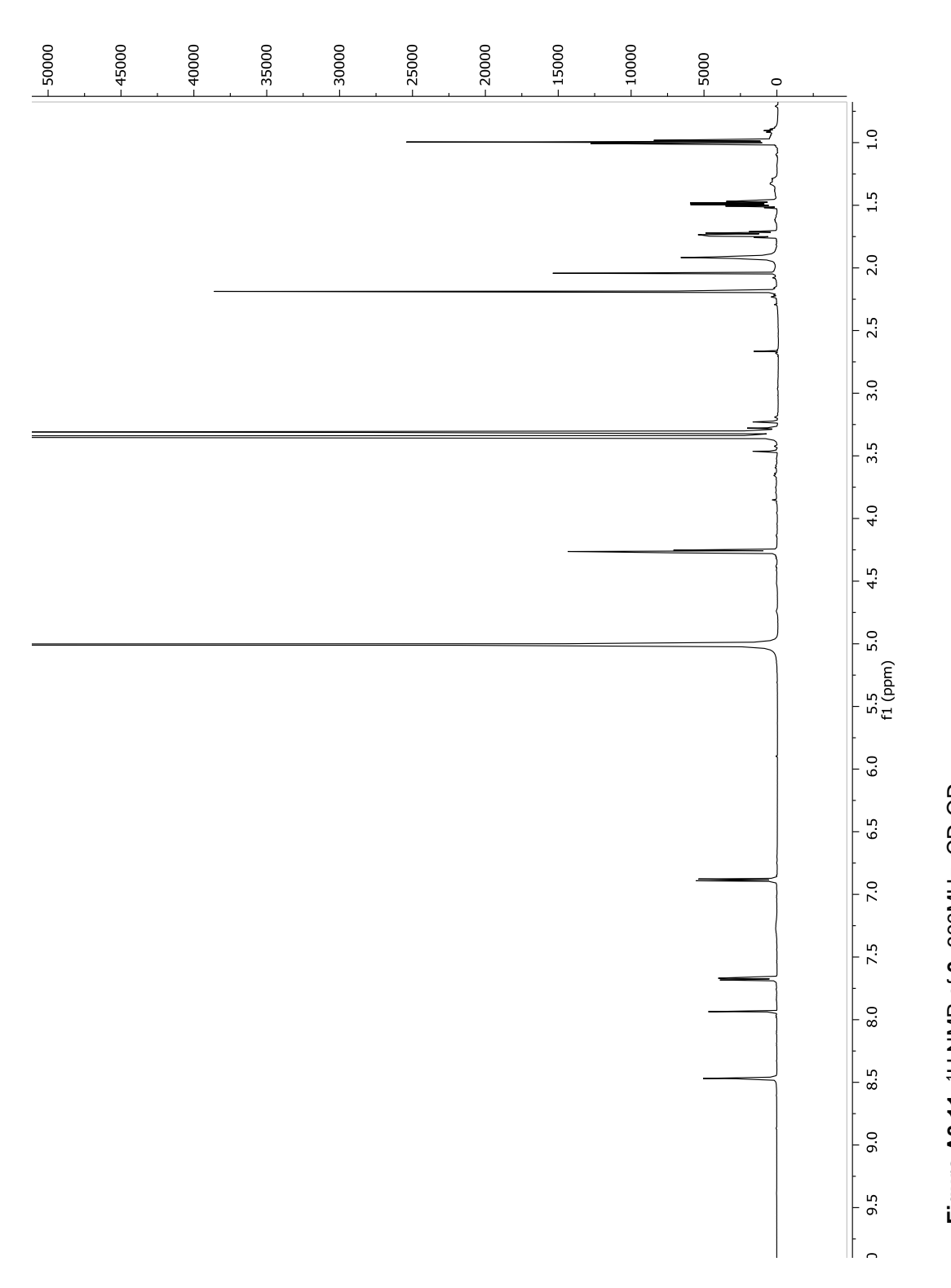


Figure A3.11.  $^1$ H NMR of 3, 600MHz, CD $_3$ OD

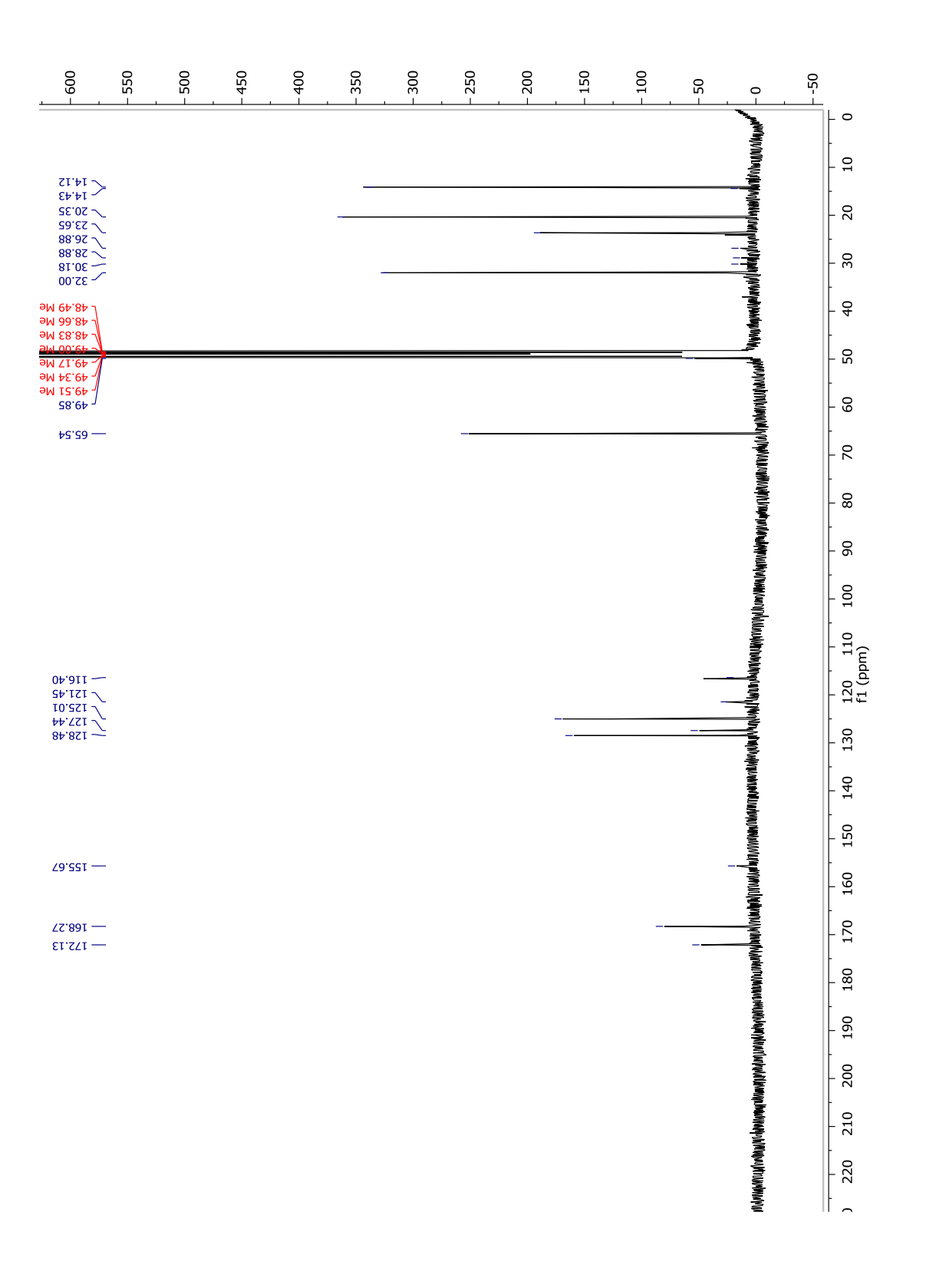
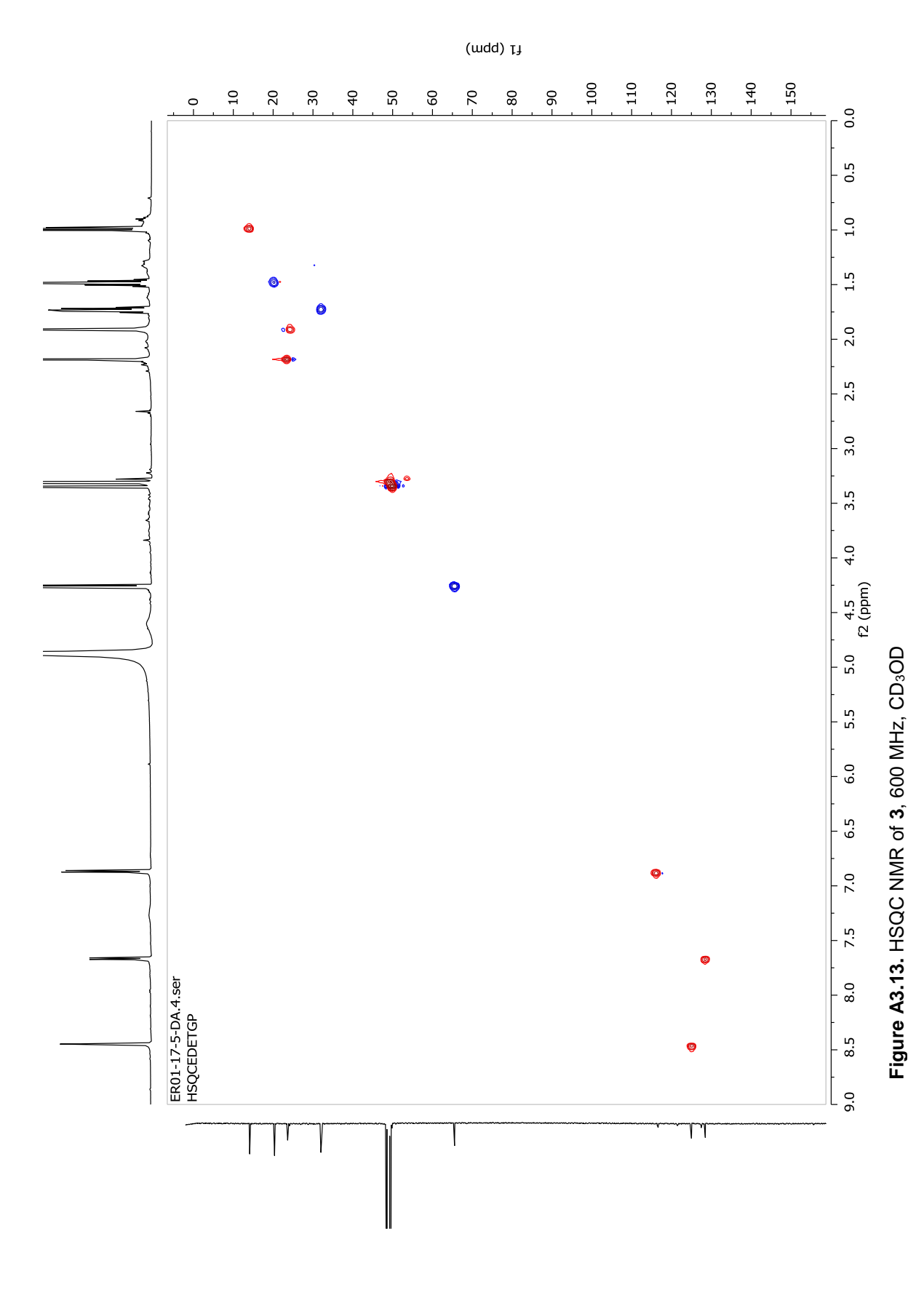
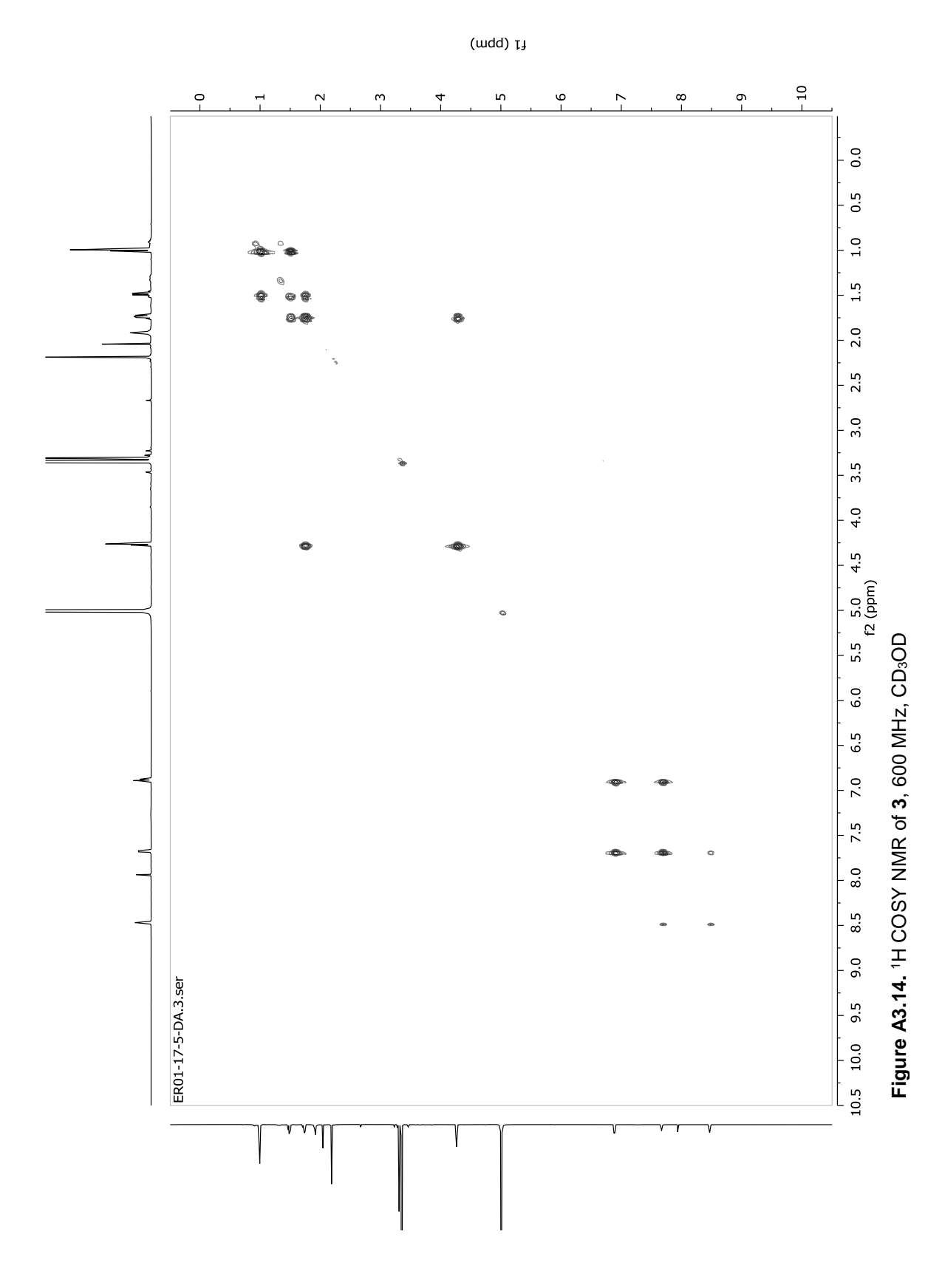


Figure A3.12. <sup>13</sup>C NMR of 3, 125 MHz, CD<sub>3</sub>OD





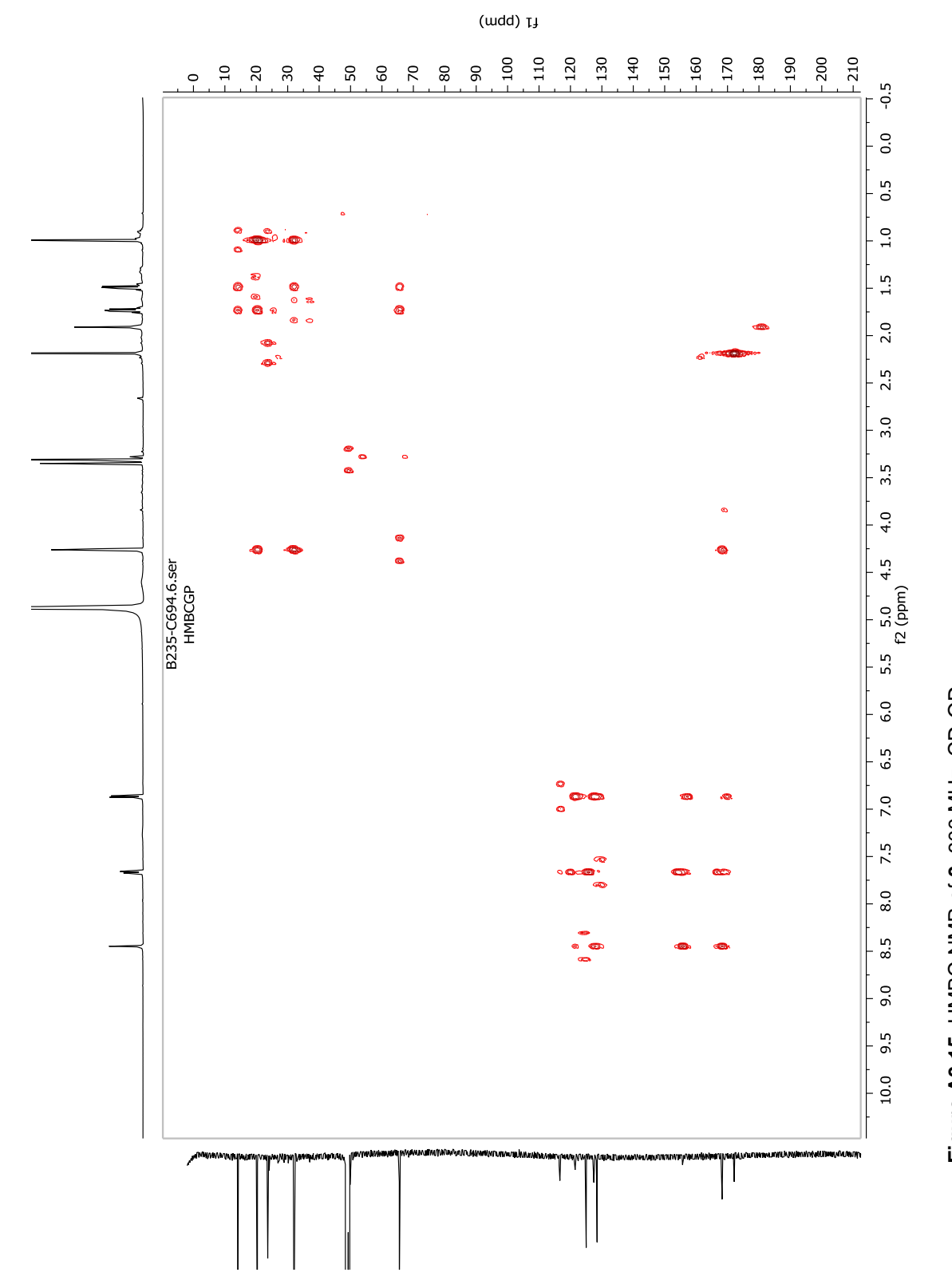


Figure A3.15. HMBC NMR of 3, 600 MHz,  $\mbox{CD}_3\mbox{OD}$ 

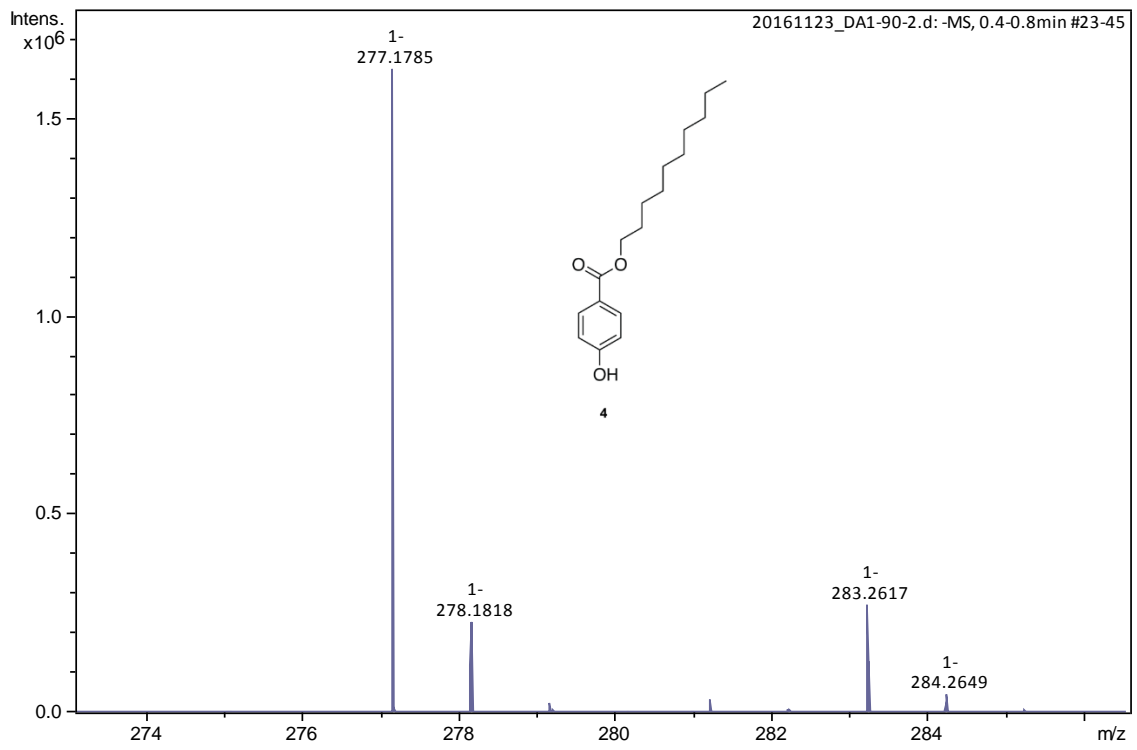


Figure A3.16. HRMS of 4 in negative ESI mode

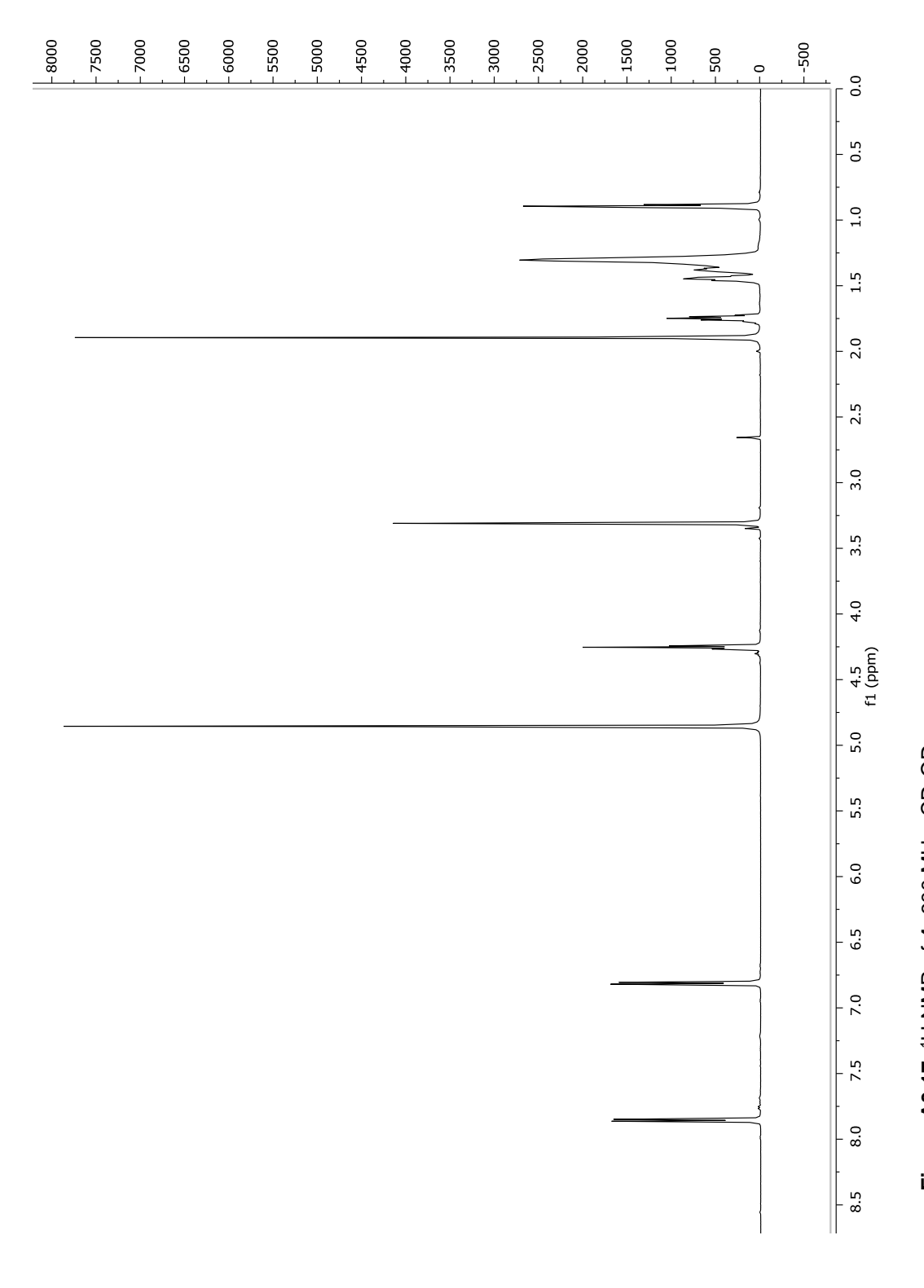
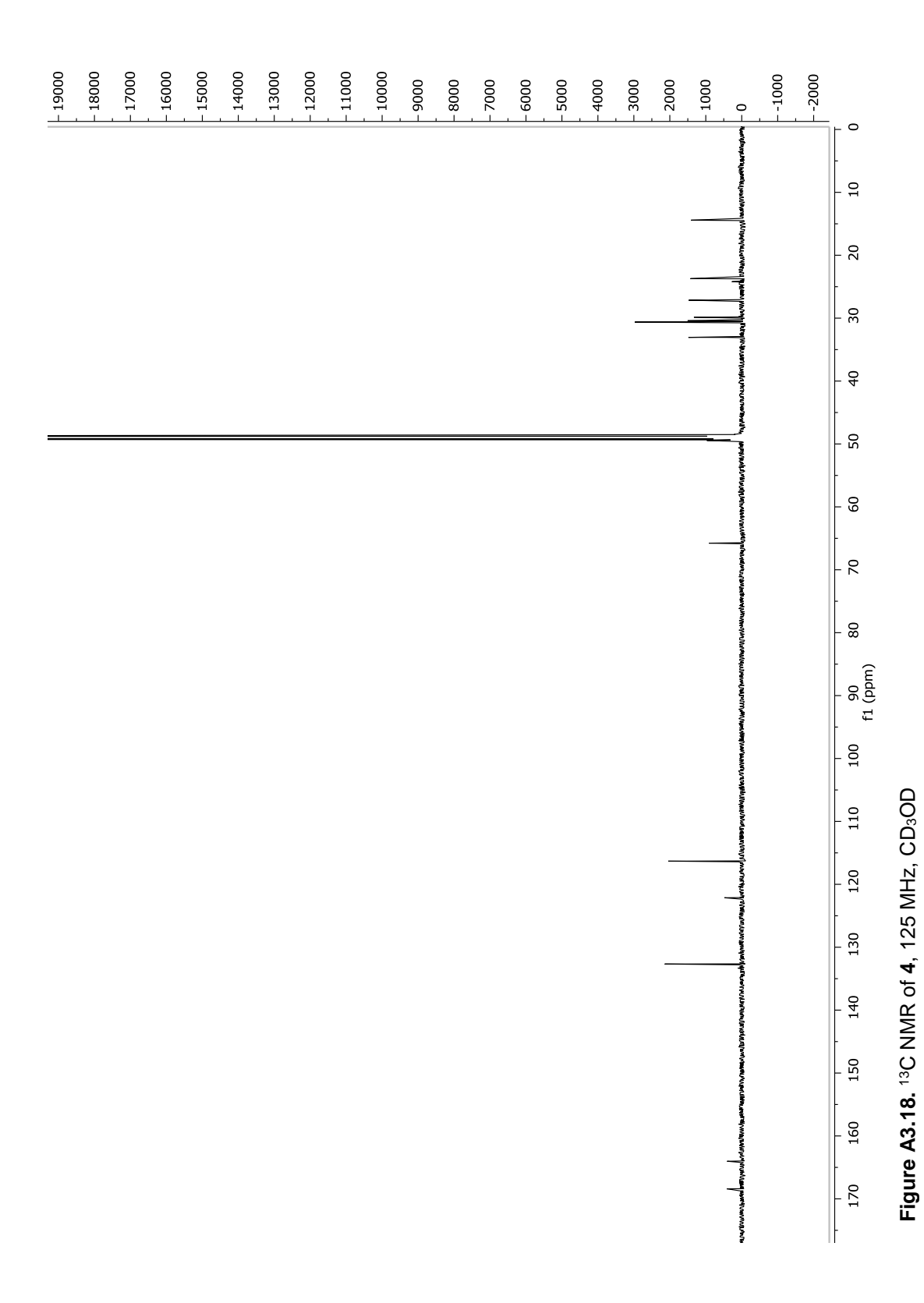
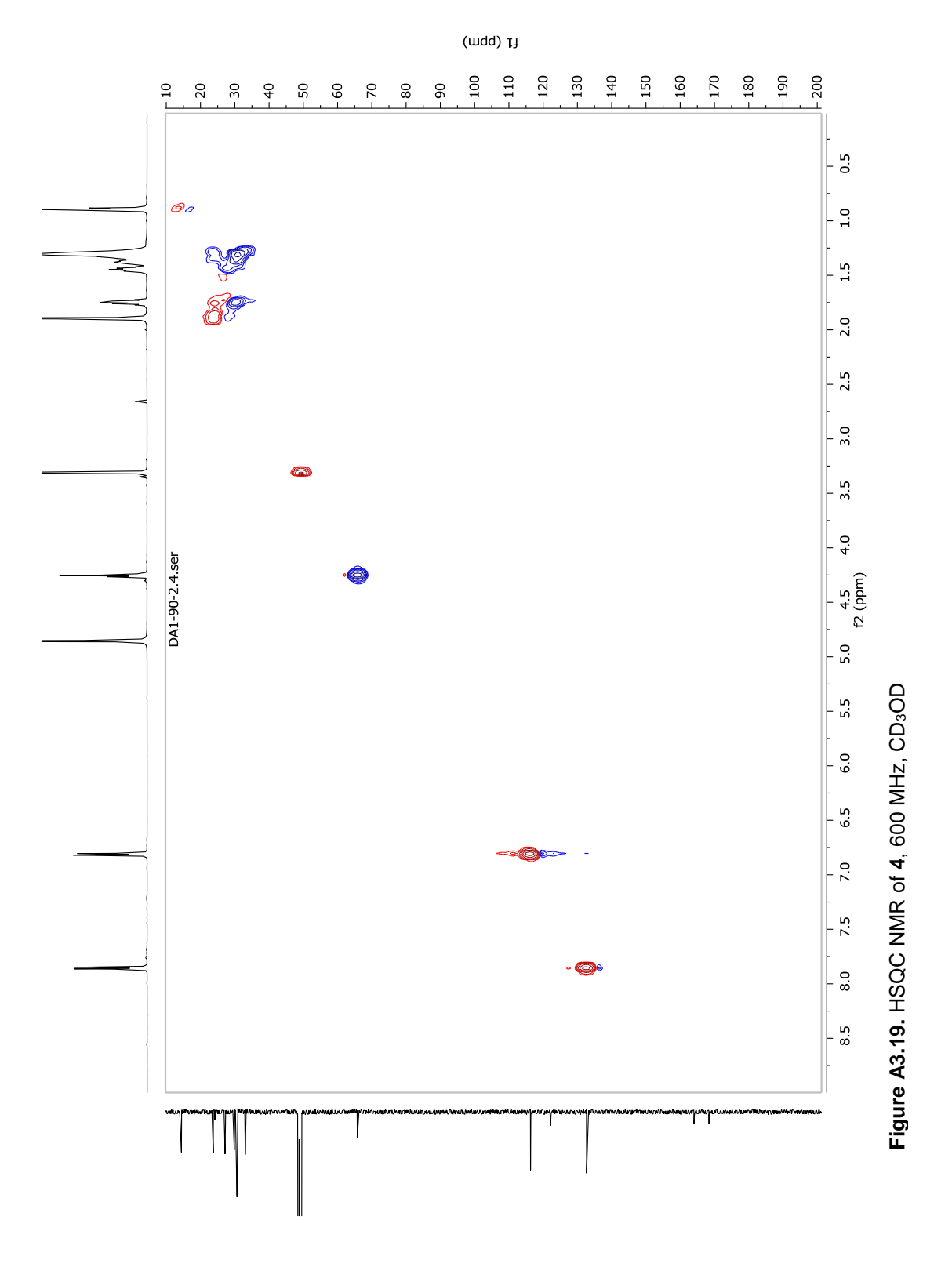


Figure A3.17.  $^1\text{H}$  NMR of 4, 600 MHz,  $\text{CD}_3\text{OD}$ 





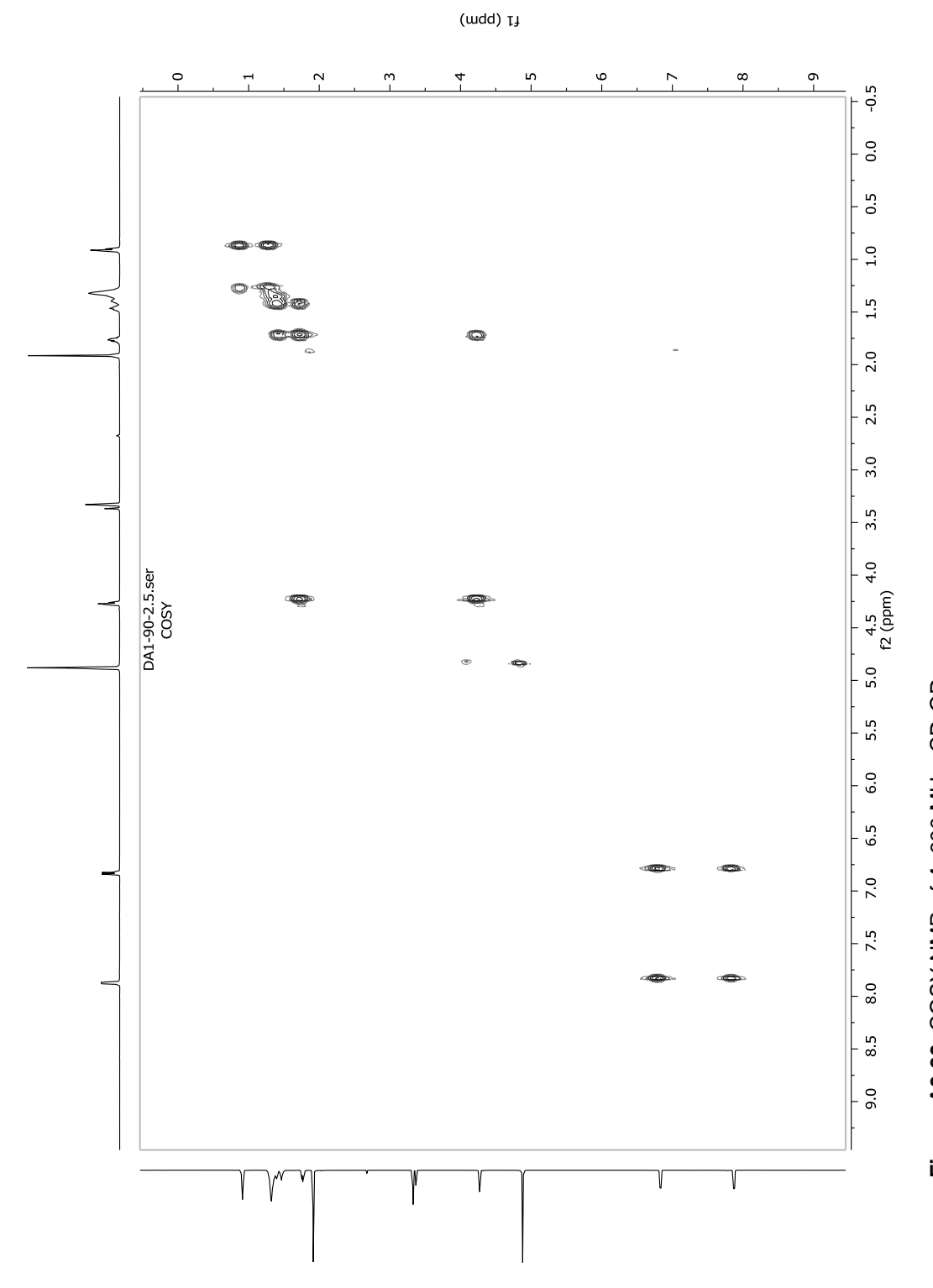
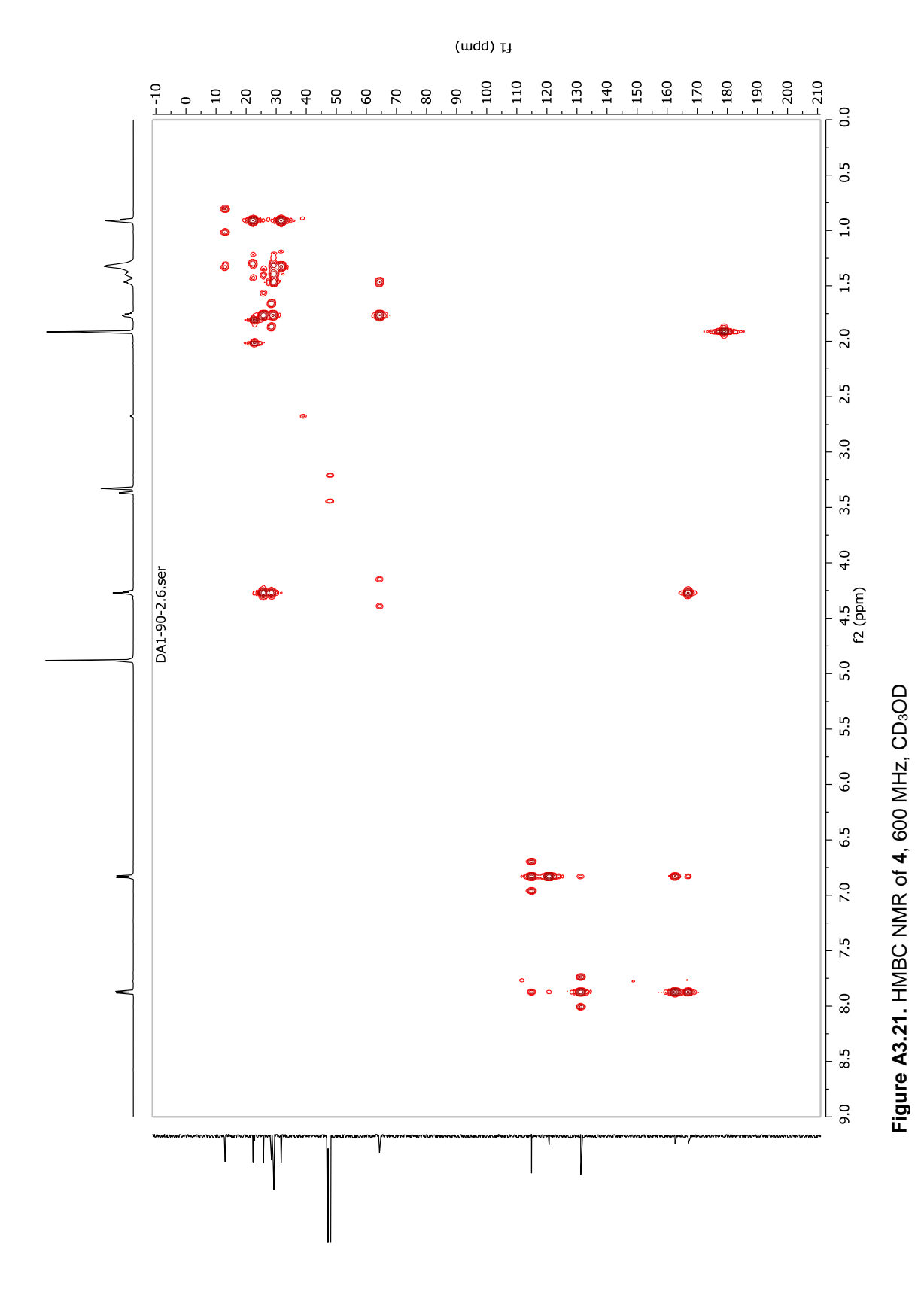


Figure A3.20. COSY NMR of 4, 600 MHz, CD<sub>3</sub>OD



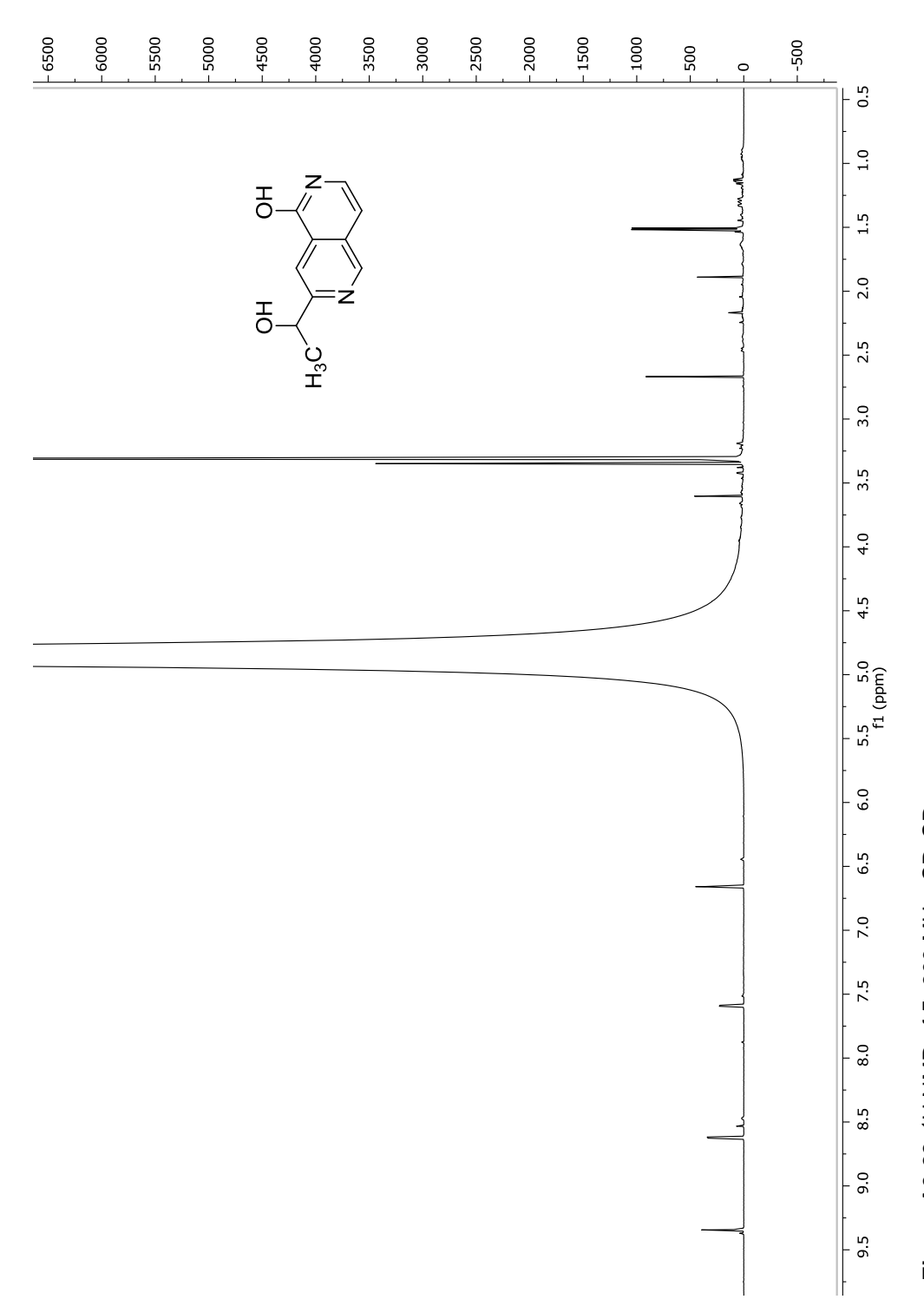
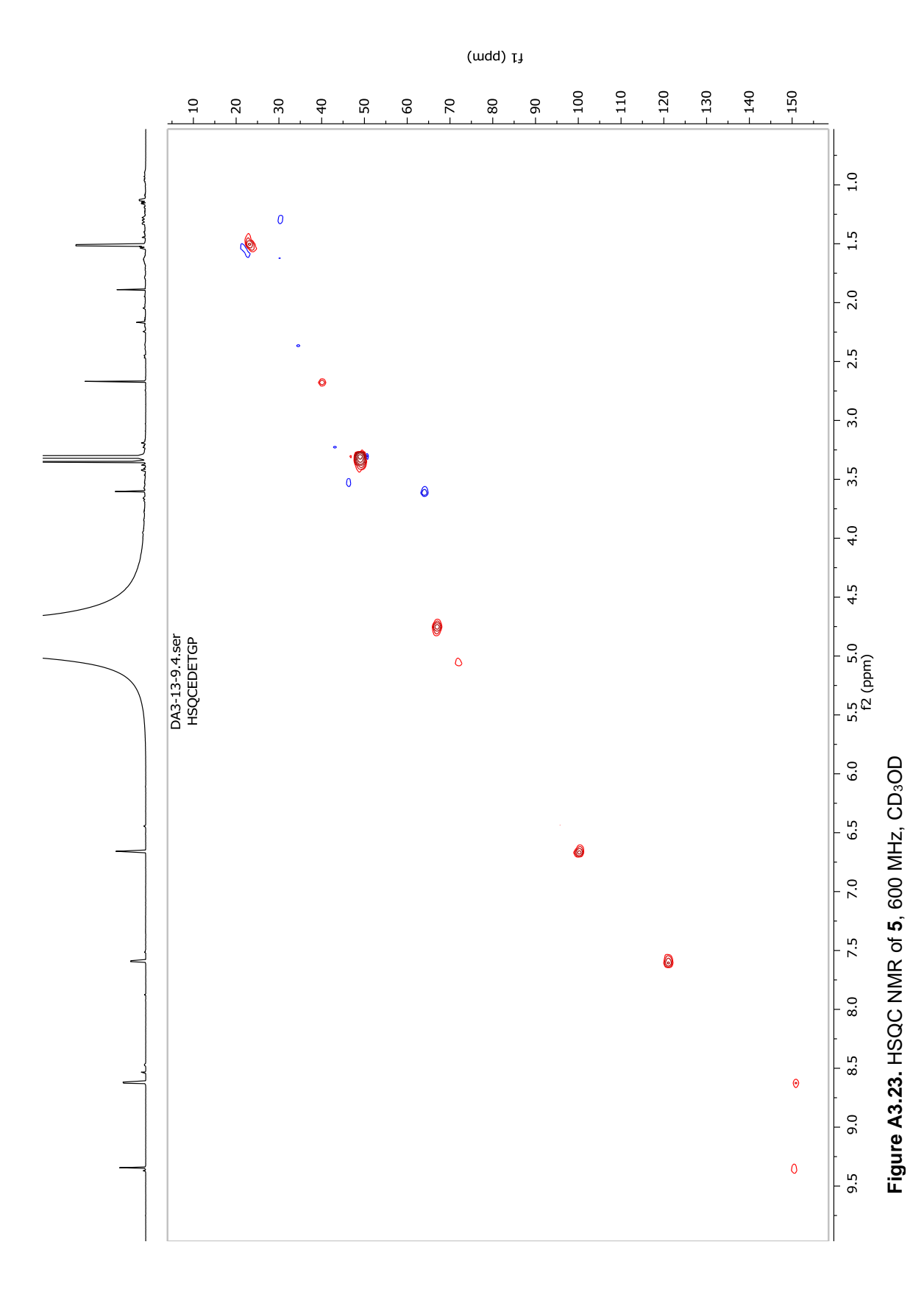
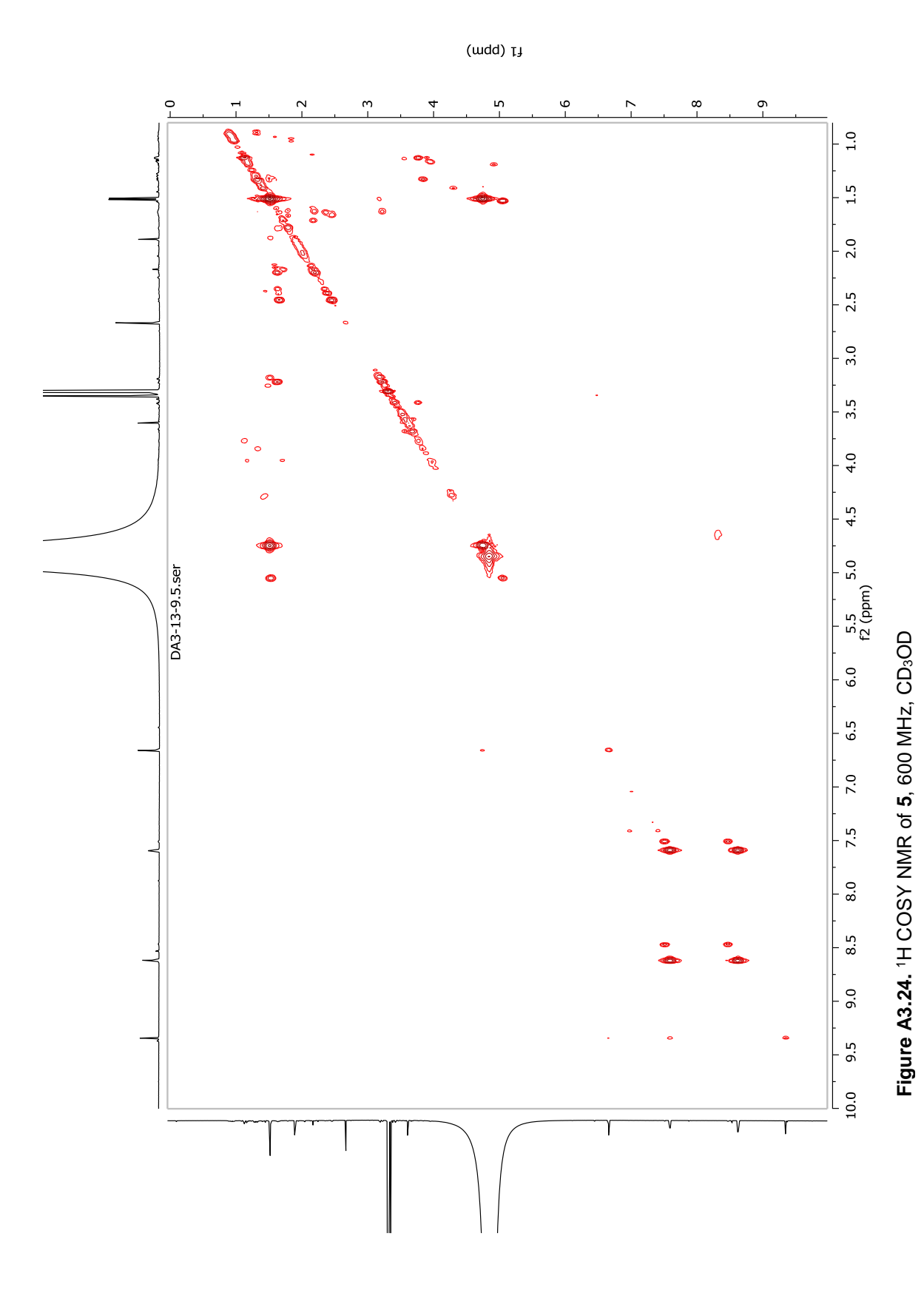
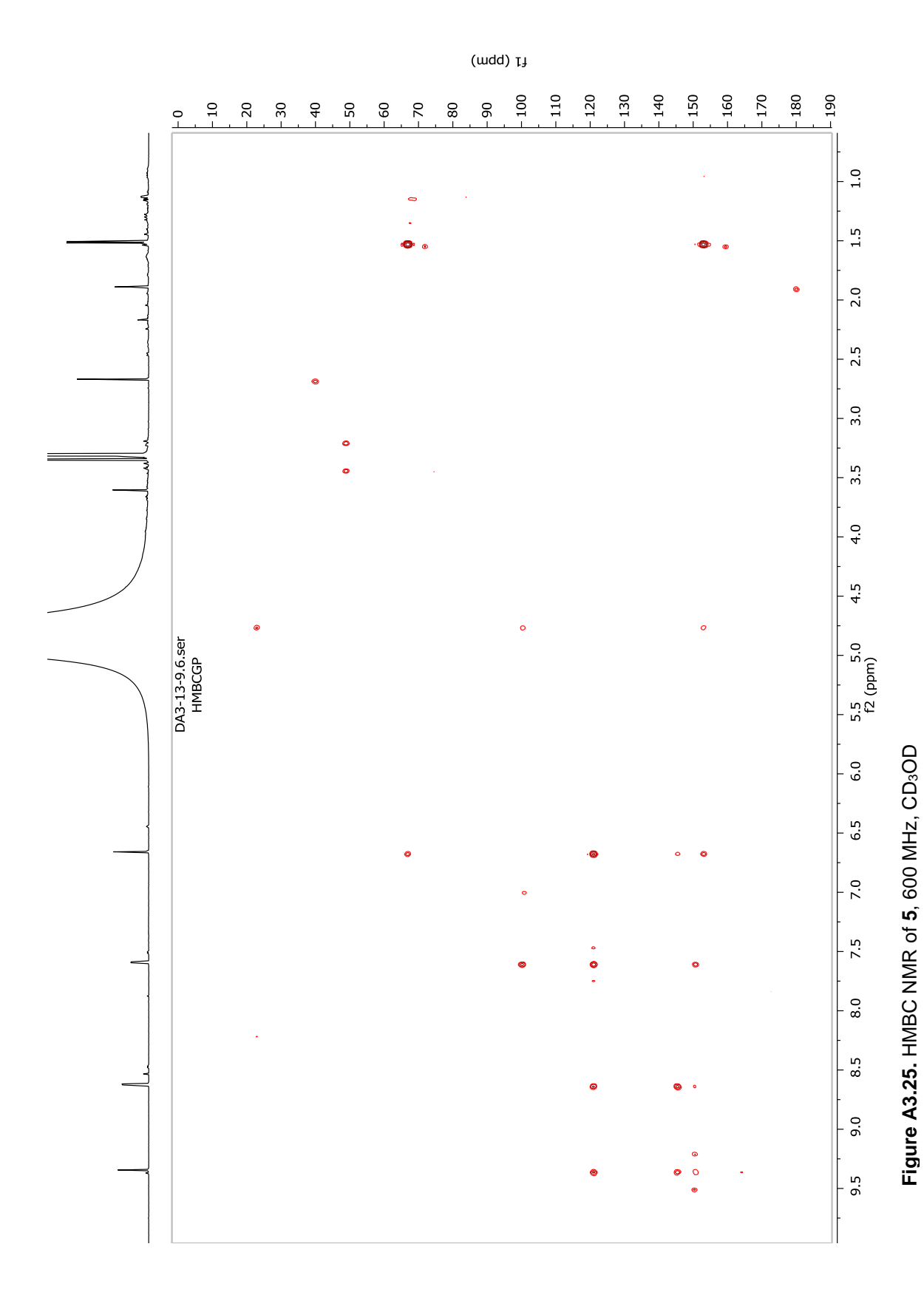


Figure A3.22. <sup>1</sup>H NMR of 5, 600 MHz, CD $_3$ OD







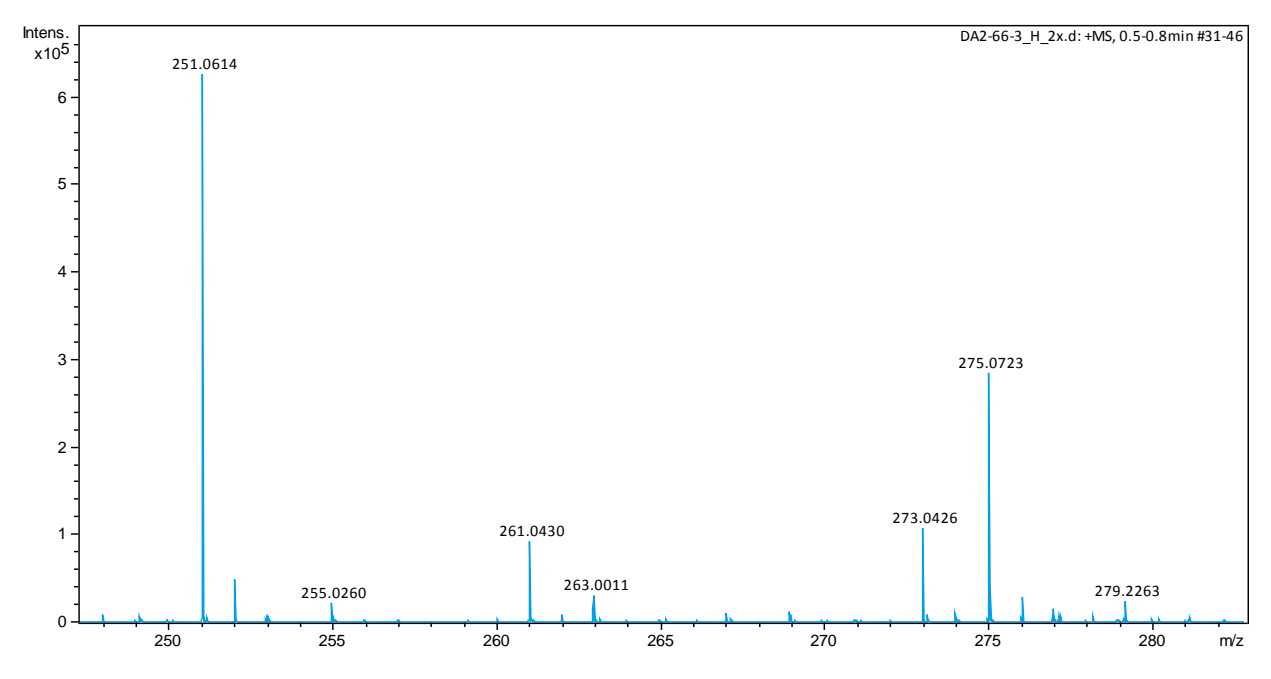


Figure A3.26. HRMS spectra of 6 taken in positive ion mode using ESI

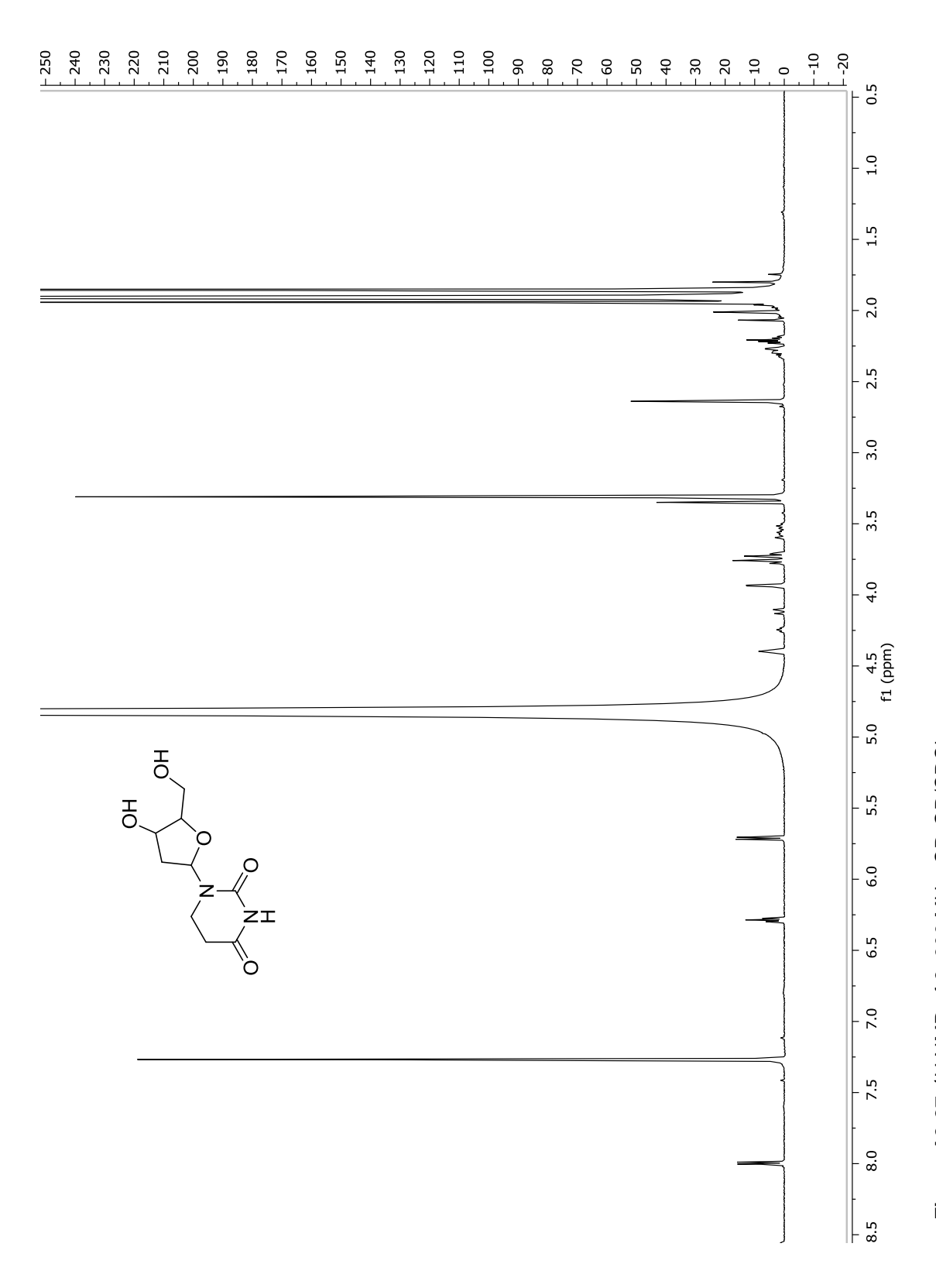
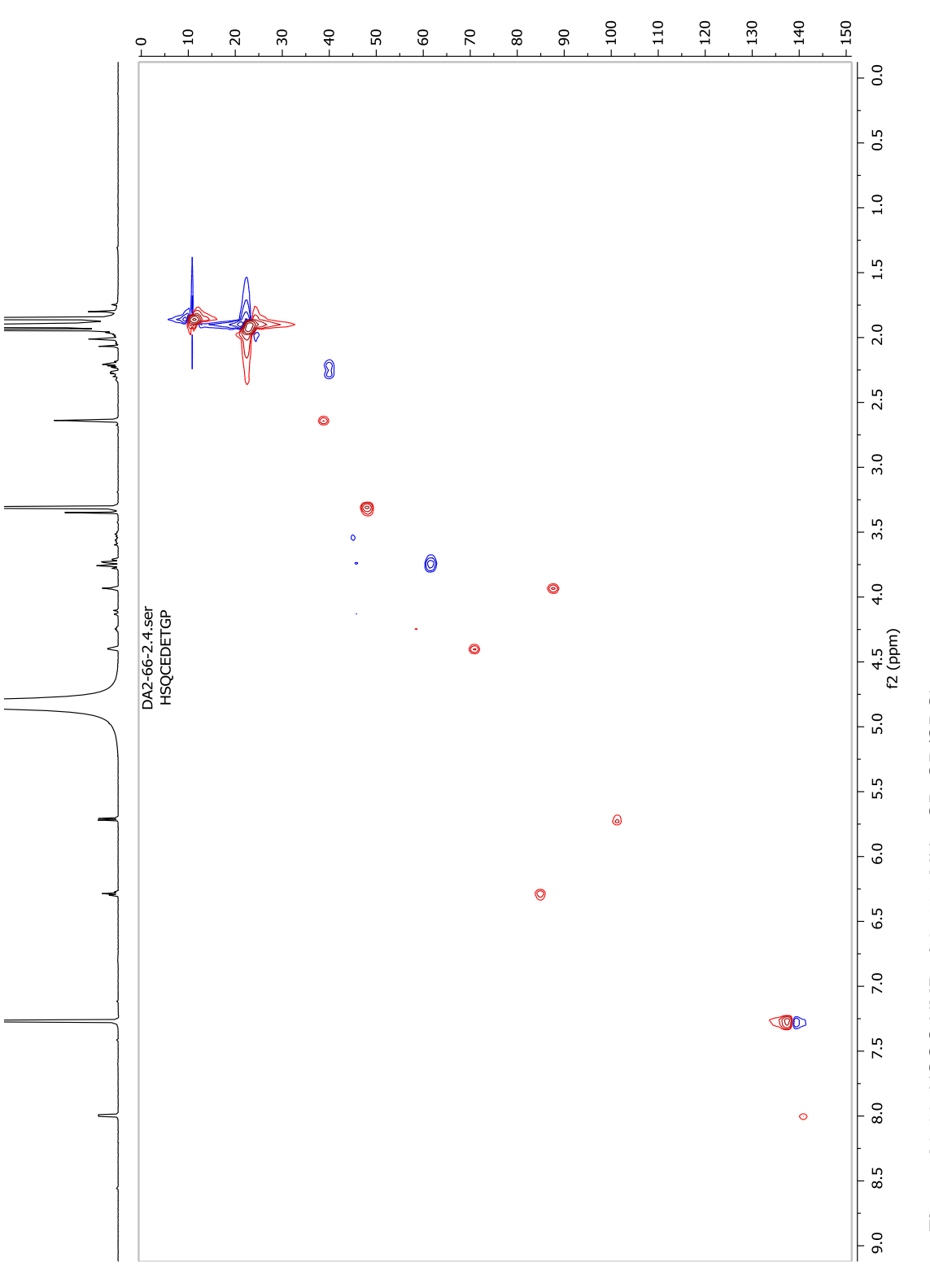


Figure A3.27. <sup>1</sup>H NMR of 6, 600 MHz, CD<sub>3</sub>OD/CDCl<sub>3</sub>



(mdd) [j

Figure A3.28. HSQC NMR of 6, 600 MHz, CD<sub>3</sub>OD/CDCl<sub>3</sub>

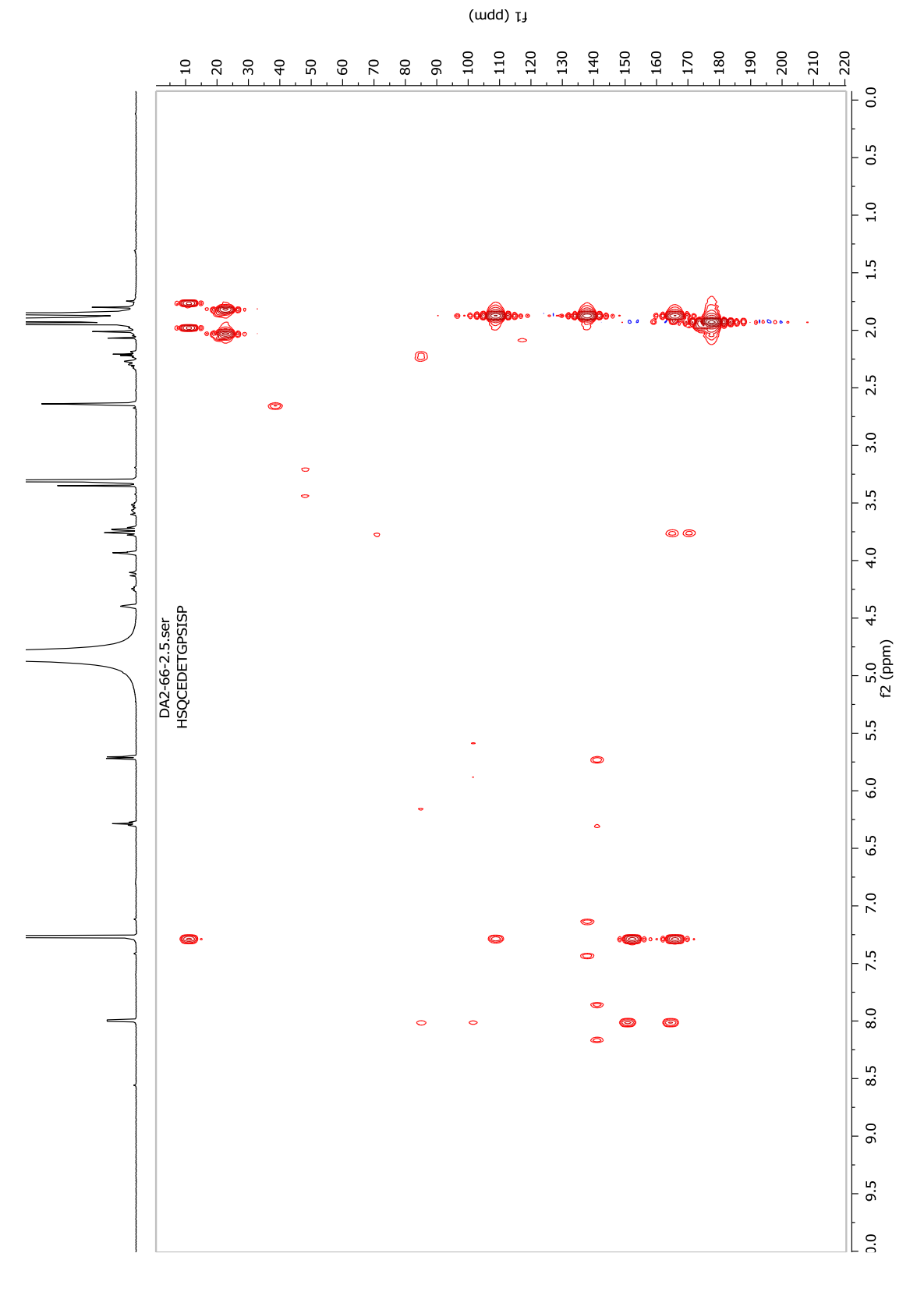


Figure A3.29. HMBC NMR of 6, 600 MHz, CD<sub>3</sub>OD/CDCl<sub>3</sub>

## **Appendix 4 Supplementary data for Chapter 5**

## Metabolomic analysis of connected flask study

To identify the molecules exclusive to R2lc or R2lc coculture, the ions also present in R2lc  $\Delta$ pks2 or R2lc  $\Delta$ pks co-culture were filtered out. Then the ions eluting between the retention times 10.30 min and 10.90 min were extracted to find molecules consistent with the UV absorption at 380 nm (as determined by the chromatograms)

Bucket	Retention	mass/	R2lc	R2lc-	R2lc Coculture	R2lc- dpks2-
10.38min: 181.161m/z	time 10.38min	charge 181.161m/z	2789	<b>dpks2</b> 0	2301	coculture ()
				_		
10.46min: 1025.654m/z	10.46min	1025.654m/z	3553	0	2412	0
10.46min: 475.236m/z	10.46min	475.236m/z	1217	0	1394	0
10.51min: 1162.690m/z	10.51min	1162.690m/z	1604	0	1433	0
10.52min: 297.110m/z	10.52min	297.110m/z	3544	0	2110	0
10.52min: 351.213m/z	10.52min	351.213m/z	909	0	1051	0
10.53min: 517.824m/z	10.53min	517.824m/z	952	0	1237	0
10.55min: 189.057m/z	10.55min	189.057m/z	4031	0	2533	0
10.56min: 173.099m/z	10.56min	173.099m/z	5326	0	3436	0
10.56min: 177.057m/z	10.56min	177.057m/z	3321	0	2466	0
10.56min: 257.118m/z	10.56min	257.118m/z	83783	0	48875	0
10.56min: 279.100m/z	10.56min	279.100m/z	36766	0	24060	0
10.59min: 321.251m/z	10.59min	321.251m/z	4536	0	4290	0
10.60min: 253.122m/z	10.60min	253.122m/z	18208	0	9723	0
10.65min: 225.056m/z	10.65min	225.056m/z	3716	0	1862	0
10.65min: 243.066m/z	10.65min	243.066m/z	7498	0	4710	0
10.65min: 263.107m/z	10.65min	263.107m/z	4280	0	2477	0
10.65min: 299.128m/z	10.65min	299.128m/z	25383	0	12909	0
10.65min: 321.109m/z	10.65min	321.109m/z	8464	0	5056	0
10.74min: 906.577m/z	10.74min	906.577m/z	558	0	410	0
10.75min: 295.130m/z	10.75min	295.130m/z	5634	0	4755	0
10.89min: 1044.625m/z	10.89min	1044.625m/z	3410	0	2992	0